MODELLING AND ALLOCATION PLANNING FOR OPEN UNIFIED POWER QUALITY CONDITIONER TO IMPROVE OPERATIONAL PERFORMANCE OF RADIAL DISTRIBUTION NETWORKS

Shubh Lakshmi

MODELLING AND ALLOCATION PLANNING FOR OPEN UNIFIED POWER QUALITY CONDITIONER TO IMPROVE OPEARTIONAL PERFORMANCE OF RADIAL DISTRIBUTION NETWORKS

A thesis submitted to
Indian Institute of Technology Guwahati
for the award of the degree of

Doctor of Philosophy

by

Shubh Lakshmi

under the guidance of

Dr. Sanjib Ganguly

DEPARTMENT OF ELECTRONICS AND ELECTRCAL ENGINEERING
INDIAN INSTITUTE OF TECHNOLOGY GUWAHATI
AUGUST 2019

Dedicated to

My Family

Department of Electronics and Electrical Engineering
Indian Institute of Technology Guwahati
Guwahati, India 781039.

CERTIFICATE

This is to certify that this thesis entitled "**Modelling and Allocation Planning for Open Unified Power Quality Conditioner to Improve Operational Performance of Radial Distribution Networks**," submitted by **Shubh Lakshmi** (156102013) to Indian Institute of Technology Guwahati is a record of bona fide research work under my supervision and I consider it worthy of consideration for the award of the degree of Doctor of Philosophy of the Institute.

(Supervisor)
Dr. Sanjib Ganguly
Department of Electronics and Electrical Engineering
Indian Institute of Technology Guwahati
Guwahati, India-781039

Declaration

I certify that

a. The work contained in this thesis is original and has been done by me under the guidance of my supervisor.
b. The work has not been submitted to any other Institute for any degree or diploma.
c. I have followed the guidelines provided by the Institute in preparing the thesis.
d. I have conformed to the norms and guidelines given in the Ethical Code of Conduct of the Institute.
e. Whenever I have used materials (data, theoretical analysis, figures, and text) from other sources, I have given due credit to them by citing them in the text of the thesis and giving their details in the references. Further, I have taken permission from the copyright owners of the sources, whenever necessary.

Shubh Lakshmi

Acknowledgements

It is my pleasure to express sincere gratitude to my supervisor, Dr. Sanjib Ganguly of the Department of Electronics and Electrical Engineering for introducing me to this area of research. His invaluable and encouraging discussions at every stage of the work helped in bringing the thesis to its present shape.

I am grateful to the Head of the Department of Electronics and Electrical Engineering for providing me all the facilities to carry out my research work. I also express my sincere gratitude to the members of doctoral scrutiny committee and all the faculty members of the department.

I would also like to acknowledge all my lab mates of Power & Control Lab-II and all other research scholars of Electronics and Electrical Engineering Department, especially, Shikha, Tilendra, and Anirban, for their help and encouragement.

My earnest thanks are to my family members who have supported this endeavor through their deeds and prayer. Their unconditional love and affection are always sources of inspiration for my future life. Many thanks to my parents for giving me the freedom of what I wanted to be. I am also thankful to my late uncle and aunt for their unconditional love and affection. Many thanks to my friends for supporting me and making my stay in IIT Guwahati memorable.

Finally, I would like to dedicate this thesis to my family.

IIT Guwahati

Date: **(SHUBH LAKSHMI)**

Abstract

The compensators are widely used in the distribution networks to improve their steady-state operational performance, such as energy efficiency and bus voltage. The capacitor bank, voltage regulator, on-load tap changer etc., are traditionally used as compensators. However, the optimal placement of these does not ensure desired power quality (PQ) level. The custom power devices are group of compensators which can mitigate PQ issues and provide reactive power compensation. Thus, their optimal allocation in distribution networks can ensure desired PQ level and improve energy efficiency. UPQC is a versatile custom power device, which can simultaneously inject a series voltage and a shunt compensating current by using its series and shunt inverters, respectively to provide reactive power compensation and to mitigate PQ problems. In UPQC, the series and shunt inverters are connected to a common DC-link. An open UPQC (UPQC-O) topology, in which, the series and shunt inverters can be placed in different locations and they do not share a common DC-link, is used in this thesis to improve the operational performance of distribution networks. This needs the modelling of UPQC-O and the formulation of planning approach to optimally allocate in distribution networks.

In this thesis, the modelling and allocation of UPQC-O without and with active power injection are presented to improve the energy efficiency of distribution networks keeping a desired PQ level intact in terms of voltage sag mitigation and harmonic elimination. A new technical constraint, i.e., percentage of voltage sag mitigated load is formulated to optimally allocate the series inverter for voltage sag mitigation. The performances of UPQC and UPQC-O models without and with active power injection are compared in view of energy efficiency improvement. The optimal allocation of UPQC-O in distribution networks significantly reduces energy loss and improves bus voltage. The modelling and allocation planning of UPQC-O integrated PV generation system are provided to improve the energy efficiency and PQ of distribution networks. The particle swarm optimization (PSO)-based solution approach is used.

The modelling and allocation planning of inverters of UPQC-O are provided to maximize the photovoltaic hosting capacity (PVHC) of a distribution network. PVHC is defined as the maximum amount of PV capacity that a network can accommodate without deteriorating its operational performance in terms of network power loss. PSO is used to optimally allocate the inverters of UPQC-O and to determine the PV generation capacity of each load bus. The simulation results show that appropriate placement of the inverters of UPQC-O increases the PVHC of a network. Since the maximization of PVHC and minimization of energy loss conflict with each other, a multi-objective planning approach is also developed for the simultaneous optimization of these two objectives. The Strength Pareto Evolutionary Algorithm-2 (SPEA2)-based multi-objective PSO (MOPSO) is used as the solution approach. This provides a set of solutions, from which a utility can choose one for the implementation according to its preference.

The proposed PV integrated UPQC-O model is used for the peak load shaving of distribution networks keeping a desired PQ level intact. For this, a multi-objective planning approach is developed to optimally allocate the UPQC-O in distribution networks. SPEA2-based MOPSO is used as the solution approach. This also provides a set of solutions, from which one solution can be selected.

An operational optimization approach is proposed to determine the time-varying reactive power injection set points for UPQC-O for time varying load and generation. This is a type of on-line optimization approach. The simulation results show that the allocation of UPQC-O with time-varying reactive power set points provides higher energy loss reduction of distribution networks for the areas where load factor is low. The CONOPT solver of General Algebraic Modelling System software is used as the solution tool.

The 33-bus and 69-bus radial distribution networks are used to validate all the proposed planning models.

Contents

List of Acronyms

ADN	Active distribution network
BESS	Battery energy storage system
BM	Bio-mass
BSS	Battery storage system
CN	Communication network
CP	Conversion planning from PDN to ADN
CP (I)	Conversion planning from PDN to ADN (investment planning)
CP (I+O)	Conversion planning from PDN to ADN (investment and operational planning)
CP (O)	Conversion planning from PDN to ADN (operational planning)
DDG	Dispatchable DG
DE	Diesel engine
DER	Distributed energy resource
DG	Distributed generation
DGHC	DG hosting capacity
DMS	Distribution management system
DNCC	Distribution network control center
DNO	Distribution network owner
DOD	Depth of discharge
DS	Distributed storage
DSTATCOM	Distribution STATCOM (static compensator)
DT	Distribution transformer
ESS	Energy storage system
EV	Electric vehicle
FC	Fuel cell
GAMS	General Algebraic Modelling System

GT	Gas turbine
HT	Hydro turbine
IC	Installation cost
LF	Load factor
MG	Micro-grid
MGP	Micro-grid planning
MGP (I)	Micro-grid planning (investment planning)
MGP (I+O)	Micro-grid planning (investment and operational planning)
MGP (O)	Micro-grid planning (operational planning)
MOPSO	Multi-objective PSO
MT	Micro turbine
OC	Operational cost
OLTC	On-load tap changer
OMC	Operational and maintenance cost
PAC	Phase angle control
PAF	Pareto approximation front
PDF	Probability density function
PDN	Passive distribution network
PI	Proportional integral
PQ	Power quality
PSO	Particle swarm optimization
PV	Photovoltaic
PV-BESS-UPQC-O	PV-BESS integrated UPQC-O
PVHC	PV hosting capacity
PVSML	Percentage of voltage sag mitigated load
SGP	ADN planning with smart grid features
SGP (I)	ADN planning with smart grid features (investment planning)
SGP (I+O)	ADN planning with smart grid features (investment and operational planning)
SGP (O)	ADN planning with smart grid features (operational planning)
SM	Smart meter
SOC	State of charge
SPEA2	Strength Pareto Evolutionary Algorithm-2
THD	Total harmonic distortion

TOU	Time-of-use
UPQC	Unified power quality conditioner
UPQC-O	Open unified power quality conditioner
UPQC-O-WB	UPQC-O with battery and PV array
UPQC-O-WOB	UPQC-O with PV array without battery
UPQC-O-WOP	UPQC-O without active power injection
UPQC-O-WP	UPQC-O with active power injection
UPQC-WOP	UPQC without active power injection
UPQC-WP	UPQC with active power injection
WT	Wind turbine

भारतीय प्रौद्योगिकी संस्थान गुवाहाटी
Indian Institute of Technology Guwahati

List of Principal Symbols

AEL_{U1}	Annual energy loss of network with UPQC-O in 1st year
AEL_{U5}	Annual energy loss of network with UPQC-O in 5th year
AEL_{base1}	Annual energy loss of base-case network (without UPQC-O) in 1st year
AEL_{base5}	Annual energy loss of base-case network (without UPQC-O) in 5th year
C^E	Unit cost of energy loss ($/kWh)
C_I^B	Investment cost of Li-ion battery
C_I^{PV}	Investment cost of PV array
$C_{O\&M}^B$	Operation and maintenance cost of Li-ion battery
$C_{O\&M}^{PV}$	Operation and maintenance cost of PV array
C_{REP}^B	Replacement cost of battery
$C_{Sh}(l)$	Investment cost of shunt inverter at location 'l'
C_{Se}	Investment cost of series inverter
C_U	Investment cost of UPQC/UPQC-O ($/kVA)
C_m^{Se}	Investment cost of series inverter at location 'm' ($/kVA)
C_n^{Sh}	Investment cost of shunt inverter at location 'n' ($/kVA)
CUF	Capacity utilization factor of PV array
$\%DOD_{max}$	Maximum depth of discharge of BESS
D^f	Discount factor
D^{f1}	Discount factor used for replacement of battery
d_{yw}	Index for load scenarios in day type 'w' of season 'y'
E_{Sh}	Energy required by the shunt inverter from the BESS connected to it
E_{Se}	Energy required by the series inverter from the BESS connected to it
$\vec{I}_{ef}$	Current flow in any line 'ef'
$\bar{I}(m)$	Load current at bus 'm'
$\bar{I}(mn)$	Current flowing through line 'mn'

I_L	Line current at the location of shunt inverter of UPQC-O
I_L'	Compensated line current with shunt inverter of UPQC-O-WOP
I_L''	Compensated line current with shunt inverter of UPQC-O-WP
$INVL_{Sh1_2}^{WP}$	UPQC-WP shunt inverter loss during off-peak hour
$INVL_{Sh_2}^{WP}$	UPQC-O-WP shunt inverter loss during off-peak hour
$INVL_{Sh_d}^{WOP}$	UPQC-WOP shunt inverter loss in load level 'd'
$INVL_{Se1_2}^{WP}$	UPQC-WP series inverter loss during off-peak hour
$INVL_{Se_d}^{WOP}$	UPQC-O-WOP series inverter loss in load level 'd'
$INVL_{Se}^{Peak}$	Series inverter losses during peak demand hours
$INVL_{md}^{Se}$	Series inverter loss in load level 'd' at location 'm'
$INVL_{nd}^{Sh}$	Shunt inverter loss in load level 'd' at location 'n'
I_{R1}	Uncompensated line current before placement of UPQC
I_{R1}'	Compensated line current with UPQC-WOP
I_{R1}''	Compensated line current with UPQC-WP
I_{R1}^{dis}	Distortion component of line current I_{R1}
I_{R1}^{fun}	Fundamental component of line current I_{R1}
I_{Re}	In-phase AC current supported by the battery of UPQC-O-WP
I_{Re1}	In-phase AC current supported by the battery of UPQC-WP
I_S	Line current at the point of connection of series inverter of UPQC-O
$I_S(t)$	Line current at the point of connection of series inverter at time 't'
I_{Sh}'	Shunt compensating current provided by the shunt inverter of UPQC-O-WOP
$I_{Sh}'(t)$	Shunt compensating current provided by the shunt inverter at time 't'
I_{Sh}''	Shunt compensating current provided by the shunt inverter of UQPC-O-WP
$I_{Sh}^{''RMS}$	RMS value of shunt compensating current I_{Sh}''
$I_{Sh}^{'RMS}$	RMS value of shunt compensating current I_{Sh}'
I_{Sh1}'	Shunt compensating current injected by the shunt inverter of UPQC-WOP
I_{Sh1}''	Shunt compensating current injected by the shunt inverter of UPQC-WP
$I_{Sh1}^{''RMS}$	RMS value of shunt compensating current I_{Sh1}''
$I_{Sh1}^{'RMS}$	RMS value of shunt compensating current I_{Sh1}'
$I_{Sh1}^{'dis}$	Distortion component of shunt compensating current I_{Sh1}'
$I_{Sh1}^{'fun}$	Fundamental component of shunt compensating current I_{Sh1}'
$I_{TH}(mn)$	Thermal limit of line 'mn'

$I_{efd_{yw}}$	Current flow in line 'ef' during load scenario 'd_{yw}'
$K_L(t)$	Percentage of peak load demand at time 't'
$K_{PV}(t)$	Percentage of peak PV generation at time 't'
K_{Re}	Ratio of in-phase AC current supported by the battery to the original line current
$K_{Sh}(t)$	Factor used to determine the injection of shunt compensating current I'_{Sh} at time 't'
$K_{Se}(t)$	Factor used to determine the injection of series voltage V_{Se}^{Hel} at time 't'
K_{Se1}	Ratio of V_{Se1} to V_{R1}
k	Amount of voltage sag in supply voltage
L_{ef}	Active power loss in line 'ef'
M_{ef}	Reactive power loss in line 'ef'
N_{Sh}	Number of shunt inverter(s) to be placed in distribution network
N	Total number of bus in a network
$P'(i)$	Modified active power demand of bus 'i'
PB_{Sh}	Rating requirement for battery connected to the shunt inverter of UPQC-O
$PB_{Sh}(l)$	Battery rating requirement for the shunt inverter of UPQC-O at location 'l'
PB_{Sh}^{WOP}	Size of battery connected to shunt inverter of UPQC-O-WOP
PB_{Sh}^{WP}	Size of battery connected to series inverter of UPQC-O-WP
PB_{Se}	Battery rating requirement for the series inverter of PV-BESS-UPQC-O
PB_{Se}^{WOP}	Size of battery connected to series inverter of UPQC-O-WOP
PB_{Se}^{WP}	Size of battery connected to series inverter of UPQC-O-WP
PB_{Tot}	Total BESS rating requirement of PV-BESS-UPQC-O
PB_{UPQC-O}^{WOP}	Total rating of battery connected to the UPQC-O-WOP
PB_{UPQC-O}^{WP}	Total rating of battery connected to the UPQC-O-WP
PB_{UPQC}^{WP}	Size of battery connected to UPQC-WP
PB_m^{Se}	Series inverter battery rating requirement at location 'm'
PB_n^{Sh}	Shunt inverter battery rating requirement at location 'n'
$PL_{HS}(mn)$	Power loss in the line 'mn' with the placement of PV-BESS-UPQC-O
PL_{PV}	Network power loss with the PV generation during minimum loading condition
PL_{base}	Base-case network power loss during minimum loading condition
P_{Lf}	Peak active power demand of bus 'f'
$PL_{mn}^{t_1}$	Power loss occurs in line 'mn' during t_1 hours
$PL_{mn}^{t_3}$	Power loss occurs in line 'mn'during t_3 hours

$PL_{mn}^{t_4}$	Power loss occurs in line 'mn' during t_4 hours
$P_{PV}(i)$	Maximum PV generation capacity of bus 'i'
$P_{PV}^{Avg}(i)$	Hourly average PV generation at bus 'i'
PPV_{Sh}	PV rating requirement for the shunt inverter of UPQC-O
$PPV_{Sh}(l)$	PV rating requirement for shunt inverter of UPQC-O at location 'l'
PPV_{Se}	PV rating requirement for the series inverter of UPQC-O
PPV_{Tot}	Total PV rating requirement of PV-BESS-UPQC-O
PPV_n^{Sh}	Shunt inverter PV rating requirement at location 'n'
$(P_{PV})_{max}$	Maximum limit of PV generation capacity in each load bus
$(P_{PV})_{min}$	Minimum limit of PV generation capacity in each load bus
P_{Sh}	Active power supplied by the shunt inverter
$P_{Sh}(l)$	Active power supplied by the shunt inverter at location 'l'
P_{Sh1}^{WOP}	Active power supplied by the shunt inverter of UPQC-WOP
P_{Sh1}^{WP}	Active power supplied by the shunt inverter of UPQC-WP
P_{Sh}^{DG}	Active power injected through DC link of shunt inverter with PV array
P_{Sh}^{WP}	Active power supplied by the shunt inverter of UPQC-O-WP
P_{Se1}^{WOP}	Active power supplied by the series inverter of UPQC-WOP
P_{Se1}^{WP}	Active power supplied by the series inverter of UPQC-WP
P_{ef}	Active power flow of line 'ef'
$P_f(t)$	Active power demand of any bus 'f' at time instant 't'
P_f^{PV}	Hourly PV generation in bus 'f'
$P_f^{PV}(t)$	PV generation in any bus 'f' at time instant 't'
P_f^{PVGEN}	PV generation capacity of bus 'f'
P_g	Active power demand of bus 'g'
$P_{total}^{Off-peak}$	Total load demand of the network during off-peak hour
P_{total}^{Peak}	Total load demand of the network during peak hour
PL_c	Total line losses in scenario 'c'
PL_d	Network power loss in load level 'd' with UPQC/UPQC-O
$P(i)$	Active power demand of bus 'i'
$PF(oe)$	Active power flowing through line 'oe'
$PL(ef)$	Active power loss in line 'ef'
$Q_{Sh1}^{\max'}$	Maximum reactive power required from the shunt inverter of UPQC-WOP

$Q_{Sh1}^{\max''}$	Maximum reactive power required from the shunt inverter of UPQC-WP
$Q_{Se1}^{\max'}$	Maximum reactive power provided by the series inverter of UPQC-WOP
$Q_{Se1}^{\max''}$	Maximum reactive power provided by the series inverter of UPQC-WP
$Q'(i)$	Modified reactive power demand of bus 'i'
Q_{Comp}	A fraction of total reactive power demand of the network
Q_{Lf}	Peak reactive power demand of bus 'f'
Q_{Sh}	Reactive power supplied by the shunt inverter
Q_{Sh_req}	Reactive power required from the shunt inverter
$Q_{Sh\_req}^{WOP}$	Reactive power required from the shunt inverter of UPQC-O-WOP
$Q_{Sh\_req}^{WP}$	Reactive power required from the shunt inverter of UPQC-O-WP
Q_{Sh1}^{WOP}	Reactive power supplied by the shunt inverter of UPQC-WOP
Q_{Sh1}^{WP}	Reactive power supplied by the shunt inverter of UPQC-WP
Q_{Sh}^{WOP}	Reactive power supplied by the shunt inverter of UPQC-O-WOP
Q_{Sh}^{WP}	Reactive power supplied by the shunt inverter of UPQC-O-WP
Q_{Se}	Reactive power supplied by the series inverter
Q_{Se1}^{WOP}	Reactive power supplied by the series inverter of UPQC-WOP
Q_{Se1}^{WP}	Reactive power supplied by the series inverter of UPQC-WP
Q_{Se}^{WOP}	Reactive power supplied by the series inverter of UPQC-O-WOP
Q_{Se}^{WP}	Reactive power supplied by the series inverter of UPQC-O-WP
Q_{ef}	Reactive power flow of line 'ef'
$Q_f(t)$	Reactive power demand of any bus 'f' at time instant 't'
Q_f^{Sh}	VAr compensation provided by the shunt inverter in bus 'f'
Q_f^{Se}	VAr compensation provided by the series inverter in bus 'f'
$Q_f^{Se}(t)$	VAr compensation provided by the series inverter in bus 'f' at time 't'
Q_f^U	VAr support provided by the series/ shunt inverter at bus 'f'
Q_g	Reactive power demand of bus 'g'
$Q_g^{Sh}(t)$	VAr compensation provided by the shunt inverter in bus 'g' at time 't'
$Q(i)$	Reactive power demand of bus 'i'
$QF(oe)$	Reactive power flowing through line 'oe'
$QL(ef)$	Reactive power loss in line 'ef'
R_{ef}	Resistance of line 'ef'

r_e	Annual energy price growth rate
$S_{Sh}(l)$	VA-rating of shunt inverter at location 'l'
S_{Sh1}^{WOP}	VA-rating of shunt inverter of UPQC-WOP
S_{Sh1}^{WP}	VA-rating of shunt inverter of UPQC-WP
S_{Sh}^{WOP}	VA-rating of shunt inverter of UPQC-O-WOP
S_{Sh}^{WP}	VA-rating of shunt inverter of UPQC-O-WP
S_{Se}	VA-rating of series inverter
S_{Se1}^{WOP}	VA-rating of series inverter of UPQC-WOP
S_{Se1}^{WP}	VA-rating of series inverter of UPQC-WP
S_{Se}^{WOP}	VA-rating of series inverter of UPQC-O-WOP
S_{Se}^{WP}	VA-rating of series inverter of UPQC-O-WP
S_{Tot}	Total VA-rating of PV-BESS-UPQC-O
S_U	Total VA-rating of UPQC/UPQC-O
S_{UPQC-O}^{WOP}	Total VA-rating of UPQC-O-WOP
S_{UPQC-O}^{WP}	Total VA-rating of UPQC-O-WP
S_{UPQC}^{WOP}	Total VA-rating of UPQC-WOP
S_{UPQC}^{WP}	Total VA-rating of UPQC-WP
S_{base}	Base kVA of network
S_m^{Se}	VA-rating of series inverter at bus 'm'
S_n^{Sh}	VA-rating of shunt inverter at bus 'n'
T^h	Planning horizon (Years)
TEL_{base}	Total energy loss of base-case network
TFL_{md}^{Se}	Series inverter transformer loss in load level 'd' at location 'm'
THD_L	Total harmonic distortion of line current
THD_{Sh}	Total harmonic distortion of shunt compensating current
t_1	Duration of peak hour in a day (hours)
t_2	Duration of off-peak hour in a day (hours)
t_3	Duration of off-peak hour with no PV generation
t_4	Operation hours of PV array (hours)
t_{Sag}	Duration of occurrence of voltage sag (seconds)
t_b	Operational hour of battery
t_c	Duration of occurrence of scenario 'c' (hours)

t_d	Duration of occurrence of load level 'd'
t_w	Total number of days in a week for which day type 'w' occurs
t_y	Total number of weeks in a year for which season 'y' occurs
t_{ywh}	Total number of hours of occurrence of load scenario 'd_{yw}' in day type 'w' of season 'y'
$\vec{V}_e$	Bus voltage at any location 'e'
$\bar{V}(m)$	Voltage at bus 'm'
V_L	Voltage at the location of shunt inverter of UPQC-O
$V_L(t)$	Voltage at the location of shunt inverter at time 't'
V_R	Receiving end voltage of a line during healthy condition
V_{R1}	Receiving end voltage of a line during healthy condition
V_R^C	Receiving end voltage of a line during healthy condition after injection of series voltage by UPQC-O
V_R^{Sag}	Receiving end voltage during voltage sag condition
V_S	Sending end voltage of a line during healthy condition
V_{Se}	Series voltage injected by the series inverter
V_{Se1}	Series voltage injected by the series inverter of UPQC
V_{Se}^{Hel}	Voltage injected by the series inverter of UPQC-O during healthy condition
$V_{Se}^{Hel}(t)$	Voltage injected by the series inverter at time instant 't' during healthy condition
$V_{Se}^{Sag}(t)$	Voltage injected by the series inverter at time 't' during voltage sag condition
V_{Se}^{sag}	Voltage injected by the series inverter of UPQC-O during voltage sag condition
V_{max}	Maximum value of bus voltage magnitude
$V_{min}^{t_1}$	Network minimum bus voltage magnitude during t_1 hours
$V_{min}^{t_3}$	Network minimum bus voltage magnitude during t_3 hours
$V_{min}^{t_4}$	Network minimum bus voltage magnitude during t_4 hours
V_{min}	Minimum value of bus voltage magnitude
w	Index for day type (weekday/ weekend) in a week
X_{ef}	Reactance of line 'ef'
x_m	Binary variable for the allocation of series inverter at bus 'm'
x_n	Binary variable for the allocation of shunt inverter at bus 'n'
y	Index for seasons in a year
Z_{ef}	Impedance of line 'ef'

$Z(mn)$	Impedance of line 'mn'
α'	Phase angle between V_S and V_R^{Sag}
α''	Phase angle between V_S and V_R (after series voltage injection)
γ_{TF}	Series inverter transformer losses (%)
γ_{loss}	Total inverter losses (%)
δ_1	Phase angle shift after series voltage injection by UPQC
δ_2	Phase angle between V_S and V_R
δ_2'	Phase angle between V_S and V_R^C
θ_L	Phase angle between V_L and I_{Sh}''
θ_{Sh1}'	Phase angle between V_{R1} (after series voltage injection) and I_{Sh1}'
θ_{Sh1}''	Phase angle between V_{R1} (after series voltage injection) and I_{Sh1}''
θ_{Se1}	Phase angle between V_{R1} and V_{Se1} during healthy condition
$\emptyset$	Phase angle between V_S and I_S
Δ	Set of seasons in a year
Λ	Set of all buses where series inverter is placed
μ	Set of all the lines of a network
ξ	Set of all the buses where shunt inverter is placed
ρ	Set of all the load buses of network
$\aleph$	Set of all downstream buses which are beyond any bus 'n'
β	Set of day type (weekday/weekend) in a week
σ	Set of incoming lines connected to any bus 'e'
τ	Set of outgoing lines connected to any bus 'e'
ψ	Set of different load and generation scenarios
∂	Set of all downstream buses which are beyond the point of connection of series inverter of UPQC-O
ϑ	Ratio of network power loss with PV generation to the base-case network power loss during minimum loading condition
$\emptyset_L$	Phase angle between V_L and I_L
$\emptyset_{R1}$	Phase angle between V_{R1} and I_{R1}
η_{INV}	Conversion efficiency of inverter
Γ_{yw}	Set of load scenarios in day type 'w' of season 'y'

List of Figures

भारतीय प्रौद्योगिकी संस्थान गुवाहाटी
Indian Institute of Technology Guwahati

List of Tables

1

Introduction and Literature Review

1.1 Introduction

In last few years, distribution network planning has attracted attention of power systems planners because it involves a number of objectives to be simultaneously optimized. The aim of distribution network planners is to develop different approaches to minimize energy loss and to maintain power quality (PQ) of a network. The distribution network planning can be done in two ways: (i) single-stage planning and (ii) multi-stage planning. In single stage planning, whole planning is performed at one step by considering discount factor for a planning horizon. In the case of multi-stage planning, the planning horizon is divided into multiple steps and the planning is performed for each step. There are some state-of-the-art review papers reported on distribution network planning [1-6]. Among these, the papers [1-3] are on review of the passive distribution network (PDN) planning. In PDN, the power flow is unidirectional. The inclusion of distributed generation (DG) in distribution network, converts the PDN to active distribution network (ADN). The works reported on ADN planning and/or PDN planning till 2015 have been reviewed in [4-6]. The different objectives and decision/optimizing variables used in the planning of PDN and ADN are shown in Table 1.1. The differences between traditional PDN and ADN are categorically shown in [6]. Some typical characteristics of ADN planning, which make it different to the traditional PDN planning are given below.

- The designed network topology/structure is to be flexible and it can automatically be reconfigured to a different structure, unlike PDN.

- The designed network should reliably work with high penetration of DG.
- The designed network should reliably work with uncertainties of the generation of renewable energy sources, such as photovoltaic (PV), wind turbine (WT) etc.
- The operation of the designed network should be automated unlike manual operation of PDN.

Table 1.1: The planning cost and decision/optimizing variables for PDN and ADN planning

Types of cost/ decision/optimizing variables	PDN planning	ADN planning
Installation/ reinforcement/ replacement cost for:	Substation, transformers, feeders, lines/ feeder branches, sectionalizing switches and tie-lines, conventional reactive power compensators, such as, voltage regulators, capacitors, and on-load tap changers etc.	DG units, storage units (i.e., battery), advanced protection and communication infrastructure, advanced automation and metering technologies, power electronics devices for reactive power compensation and PQ improvement etc.
Operational cost:	Cost of energy loss and maintenance cost for each equipment associated with PDN	Cost of energy loss and maintenance cost for each equipment associated with ADN
Decision/optimizing variables:	Size and location for new substation, number of feeders, feeder routing, number and locations for sectionalizing switches and tie-lines, conductor types and sizes etc.	Sizes and locations for DG units, sizes and locations for battery, appropriate coordination of protection and automation technologies, generation mix among different types of DG units etc.

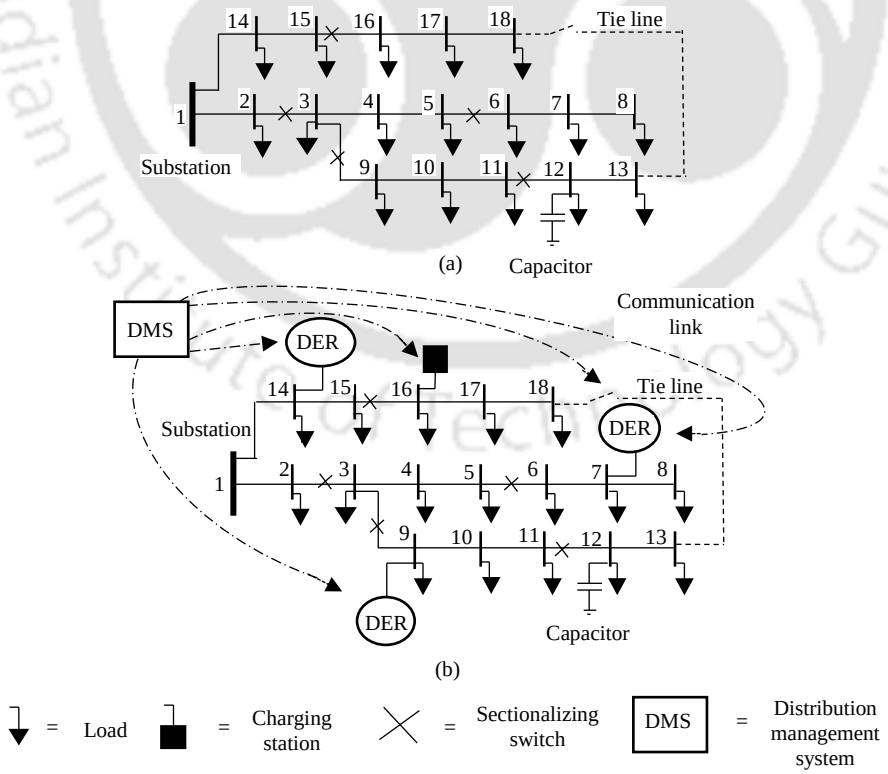

Fig. 1.1: The different features of typical distribution networks: (a) PDN and (b) ADN

The difference in features between PDN and ADN is shown with example networks in Fig. 1.1. Usually, a typical PDN consists of single or multiple feeders, several sectionalizing switches, tie line(s), and capacitor bank(s) as shown in Fig. 1.1(a). In addition to these, a typical ADN, as shown in Fig. 1.1(b), consists of distributed energy resources (DERs), charging station for electric vehicles (EVs), smart meters (SMs), and distribution management system (DMS), which includes smart communication devices, advanced metering technologies, demand side management technologies, energy management technologies, smart automation technologies etc. Traditionally, the tie-line and sectionalizing switches in PDN are manually operated, whereas, advanced automation technologies are used to operate these in ADN. The scheduling for the operation of different DER units and charging station(s) is done using DMS. Hence, there are differences among the objectives and optimizing variables in PDN and ADN planning as summarized in Table 1.1. Thus, the ADN planning is an involved multi-objective optimization process with a number of objectives, such as, (i) minimization of installation/ reinforcement/ replacement cost for DG units and storage units (if any), (ii) minimization of operational cost (cost of energy loss and maintenance cost), (iii) maximization of reliability, (iv) maximization of DG capacity, (v) minimization of carbon emission, (vi) determination of optimal operational strategy for DG units, (vii) PQ mitigation etc. These objectives are optimized subjected to several technical and operational constraints, such as, active and reactive power balance, bus voltage magnitude, line current flow, PV capacity etc. In many occasions, these objectives do conflict with each other. For example, the integration of renewable DG unit reduces the carbon emission at the expense of higher investment cost. Hence, to solve the ADN planning problem consisting of several such conflicting objectives, one needs multi-objective optimization approach. There are various multi-objective optimization approach available in the literature. These are weighted aggregation-based approach, Pareto-based approach, ε-constrained approach etc. It is seen that the Pareto-based approach is popularly used in solving most of the multi-objective ADN planning problems.

The power systems researchers around the globe have significantly contributed on ADN planning during last 2-3 years. Hence, in this chapter, these works are systematically presented. A classification tree is developed for ADN planning, as shown in Fig. 1.2. It

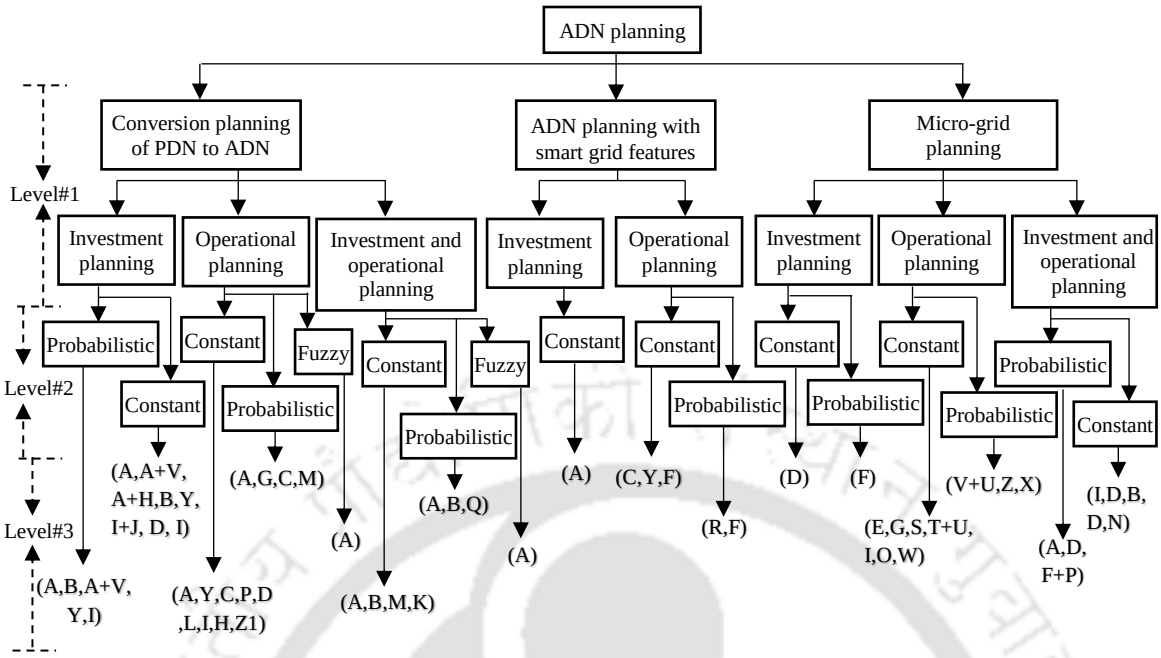

A- Genetic algorithm (GA) and its variants
B- Particle swarm optimization (PSO) and its variants
C- Non-linear programming (NLP)
D- Mixed integer programming (MIP)
E- Dynamic programming (DP)
F- Stochastic programming (SP)
G- Mixed integer non-linear programming (MINLP)
H- Ant colony optimization (ACO)
I- Mixed integer linear programming (MILP)
J- Simulated annealing (SA)
K- Chaotic local search with modified honey bee mating optimization (CLSMHBMO)
L- Multi period OPF (MOPF)
M- Interior point method (IPM)
N- Linear programing (LP)
O- Semi definite programming (SDP)
P- Monte Carlo method (MCM)
Q- Mixed integer second order cone programming (MISOCP)
R- Nash bargaining theory
S- Predictor corrector proximal multiplier (PCPM)
T- Integer programming (IP)
U- Graph theory
V- Tabu search (TS)
W- Cultural algorithm (CA)
X- Self adaptive imperialist competitive algorithm (SAICA)
Y- Heuristic algorithm (HA)
Z- Active set optimization algorithm (ASOA)
Z1- Multi-objective evolutionary algorithm (MOEA)

Fig. 1.2: Classification tree of ADN planning

consists of three levels based on different attributes of planning. The different types of ADN planning are grouped in Level #1 classification. The Level # 2 further categorizes the Level #1 based on different load and generation models used. The Level # 3 classification is based on the different solution strategies reported in solving the ADN planning optimization problem. The special emphasis is given in the literature review to identify the inclusion of two important features of modern sustainable energy planning: (i) mitigation of the PQ problems and (ii) integration of storage units.

1.2 Literature review on ADN planning

In view of different approaches on ADN planning, a three-level classification tree structure is developed as shown in Fig. 1.2. The level #1 classification is based on the type of the planning. There are three different types found and these are: (i) conversion planning from PDN to ADN (CP), (ii) ADN planning including smart grid features (SGP) and (iii) micro-grid (MG) planning (MGP). In the conversion planning, [7-43], the traditional PDN is converted to ADN with at least one DG unit of either conventional or renewable type. In ADN planning with smart grid features [44-49], the planning approaches consist of smart technologies, such as, charging of EV, fault passage indicator, distribution automation, advanced metering techniques, advanced communication techniques, energy management technologies, demand management technologies etc. The MG is a kind of low/medium-voltage distribution network consisting of DG units and controllable loads, which can be operated in either islanded or grid-connected mode. The MG planning [50-69] is done to improve system self-adequacy and to design self-sufficient network. These three types of planning are further divided into three sub-categories based on the objective function formulations. They are: (i) investment planning, (ii) operational planning, and (iii) combined investment and operation planning. In investment planning, a planner's job is to find out the amount of fund to be optimally invested for achieving particular objectives within a planning horizon. In the ADN operational planning, a planner's job is to determine the optimal operational strategy for the devices connected with the distribution networks for achieving particular objectives. This is done by maximizing the profit with energy export/import, by finding the optimal power flow, by finding the optimal exchange of power with main grid, and by improving different operational parameters of distribution network, such as power loss, voltage deviation, carbon emission etc. The combined investment and operation planning is an approach combining both investment and operational planning objectives. The investment planning is long-term planning process, whereas the operational planning is a short-term planning process. The different attributes of individual work are given in Table 1.2.

The Level #2 further categorizes the Level #1 based on different types of load and generation models. Basically, three types of load and generation models are used in the

literature: (i) constant, (ii) probabilistic and (iii) fuzzy set theory-based. The probability-based load models are reported in [9, 11, 13, 16-18, 23, 28, 33, 35, 39-40, 42, 46, 51, 55-56, 58-59, 67]. In [9, 11, 13, 17, 18, 22-23, 28, 30, 31, 33, 35, 39-40, 42, 46, 49, 51-52, 55-56, 58-59, 67-68], probability-based generation models are used. Probabilistic load and generation are usually modelled by using a chosen probability density function (PDF), such as normal distribution, beta PDF, Weibull PDF, Rayleigh PDF etc. In some of the approaches [8, 10], the fuzzy set theory is used to model the uncertain load and generation. The rest of the works are based on constant load and generation values.

The Level #3 classification is based on the solution strategies used in ADN planning. Several solution strategies are used to solve the planning optimization problems. The reported solution strategies can be categorized into two groups: (i) classical and enumerative search techniques and (ii) meta-heuristic approaches. Different conventional mathematical approaches and enumerative search techniques used are linear programming (LP), non-linear programming (NLP), mixed integer programming (MILP), mixed integer non-linear programming (MINLP), mixed integer second order cone programming (MISOCP), semi definite programming (SDP), Nash bargaining approach, dynamic programming (DP), and predictor corrector proximal multiplier (PCPM) etc. The meta-heuristic methods use problem-independent set of rules to search feasible solutions. Some of the meta-heuristic approaches used are genetic algorithm (GA) and its different variants, particle swarm optimization (PSO) and its different variants, heuristic algorithm (HA), ant colony optimization (ACO), simulated annealing (SA), tabu search (TS), and cultural algorithm (CA) etc. In some of the approaches, hybrid solution strategy combining both classical and meta-heuristic approaches is used, for example, hybrid MILP and SA, and hybrid TS and graph theory, etc. The individual approaches are summarized in Table 1.2.

Table 1.2: Different features of different ADN planning approaches

Ref. No.	Planning category	Objective functions	Type of DG unit	Solution strategy	PQ problem mitigation included?	Integration of storage included?
[7]	CP (I)	IC and OC for substation, feeder, DG units, and ESS, replacement cost of ESS, and cost of outage	Not mentioned	TS-GA, GA-ACO and PSO	No	Yes
[8]	CP (O)	Power loss and voltage deviation	Not mentioned	Adaptive GA	No	No
[9]	CP (O)	Energy loss	WT	MINLP	No	No

[10]	CP (I+O)	IC and OC of DG units, cost of energy loss, risk of overloading in substations and line segments, risk of over/under voltage in buses, and economic risk due to electricity price uncertainty	Not mentioned	NSGA-II	No	No
[11]	CP (I+O)	Cost of line up-gradation, cost of energy loss, IC and OMC of DG units, cost of energy produced by DG units, and emission from DG units and for the purchased energy from the grid	PV, WT and GT	NSGA-II	No	No
[12]	CP (I+O)	IC and OC of DG units, costs of substation and feeder reinforcement, cost of purchased energy from the grid, emission cost, and voltage satisfaction	GT, MT and FC	CLSMH BMO	No	No
[13]	CP (I+O)	Technical constraints dissatisfaction, cost of energy purchase from the grid, reinforcement of substation and feeder, IC and OC of DG units, and total emission from DG units and the grid	WT, GT and MT	Binary PSO	No	No
[14]	CP (I)	IC and OC of DG units, capital cost to upgrade substation and feeders, and cost for import and export of energy	GT	HA	No	No
[15]	CP (I)	IC and OMC of DDG units, capacitors, lines and transformers, cost of energy loss, reliability cost, and cost of the reduction in purchased energy from the grid	DE	Modified discrete PSO	No	No
[16]	CP (I)	IC of substation, feeder and DG units, and OC of DG units and substation	Not mentioned	PSO	No	No
[17]	CP (I)	Costs of energy loss, imported energy from the grid, and non-distributed energy, cost of reconfiguration using switches, IC of DG units, and costs of conductor replacement and additional lines	Thermal and WT	GA	No	No
[18]	CP (I)	IC, OMC, and capacity adequacy cost of DG units and cost of energy loss	WT, PV and DE	Point estimated GA	No	No
[19]	CP (I)	Costs of new lines, cost of energy losses, cost of undelivered energy due to faults, and cost of production loss of DG units due to faults in lines	Not mentioned	MILP & SA	No	No
[20]	CP (O)	Costs of energy not supplied and energy loss	WT and PV	HA	No	Yes
[21]	CP (O)	Maximization of energy export and revenue from energy export	Not mentioned	NLP	No	Yes
[22]	CP (O)	Cost of energy loss	WT, PV and HT	GA	Yes	No
[23]	CP (I)	Costs of energy loss, imported energy, and non-distributed energy, cost of reconfiguration using switches, IC of DG units and new lines, and cost of conductor replacement	WT and Thermal	GA	No	No
[24]	CP (O)	Energy loss	WT and PV	MCM	No	Yes
[25]	CP (O)	Load curtailment minimization	Fossil fuel based DG	MIP	No	No
[26]	CP (O)	DG capacity maximization	WT	MOPF	No	No
[27]	CP (O)	Cost of energy loss, generation cost of wind energy, and cost of ESS	WT	NLP	No	Yes
[28]	CP (I+O)	IC and MC of DS systems and OC of grid (voltage deviation, energy purchase from the grid, energy losses, and load curtailment)	WT, PV and DE	MISOCP	No	Yes
[29]	CP (O)	Network power loss and voltage deviation	Not mentioned	GA	No	No
[30]	CP (I)	IC and OC of DG units and capacitor, and cost of purchase energy from the grid	WT	TS and GA	No	No
[31]	CP (I)	IC and OC of substation and lines, cost of energy loss, and fault cost	WT	NSGA-II	No	No
[32]	CP (I+O)	Costs of energy loss, voltage regulation, and peak demand, and IC and OMC of ESS	-	IPM	No	Yes
[33]	CP (O)	OC of PV units, cost of reduction in demand with the integration of demand response program, and energy loss	PV	IPM	No	No
[34]	CP (O)	DG hosting capacity maximization	Not mentioned	MILP	No	No

[35]	CP (I)	Cost of substation expansion, IC of substation, DG units, and feeder, replacement cost of feeder, OC of DG units, cost of energy purchase from the grid, cost of energy loss, cost of energy not supplied due to faults, and pollutant emission cost	WT and DDG	GA and OPF	No	No
[36]	CP (O)	Power loss, voltage improvement, and load balancing of the lines in feeder	PV	ACO and fuzzy	No	No
[37]	CP (I+O)	Profit due to sale of energy, IC of ESS and DG units, and OMC of ESS and DG units	Not mentioned	PSO	No	Yes
[38]	CP (I)	IC of ESS, OC of ESS and lines, cost of conductor replacement, cost of power imported from the substation, outage cost, and value of lost load	-	MIP	No	Yes
[39]	CP (I+O)	Substation expansion cost, IC of substation, feeder and DG units, conductor replacement cost of feeder, OC of DG units, cost of energy purchase from the grid, cost of energy loss, cost of expected energy not supplied, and emission cost	WT and DDG	GA	No	No
[40]	CP (O)	Cost of energy	WT	NLP	No	No
[41]	CP (I)	IC and OMC of DG units, cost of energy purchase from the grid, cost of unserved energy, cost of energy loss, and emission cost	WT, PV, HT, GT, Geothermal, Heavy fuel oil turbine, BM	MILP	No	No
[42]	CP (I)	IC and OMC of feeder, transformer, substation and DG units, cost of energy loss, and cost of unserved energy	WT and PV	MILP	No	No
[43]	CP (O)	Active and reactive power losses of the network	PV, MT etc.	MOEA	No	No
[44]	SGP (I)	IC and OMC of substation, lines, fault passage indicator and parking lot, and expected energy not supplied	-	NSGA-II	No	Yes (EV)
[45]	SGP (I)	Revenue earned from energy export, IC and OMC of substations, feeders, and lines, cost of energy loss, and interruption and fault repairing cost of lines	-	GA	No	No
[46]	SGP (O)	Saving cost for reactive power compensation and the voltage deviation	Not mentioned	Nash Bargaining theory	No	No
[47]	SGP (O)	Economic benefit from load and plug-in EV (PEV), OC of DG units, and cost of energy purchase from the grid	WT and PV	NLP	No	Yes (PEV)
[48]	SGP (O)	Generation curtailment for DG units and load curtailment minimization	WT	HA	No	Yes (EV)
[49]	SGP (O)	OC of DDG unit, cost of import and export of energy, and cost of battery degradation due to vehicle-to-grid connection	WT, PV and DDG	SP	No	Yes (EV)
[50]	MGP (I+O)	IC and OMC of lines and DG units, cost of energy purchase from the grid, and cost of lost load	Not mentioned	MILP	No	No
[51]	MGP (I+O)	IC, OMC, and replacement cost of BESS and DG units, fault repairing cost of all equipment, and pollutant emission cost	WT, DE and PV	NSGA-II	No	Yes
[52]	MGP (I+O)	IC of BESS and OC of MG (fuel cost, start-up and shutdown costs of units, and cost of energy purchase)	WT and thermal	MIP	No	Yes
[53]	MGP (I)	IC of DG units, OC of MG, and reliability cost	WT, PV, FC and GT	MIP	No	Yes
[54]	MGP (I+O)	IC, OMC and replacement cost of components, cost of lost load, and cost of purchased energy from the grid, and cost of energy sale to the grid	WT, PV and FC	PSO	No	Yes
[55]	MGP (I)	IC and OMC of DG units, cost of energy sale, and cost of purchased energy from the grid	WT, MT and PV	MIP	No	No
[56]	MGP (I)	IC and OMC of ESS and DG units and interruption cost	WT and DE	SP	No	Yes
[57]	MGP (I+O)	Revenue from electrical and thermal energy sale, IC and OMC of ESS and DG units, cost of energy exchange with the grid, and emission cost	WT, PV, DE, MT and FC	PSO	No	Yes

[58]	MGP (O)	Energy losses, load and generation balance within MG, and MG self-adequacy	WT, PV and BM	TS and Graph theory	No	Yes
[59]	MGP (O)	MC of ESS, OC of DG units, and cost of energy exchange	Renewable source, MT, DE and FC	ASOA	No	Yes
[60]	MGP (O)	Cost of energy purchase from the grid	WT and PV	DP and Gauss-Seidel	No	Yes
[61]	MGP (O)	Cost of energy purchase from the grid, OC of DG units, cost of peak loading, emission cost, and cost of non-delivered energy	WT, PV and DE	MINLP	No	No
[62]	MGP (O)	OC of DG units, cost of storing energy and energy purchase from the grid, customer dissatisfaction, and power loss	WT, PV and DE	PCPMA	No	Yes
[63]	MGP (O)	Generation-load balance and ESS capacity sharing	Not mentioned	IP and graph theory	No	Yes
[64]	MGP (O)	Start-up cost of DG units, OMC of DG units and BESS, cost of energy sale/purchase from the grid, and cost of load curtailment	PV and FC	MILP	No	Yes
[65]	MGP (O)	Power loss, cost of energy purchase from the grid, and cost of energy supplied by DG units	Convention -al DG	SDP	No	No
[66]	MGP (O)	IC and OMC of BESS and DG units, OC of MG, and cost of energy purchase and sale to the grid	PV, FC and BM	Cultural algorithm	No	Yes
[67]	MGP (O)	Cost of energy purchase from the grid, cost of EVs charging, and cost of degradation of battery	WT	SAICA	No	Yes
[68]	MGP (I+O)	Power procurement cost, OC of battery, and IC of DG units	WT and PV	MIP and convex optimizat -ion	No	Yes
[69]	MGP (I+O)	IC and OC of DG units and ESS, cost of unserved energy, and cost of energy purchase/sale to the grid	WT, PV and DDG	LP	No	Yes

1.3 Motivation behind this thesis

The conventional distribution networks suffer from poor energy efficiency and lower bus voltage magnitude due to the high R/X ratio of distribution line. The DG integration can improve the energy efficiency and bus voltage of a network. It is one of the solutions to meet increasing load growth with uninterrupted power supply to the consumers. The shortage of power generation during peak load demand hours is a common problem for the developing nations, such as India. This results in load curtailment. To avoid this, the energy generated by renewable sources, such as PV units can be stored in storage units so as to utilize during peak load demand hours. In the coming years, it is also expected that the installation capacity of rooftop PV will rapidly grow due to the need of clean/carbon free energy source. The general tendency of rooftop PV owner is to inject the surplus PV generation into the distribution networks. But, the injection of large PV generation may increase power/energy loss, create over voltage problem, and deteriorate PQ in distribution

networks. Thus, the determination of total amount of PV capacity that a network can accommodate without deteriorating its operational performance is a matter of interest. This is called PV hosting capacity (PVHC) of a network. There are several ways to improve the PVHC of a network, in which, reactive power compensation is one of them. The use of non-linear loads in distribution networks increases harmonics. The excessive harmonics in line current may result in mal-operation of the sensitive equipment, additional network losses etc. The single line to ground fault and the presence of arc furnaces cause voltage sag, which may create operational problem for some of the sensitive loads, such as adjustable speed drives, certain medical equipment, data processing centers etc. This results in production loss for the process industries, loss of data for the data processing centers etc. Hence, an appropriate measure should be taken to ensure a desired PQ level to all the customers. The installation of the custom power devices [70] can be one of the approaches. The custom power devices are power electronics-based devices, which can provide reactive power compensation to a distribution network in addition to the mitigation of PQ issues. Thus, the allocation of any combination of the custom power devices, DG unit, and storage unit can solve many of the above-mentioned issues for radial distribution networks.

In view of the above mentioned issues, the following research gaps are identified:

- Unified power quality conditioner (UPQC) is a versatile custom power device used in PQ mitigation of distribution networks. In UPQC, two inverters, i.e., series and shunt inverters are usually placed in same location and they share a common dc-link. A new open UPQC (UPQC-O) topology is reported in [71], in which the series and shunt inverters can be placed in different locations of a network, unlike connected UPQC topology, and they do not share common dc-link. The reactive power compensation capability of connected UPQC topology for the improvement of energy efficiency of distribution networks is investigated in [72-75]. However, the optimal placement of UPQC-O with and without active power injection in distribution networks and a study to assess its ability to enhance energy efficiency and PQ of distribution networks have not been investigated.
- As mentioned above, the optimal placement of DG in the distribution networks has several advantages. The optimal allocation of custom power devices, such as UPQC-O

can also improve energy efficiency and PQ of distribution networks. Thus, the allocation of custom power device connected with DG can be a solution to many of the above-mentioned problems. Thus, there is a need of development of UPQC-O model with DG and its optimal allocation strategy to distribution networks so as to improve the energy efficiency and PQ.

- The network power/energy loss is one of the parameters of distribution network which greatly varies with the injection of PV generation into a network. But, none of the works considers the power loss as a constraint in defining the PVHC of distribution networks. Although the maximization of PVHC and minimization of energy loss are two conflicting objectives, none of the works has considered the simultaneous optimization of these two. The optimal allocation of series and shunt inverters of UPQC-O for the improvements of PVHC, energy efficiency, and PQ of distribution networks has not been studied.
- The active power compensation capability of PV-BESS integrated UPQC-O (PV-BESS-UPQC-O) for the peak load shaving of distribution networks has not been investigated.
- The time varying reactive power (VAr) compensation capability of UPQC-O for energy loss minimization in distribution networks during time varying load and PV generation variations has not been investigated. Thus, there is need of operational optimization approach for setting the optimal VAr set point for UPQC-O in each load and PV generation scenario for the energy loss minimization of distribution networks.

These research gaps are the motivations behind the present work.

1.4 Organization of this thesis

This thesis is organized as follows:

- In Chapter-2, the modelling of UPQC-O without and with active power injection is formulated for distribution networks. The PSO-based planning approach is used for the optimal allocation of these UPQC-O models in distribution networks for energy efficiency and PQ improvement. A new technical constraint, named as percentage of

voltage sag mitigated load (PVSML), is proposed to include the voltage sag mitigation criteria in the planning problem. The performances of UPQC-O models without and with active power injection are compared with the UPQC models without and with active power injection to assess their potential in enhancing the energy efficiency and PQ of distribution networks. The charging schemes for the battery connected to the UPQC models are also discussed in this chapter.

- In Chapter-3, the modelling and allocation planning of UPQC-O integrated PV generation system are provided to improve the energy efficiency and PQ of distribution networks. The two UPQC-O models with PV array are formulated in this chapter. The relative merits and demerits for the deployment of these UPQC-O models are highlighted. The performance comparison of proposed approach with other similar approaches of power/energy loss minimization is also provided.
- In Chapter-4, mono- and multi-objective planning approaches are proposed to improve the PVHC and energy efficiency of distribution networks with the optimal allocation of inverters of UPQC-O. In mono-objective planning, PVHC is maximized considering the network power loss as a technical constraint to determine the maximum integration of PV capacity in each load bus and locations of the inverters of UPQC-O for reactive power compensation. The modelling of inverters of UPQC-O is also formulated. The effect of placement of single series/shunt inverter on PVHC is also provided. The performance of the proposed mono-objective planning approach of maximization of PVHC is qualitatively compared with the other approaches of maximization of PVHC. In multi-objective planning, PVHC and energy loss of distribution network are simultaneously optimized. Multi-objective PSO (MOPSO) based optimal allocation strategy for the inverters of UPQC-O is developed.
- In Chapter-5, a multi-objective planning approach is provided for the optimal allocation of PV-BESS integrated UPQC-O for peak load shaving of radial distribution networks. The performance of proposed approach of peak load shaving is qualitatively compared with other similar approaches.
- In Chapter-6, an operational optimization approach for the determination of time varying VAr injection set points of UPQC-O with time varying load demand and PV generation is proposed to minimize the energy loss in distribution networks. An

appropriate solution strategy is devised for this approach. The infrastructure required for the real-time implementation of the proposed methodology, impact of load growth on the VAr set points of UPQC-O, and the cost-benefit analysis with single and multi-point compensations are also provided.

- In Chapter-7, the conclusion of the whole work is presented along with some future directions of the research in this area.

The Appendix of this thesis provides the simulation data for the 33-bus and 69-bus radial distribution networks, and time varying load demand and PV generation.

1.5 Contributions of this thesis

The main contributions of this thesis are summarized below:

- Development of UPQC-O models without and with active power injection to improve energy efficiency and PQ of radial distribution networks.
- Formulation of planning problem to optimally allocate UPQC-O-integrated PV generation system to improve energy efficiency and PQ of radial distribution networks.
- Development of mono- and multi-objective planning approaches to improve PVHC and energy efficiency of radial distribution networks with the UPQC-O placement.
- Development of multi-objective planning approach to optimally allocate the PV-BESS integrated UPQC-O for peak load shaving of radial distribution networks.
- Development of an online operational optimization approach for UPQC-O to minimize the energy loss in radial distribution networks during time varying load demand and PV generation.

In this thesis, the following performance indices are considered to analyze the performance of distribution networks:

- *Energy loss/power loss*: In Chapter 2, the network power loss of peak hour and off-peak hour load levels are used to compute the daily energy loss. In Chapters-3 and 4, three load-generation scenarios: peak load with no PV generation, off-peak load with no PV

generation, and off-peak load with PV generation are considered to compute the daily energy loss. In Chapter-5, total power loss during peak load hour which includes the line losses, series transformer loss, and inverter losses is used for performance evaluation. In Chapter-6, hourly energy loss is computed considering the hourly variations of load and/or PV generation.

- *Minimum bus voltage magnitude*: The load-generation scenarios used for the computation of energy loss/power loss are also considered for the determination of minimum bus voltage magnitude of distribution networks.
- *Voltage sag mitigation and current harmonics elimination*: In this thesis, the supply voltage sag and current harmonics are considered as the PQ issues. In all the planning models, a fixed percentage of sag in supply voltage (i.e., 30%) and current harmonics in line current (i.e., 20%) is mitigated by the UPQC-O.
- *PVHC*: It is computed considering the worst-case scenario, i.e., minimum load demand (i.e., 20% of peak load) and maximum PV generation in each bus of the network except substation bus.
- *Peak load shaving*: It is defined as the percentage of total peak load to be supplied by the PV-BESS integrated UPQC-O during peak load hours.

2

A Comparative Study among UPQC Models with and without Active Power Injection to Improve Energy Efficiency of Radial Distribution Networks

2.1 Introduction

The energy efficiency and PQ are two important aspects to any power distribution systems planner. The high resistance to reactance ratio of distribution line and the increasing use of non-linear loads lead to poor energy efficiency and deterioration of PQ, respectively. Hence, to maintain the standard of electricity, utilities have to look into both these issues together. The development of the custom power devices [70] can facilitate to achieve this. The custom power devices are the power electronic-based devices, which are used to provide reactive power compensation and to mitigate the PQ problems such as voltage sag/ swell, harmonics etc. UPQC is a type of custom power device which can provide both series and shunt compensations by using series and shunt inverters, respectively. The proper allocation of this device can ensure a specified PQ level and can significantly reduce the network power loss [72-75]. A state-of-art review on UPQC can be found in [76]. In UPQC connected topology, its two inverters are connected back-to-back to a DC link [77].

Based on research reported on UPQC, various UPQC models are found, in which some are developed based on different types of series compensation [76], for example UPQC-P, UPQC-Q, UPQC-S etc. In UPQC-P and UPQC-Q, a series voltage is injected in phase and in quadrature with the bus voltage, respectively to mitigate the voltage sag. A performance comparison between these two models is reported in [78]. In UPQC- S, series voltage is injected in such a way that it can provide both active and reactive power compensations [79]. Some UPQC models are based on minimization of VA-rating, for example UPQC-VAmin [80]. Some works are reported on the development of different UPQC inverter topologies, such as, 3-phase 4-wire structure [81], interline UPQC [82], in which two inverters are placed in different feeders of a network, OPEN UPQC [71], in which the series and shunt inverters are not connected to a common DC link etc. In [83], a new topology of UPQC based on current sourced converters is developed, in which shunt inverter is placed on the left side of series inverter and these two inverters share a common DC reactor for the power exchange. In some of these works, different control schemes for UPQC are developed, for example phase angle control (PAC) [84], simultaneous voltage and current compensation scheme [85], design of a feedback controller using PSO [86] etc. In [87], the impact of fixed and variable PAC approaches on the VA loadings of series and shunt inverters of UPQC are studied under voltage sag and swell conditions. In [88-89], variable PAC based method is used to determine the optimal size of UPQC. In [88], the size of series inverter, shunt inverter, and series transformer are determined. However, in [89], only the sizes of the series and shunt inverters are determined. In [90], a control scheme is designed for the series and shunt inverters of UPQC to mitigate various types of PQ issues, such as, voltage sag, unbalance, distortions, load current harmonics etc. The proportional resonant controller is used to control the series inverter and proportional integral (PI) controller and three vector PI controller are used to control the shunt inverter. In [91], a control scheme is developed for UPQC to reduce the reactive power circulation between the inverters and overloading on UPQC due to unbalanced load. In [92], UPQC cost minimization is considered to be the objective function. In [93-94], the UPQC model with distributed generation is reported. In [95], the PV integrated UPQC is designed and the simulation and experimental results are provided by varying the load unbalancing, voltage sags/swells,

and solar irradiation. The shunt inverter is used to extract the power from PV and to compensate the load harmonics and the series inverter is used to mitigate grid side voltage sags/swells.

In most of the above mentioned works, UPQC is used to protect single load, i.e., most sensitive load of the network from PQ problems. But, there might be a number of equally sensitive loads in a distribution network. The potential of UPQC in improving energy efficiency of a distribution network is not fully explored, except the works [72-75]. In [72], a study to determine the impact of the placement of UPQC on network power loss, line loadability, and voltage stability is reported. In [73], a multi-objective optimization-based planning approach is adopted to find the optimal location(s) and size(s) for UPQC in distribution networks. In [74], PSO is used to determine the optimal location, size, amount of VAr compensation required at the location, and ratio of series voltage injected to the desired voltage by minimizing the power loss and voltage drop in the network. In [74], the optimal location and size of UPQC are determined by minimizing the cost of UPQC, cost of energy loss, and cost of load interrupted due to the voltage sag. These works [72-75] show that an UPQC placed at an appropriate location can be used to reduce the network power loss, to mitigate the voltage sag, to eliminate the harmonics, and to improve the bus voltages etc. Since the series inverter of UPQC protects downstream load from voltage sag, it can provide the protection to large number of load, if it is placed near the substation. But, it increases its VA-rating. Moreover, if the shunt inverter of UPQC is placed near the substation it may not result optimal power loss reduction [72]. Hence, a unique location for UPQC may not fulfil both the aspects. The concept of OPEN UPQC (UPQC-O) [71] has given the flexibility to place both series and shunt inverters at different locations. The recently reported works on UPQC-O can be found in [96-102]. But, these works are mostly focused on the design of control schemes for the series [96] and shunt inverters [97] for PQ improvement. In [98], a design approach is reported, in which VA-rating of UPQC-O, is determined to mitigate the voltage sag. In [99], UPQC-O is used with renewable generation to improve PQ. In [100], enhanced phase locked loop and non-linear adaptive filter-based control schemes are designed for

series and shunt inverters. In [101], the UPQC-O is designed, simulated, and implemented for the improvement of PQ of a real low voltage distribution network. In [102], a performance comparison is provided in between UPQC and UPQC-O by considering non-linear loads and different types of voltage sag. From the above mentioned literature, the motivating factors behind this work are given below.

- There is no work available in the literature, in which the modelling of UPQC-O with and without active power injection to improve energy efficiency and PQ of distribution networks is reported.
- There is no comparative study among the UPQC and UPQC-O models designed to improve energy efficiency and PQ of distribution networks.

To fill the above-mentioned research gaps, four different UPQC models are presented in this chapter. They are: (i) UPQC without active power injection (UPQC-WOP), (ii) UPQC with active power injection (UPQC-WP), (iii) UPQC-O without active power injection (UPQC-O-WOP), and (iv) UPQC-O with active power injection (UPQC-O-WP). The UPQC-WOP model is taken from [73] to provide comparative study with these models. In UPQC-O, the series and shunt inverters, placed in different locations in the network, are designed to communicate with each other so as to coordinate the VAr sharing among them. A planning optimization model is formulated to determine the optimal locations and ratings of the series and shunt inverters. The PSO algorithm is used to solve the planning model.

The work is demonstrated on a 69-bus and a 33-bus radial distribution networks.

2.2 UPQC and UPQC-O modelling without and with active power injection

To demonstrate the UPQC and UPQC-O models, a 6-bus radial distribution network is chosen, as shown in Figs. 2.1(a) and 2.1(b), respectively. The bus 1 is the substation bus and remaining buses are load buses. Both UPQC and UPQC-O consist of two voltage source inverters, i.e., series and shunt inverters. The series inverter injects series voltage to mitigate the supply voltage sag and the shunt inverter injects shunt compensating current to provide harmonic compensation and to inject reactive power into the network. In case of UPQC,

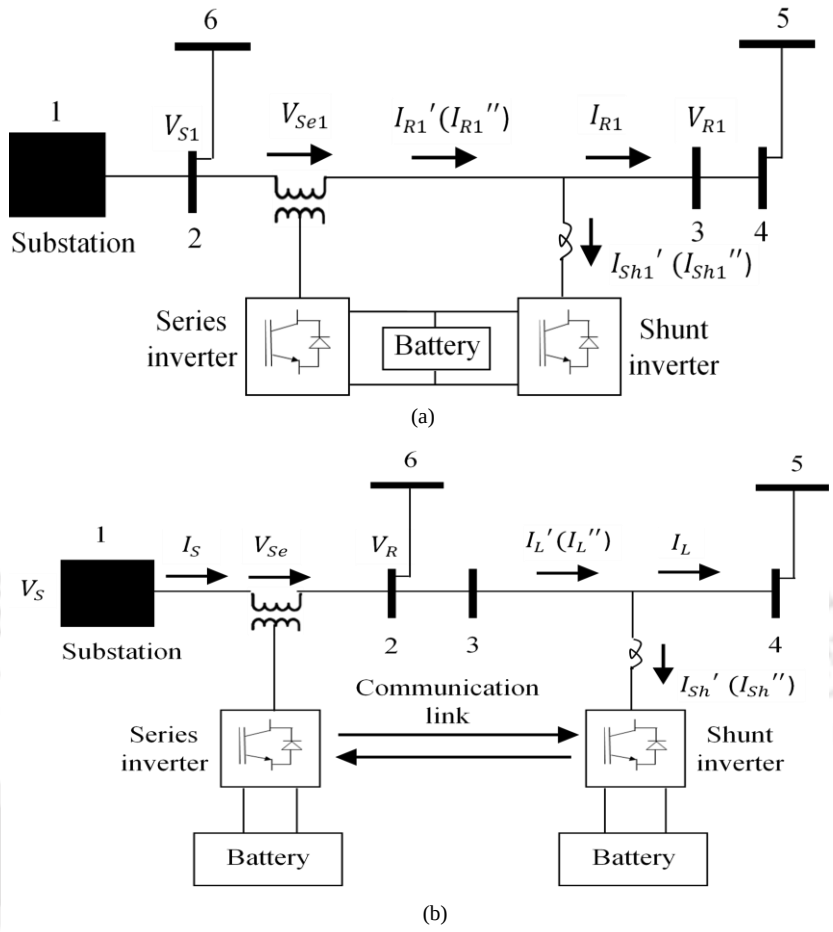

Fig. 2.1: A 6-bus radial distribution network with (a) UPQC (b) UPQC-O {symbols used in bracket are for the model with active power injection}

these two inverters are connected to a DC link and placed at the same location as shown in Fig. 2.1(a). But, in case of UPQC-O, these two inverters can be placed in different locations and these are connected via communication link to coordinate the VAr sharing. To do this, firstly, the total reactive power (Q_{Comp}) required in a network is decided. It is usually a fraction of the sum total of reactive power demand of the loads. Then, the amount of reactive power, that the series inverter could provide, is computed. Let, this amount be Q_{Se}. From these, the amount of reactive power required from the shunt inverter(s) is computed as,

$$Q_{Sh\_req} = Q_{Comp} - Q_{Se} \tag{2.1}$$

In case of multiple shunt inverters, Q_{Sh_req} is distributed among all the shunt inverters based on their reactive power support capacity. For example, the reactive power required from the n^{th} shunt inverter is set as:

$$Q_{Sh_n} = \frac{Q^c_{Sh_n}}{\sum_n Q^c_{Sh_n}} Q_{Sh\_req} \quad (2.2)$$

where, $Q^c_{Sh_n}$ is the maximum reactive power support capacity or rating of the n^{th} shunt inverter. If the reactive power required from the n^{th} shunt inverter unit (Q_{Sh_n}) is found to be greater than its rated VAr support capacity, i.e., $Q^c_{Sh_n}$, then $Q^c_{Sh_n}$ is set as its reactive power injection amount. The functions of series and shunt inverters during healthy and voltage sag conditions are summarized in Table 2.1.

Table 2.1: Function of series and shunt inverters for different UPQC models

UPQC models	Function of the series inverter		Function of the shunt inverter during voltage sag and healthy conditions
	Voltage sag condition	Healthy condition	
UPQC-WOP	Mitigates voltage sag	Reactive power injection	Reactive power injection and harmonic compensation
UPQC-WP	Mitigates voltage sag	Reactive power injection	Active and reactive power injections as well as harmonic compensation
UPQC-O-WOP	Mitigates voltage sag	Reactive power injection	Reactive power injection and harmonic compensation
UPQC-O-WP	Mitigates voltage sag	Reactive power injection	Active and reactive power injections as well as harmonic compensation

In case of UPQC-WOP, the active power circulates in between two inverters to maintain the DC link voltage constant [84]. With the appropriate size of battery, UPQC and UPQC-O both are capable of providing active power to the network. The battery rating requirements in different UPQC models are computed as:

- In UPQC-WP model, the battery connected to the DC link is designed such that it can provide active power during peak hour and can compensate inverter losses.
- In UPQC-O-WOP model, the battery connected to the series inverter is designed such that it can mitigate k % of voltage sag and can compensate inverter losses. The battery connected to the shunt inverter is also designed to compensate inverter losses.
- In UPQC-O-WP model, the design of battery connected to the series inverter is similar to the UPQC-O-WOP model. But, the battery connected to the shunt inverter is designed to inject active power during peak hour and to compensate inverter losses.

Hence, in this work, four different models are provided. They are:

- Model A: UPQC-WOP
- Model B: UPQC-WP
- Model C: UPQC-O-WOP
- Model D: UPQC-O-WP

The model of UPQC-WOP is taken from [73] and other three models are proposed in this work. It is to be noted that the current flowing through the shunt inverter would be equal to the phasor sum of the in-phase current supported by the battery and a quadrature component of the shunt compensation current if the battery is designed for active power injection, i.e., Models B and D. In other two models, the current flowing through the shunt inverter is in quadrature with the voltage to ensure only reactive power injection.

2.2.1 Model A: UPQC-WOP

The phasor diagram of UPQC-WOP is shown in Fig. 2.2. The detailed steady-state modelling of UPQC-WOP is found in [73]. In healthy condition, a fraction (K_{Se1}) of V_{R1} i.e, V_{Se1} is injected by the series inverter to maintain V_{R1} by shifting the receiving end voltage phase angle by δ_1. The amount of voltage sag (k) to be mitigated by the series inverter of UPQC is obtained as [73]:

$$k = K_{Se1}^2 \tag{2.3}$$

The receiving end voltage phase angle shift is obtained as [73]:

$$\delta_1 = \cos^{-1}(1 - 0.5\,K_{Se1}^2) \tag{2.4}$$

The maximum reactive power provided by the series inverter of UPQC-WOP is obtained as [73]:

$$Q_{Se1}^{\max\prime} = V_{R1} I'_{R1} \sin\delta_1 \tag{2.5}$$

The maximum reactive power required from shunt inverter is obtained by Eq. (2.6),

$$Q_{Sh1}^{\max\prime} = Q_{Comp} - Q_{Se1}^{\max\prime} \tag{2.6}$$

From Fig. 2.2., the series voltage injected by the series inverter is computed as:

$$\begin{aligned} V_{Se1} &= \sqrt{{V_{R1}}^2 + {V_{R1}}^2 - 2V_{R1}V_{R1}\cos\delta_1} \\ &= V_{R1}\sqrt{2(1-\cos\delta_1)} \end{aligned} \tag{2.7}$$

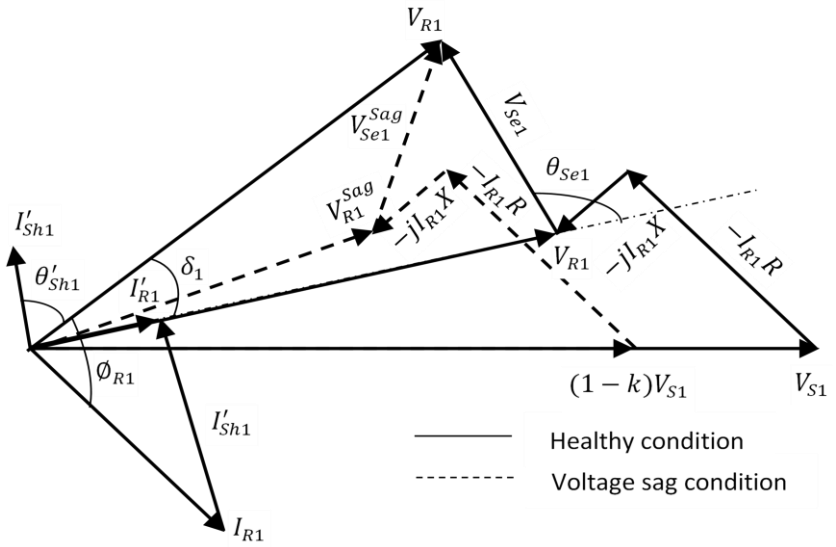

Fig. 2.2: Phasor diagram for Model A

For lossless UPQC-WOP, the active power drawn by the load will be equal to the active power supplied by the source, i.e.,

$$V_{R1}I'_{R1} = V_{R1}I_{R1}\cos\emptyset_{R1} \tag{2.8}$$

$$I'_{R1} = I_{R1}\cos\emptyset_{R1} \tag{2.9}$$

The VA-rating of series inverter of UPQC-WOP is computed as:

$$S_{Se1}^{WOP} = V_{Se1}I'_{R1} \tag{2.10}$$

The active and reactive power to be supplied by the series inverter of UPQC-WOP are computed as:

$$P_{Se1}^{WOP} = S_{Se1}^{WOP}\cos\theta_{Se1} \tag{2.11}$$

$$Q_{Se1}^{WOP} = S_{Se1}^{WOP}\sin\theta_{Se1} \tag{2.12}$$

The phase angle θ_{Se1} is computed as [73]:

$$\theta_{Se1} = 90° + \frac{\delta_1}{2} \tag{2.13}$$

From Fig. 2.2, the shunt compensating current to be provided by the shunt inverter is computed as:

$$I'_{Sh1} = \sqrt{{I_{R1}}^2 + {I'_{R1}}^2 - 2I_{R1}I'_{R1}\cos(\emptyset_{R1} - \delta_1)} \tag{2.14}$$

From Eqs. (2.9) and (2.14),

$$I'_{Sh1} = I_{R1}\sqrt{1 + \cos^2\emptyset_{R1} - 2\cos\emptyset_{R1}\cos(\emptyset_{R1} - \delta_1)} \tag{2.15}$$

In addition to the reactive power compensation, the UPQC-WOP provides harmonic compensation by eliminating the distortion components present in the line current. The distortion components of line current I_{R1}^{dis} is nullified by the distortion components of shunt compensating current $I_{Sh1}^{\prime dis}$, i.e.,

$$I_{R1}^{dis} = I_{Sh1}^{\prime dis} \tag{2.16}$$

From the definition of total harmonic distortion (THD), i.e,

$$THD = \frac{I^{dis}}{I^{fun}} \tag{2.17}$$

From Eqs. (2.16) and (2.17),

$$THD_L I_{R1}^{fun} = THD_{Sh} I_{Sh1}^{\prime fun} \tag{2.18}$$

From Eqs. (2.15) and (2.18),

$$THD_{Sh} = \frac{THD_L}{\sqrt{1+\cos^2 \emptyset_{R1} - 2\cos\emptyset_{R1}\cos(\emptyset_{R1}-\delta_1)}} \tag{2.19}$$

The RMS value of the shunt compensating current is computed as:

$$I_{Sh1}^{\prime RMS} = I_{Sh1}^{\prime fun}\sqrt{1+{THD_{Sh}}^2} \tag{2.20}$$

From Eqs. (2.19) and (2.20),

$$I_{Sh1}^{\prime RMS} = I_{R1}\sqrt{1+\cos^2\emptyset_{R1} - 2\cos\emptyset_{R1}\cos(\emptyset_{R1}-\delta_1) + {THD_L}^2} \tag{2.21}$$

The VA-rating of shunt inverter of UPQC-WOP is computed as:

$$S_{Sh1}^{WOP} = V_{R1} I_{Sh1}^{\prime RMS} \tag{2.22}$$

The active and reactive power supplied by the shunt inverter are computed as:

$$P_{Sh1}^{WOP} = V_{R1} I_{Sh1}^{\prime} \cos\theta_{Sh1}^{\prime} \tag{2.23}$$

$$Q_{Sh1}^{WOP} = V_{R1} I_{Sh1}^{\prime} \sin\theta_{Sh1}^{\prime} \tag{2.24}$$

The phase angle $\theta_{Sh1}^{\prime}$ is computed as [73]:

For $(\delta_1 > \emptyset_R)$, $\theta_{Sh1}^{\prime}$ is calculated as,

$$\theta_{Sh1}^{\prime} = \tan^{-1}\left[\frac{\cos(\delta_1-\emptyset_{R1})-\cos\emptyset_{R1}}{\sin(\delta_1-\emptyset_{R1})}\right] + 90° - \delta_1 \tag{2.25}$$

Otherwise,

$$\theta'_{Sh1} = \tan^{-1}\left[\frac{\cos(\emptyset_{R1}-\delta_1)-\cos\emptyset_{R1}}{\sin(\emptyset_{R1}-\delta_1)}\right]+90° - \delta_1 \quad (2.26)$$

If $Q_{Sh1}^{\max'}$ is found to be higher than Q_{Sh1}^{WOP} then $Q_{Sh1}^{\max'}$ is set to Q_{Sh1}^{WOP}.

The total VA-rating of UPQC-WOP is computed as [103-104]:

$$S_{UPQC}^{WOP} = S_{Sh1}^{WOP} + S_{Se1}^{WOP} \quad (2.27)$$

2.2.2 Model B: UPQC-WP

The phasor diagram of UPQC-WP is shown in Fig. 2.3. Here, a fraction (K_{Re}) of line current I_{R1} is to be supported by the battery to provide the active power compensation to the network. i.e.,

$$I_{Re1} = K_{Re} I_{R1} \quad (2.28)$$

The Eqs. (2.3) and (2.4) are also used in this model to find k and δ_1, respectively. The maximum reactive power supplied by the series inverter of UPQC-WP is obtained as:

$$Q_{Se1}^{\max''} = V_{R1} I''_{R1} \sin\delta_1 \quad (2.29)$$

The maximum reactive power required from the shunt inverter of UPQC-WP is obtained as:

$$Q_{Sh1}^{\max''} = Q_{Comp} - Q_{Se1}^{\max''} \quad (2.30)$$

By applying the active power balance equation,

$$I''_{R1} V_{R1} = V_{R1} I_{R1} \cos\emptyset_{R1} + V_{R1} I_{Re1} \quad (2.31)$$

The right hand side of Eq. (2.31) consists of two components. These are the active power drawn by the load buses and the active power to be injected through the shunt inverter. The left hand side of Eq. (2.31) shows total active power flowing from the preceding bus to the bus, at which UPQC is located.

From Eqs. (2.28) and (2.31),

$$I''_{R1} = I_{R1}(\cos\emptyset_{R1} + K_{Re}) \quad (2.32)$$

In UPQC-WP model, the series voltage supplied by the series inverter is equal to the V_{Se1} obtained for UPQC-WOP model. Thus, the VA-rating of series inverter of UPQC-WP can be computed as:

$$S_{Se1}^{WP} = V_{Se1} I''_{R1} \quad (2.33)$$

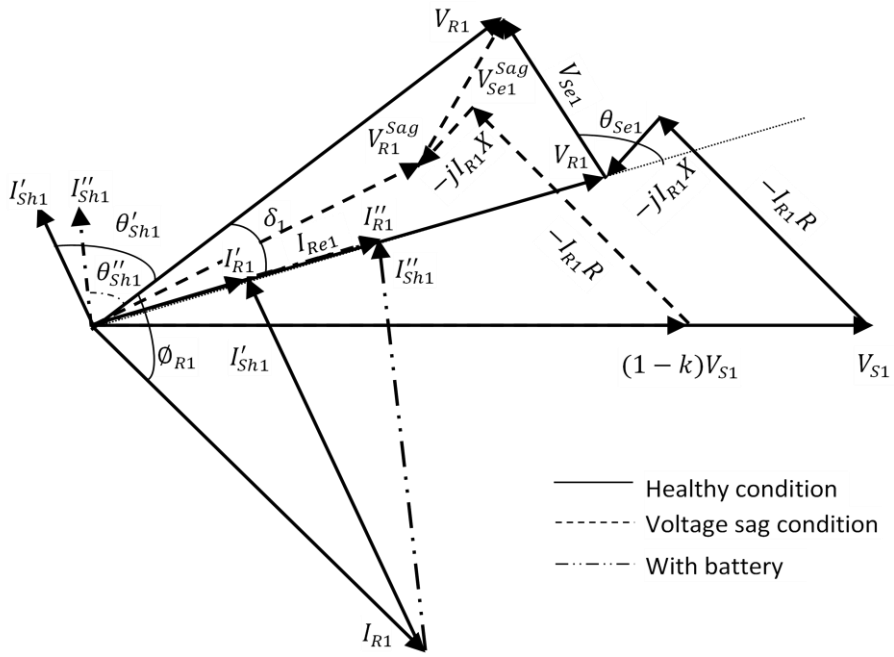

Fig. 2.3: Phasor diagram for Model B

The active and reactive power supplied by the series inverter of UPQC-WP are computed as:

$$P_{Se1}^{WP} = S_{Se1}^{WP}\cos\theta_{Se1} \tag{2.34}$$

$$Q_{Se1}^{WP} = S_{Se1}^{WP}\sin\theta_{Se1} \tag{2.35}$$

The phase angle θ_{Se1} can be computed by using Eq. (2.13).

From Fig. 2.3, the shunt compensating current provided by the shunt inverter of UPQC-WP is computed as:

$$I''_{Sh1} = \sqrt{{I''_{R1}}^2 + {I_{R1}}^2 - 2I''_{R1}I_{R1}\cos(\emptyset_{R1} - \delta_1)} \tag{2.36}$$

From Eqs. (2.32) and (2.36),

$$I''_{Sh1} = I_{R1}\sqrt{1 + (\cos\emptyset_{R1} + K_{Re})^2 - 2\,(\cos\emptyset_{R1} + K_{Re})\cos(\emptyset_{R1} - \delta_1)} \tag{2.37}$$

The RMS value of I''_{Sh1} can be computed by following the similar steps as followed for the computation of $I_{Sh1}^{'RMS}$ (*Refer section 2.2.1*).

$$I_{Sh1}^{''RMS} = I_{R1}\sqrt{1 + (\cos\emptyset_{R1} + K_{Re})^2 - 2\,(\cos\emptyset_{R1} + K_{Re})\cos(\emptyset_{R1} - \delta_1) + {THD_L}^2} \tag{2.38}$$

The VA-rating of shunt inverter of UPQC-WP is computed as:

$$S_{Sh1}^{WP} = V_{R1} I_{Sh1}^{''RMS} \tag{2.39}$$

The active and reactive power supplied by the shunt inverter of UPQC-WP are computed as:

$$P_{Sh1}^{WP} = V_{R1} I_{Sh1}'' \cos\theta_{Sh1}'' \tag{2.40}$$

$$Q_{Sh1}^{WP} = V_{R1} I_{Sh1}'' \sin\theta_{Sh1}'' \tag{2.41}$$

The expression for the computation of phase angle θ_{Sh1}'' can be derived by following the similar steps as used for the derivation of θ_{Sh1}' [84].

For $(\delta_1 > \emptyset_R)$, θ_{Sh1}'' is calculated as,

$$\theta_{Sh1}'' = \tan^{-1}\left[\frac{\cos(\delta_1 - \emptyset_{R1}) - \cos\emptyset_{R1} - K_{Re}}{\sin(\delta_1 - \emptyset_{R1})}\right] + 90° - \delta_1 \tag{2.42}$$

Otherwise,

$$\theta_{Sh1}'' = \tan^{-1}\left[\frac{\cos(\emptyset_{R1} - \delta_1) - \cos\emptyset_{R1} - K_{Re}}{\sin(\emptyset_{R1} - \delta_1)}\right] + 90° - \delta_1 \tag{2.43}$$

If $Q_{Sh1}^{\max''}$ is found to be higher than Q_{Sh1}^{WP} then $Q_{Sh1}^{\max''}$ is set to Q_{Sh1}^{WP}.

The total VA-rating of UPQC-WP is computed as:

$$S_{UPQC}^{WP} = S_{Sh1}^{WP} + S_{Se1}^{WP} \tag{2.44}$$

The rating/size of battery connected to the DC link of UPQC-WP is computed as:

$$PB_{UPQC}^{WP} = \frac{V_{R1} I_{Re1} t_1}{\eta_{INV}} + INVL_{Sh1_2}^{WP} t_2 + INVL_{Se1_2}^{WP} t_2 \tag{2.45}$$

The 1st part of Eq. (2.45) represents the battery rating required to provide active power compensation and to compensate inverter losses during peak load hours. The 2nd and 3rd parts of Eq. (2.45) represent the battery rating required to compensate the series and shunt inverter losses during off-peak hours, respectively.

2.2.3 Model C: UPQC-O-WOP

The phasor diagrams for the series and shunt inverters of UPQC-O-WOP are shown in Figs. 2.4(a) and 2.4(b), respectively. In this case, phase angle between V_{Se}^{sag} and I_S is maintained at 90° to provide only reactive power to the network.

From Fig. 2.4(a),

$$V_R \cos\alpha'' = V_R^{Sag} \cos\alpha' + V_{Se}^{Sag} \sin\emptyset \quad (2.46)$$

$$V_R \sin\alpha'' = V_R^{Sag} \sin\alpha' + V_{Se}^{Sag} \cos\emptyset \quad (2.47)$$

From Eqs. (2.46) and (2.47),

$$V_R \cos(\alpha'' + \emptyset) = V_R^{Sag} \cos(\alpha' + \emptyset) \quad (2.48)$$

From Eq. (2.48), α'' can be found as:

$$\alpha'' = \cos^{-1}\left\{\frac{V_R^{Sag}}{V_R}\cos(\alpha' + \emptyset)\right\} - \emptyset \quad (2.49)$$

From Fig. 2.4(a), the series voltage (V_{Se}^{Sag}) injected by the series inverter of UPQC-O-WOP is obtained as:

$$V_{Se}^{Sag} = \sqrt{{V_R}^2 + (V_R^{Sag})^2 - 2V_R V_R^{Sag} \cos(\alpha'' - \alpha')} \quad (2.50)$$

The same magnitude of series voltage, as injected during voltage sag condition, is also injected ($V_{Se}^{Hel} = V_{Se}^{Sag}$) in the healthy condition to provide the reactive power to the network. Thus, the VA-rating of series inverter of UPQC-O-WOP is computed as:

$$S_{Se}^{WOP} = V_{Se}^{Hel} I_S \quad (2.51)$$

The reactive power supplied by the series inverter of UPQC-O-WOP is equal to the S_{Se}^{WOP}. i.e.,

$$Q_{Se}^{WOP} = S_{Se}^{WOP} \quad (2.52)$$

Using the communication link, the series inverter sends the information of the amount of its VAr sharing to the shunt inverter. Then, the VAr sharing of the shunt inverter is computed as:

$$Q_{Sh\_req}^{WOP} = Q_{Comp} - Q_{Se}^{WOP} \quad (2.53)$$

The rating of battery connected to the DC link of series inverter of UPQC-O-WOP is computed as:

$$PB_{Se}^{WOP} = \frac{kt_{Sag} \sum_{i\epsilon\partial} P(i)}{3600} + \sum_{d\epsilon[1,2]} INVL_{Se_d}^{WOP} t_d \quad (2.54)$$

where, ∂ is the set of all downstream buses which are beyond the point of connection of series inverter.

From Fig. 2.4(b), the shunt compensating current provided by the shunt inverter of UPQC-O-WOP is computed as:

$$I'_{Sh} = I_L \sin\emptyset_L \quad (2.55)$$

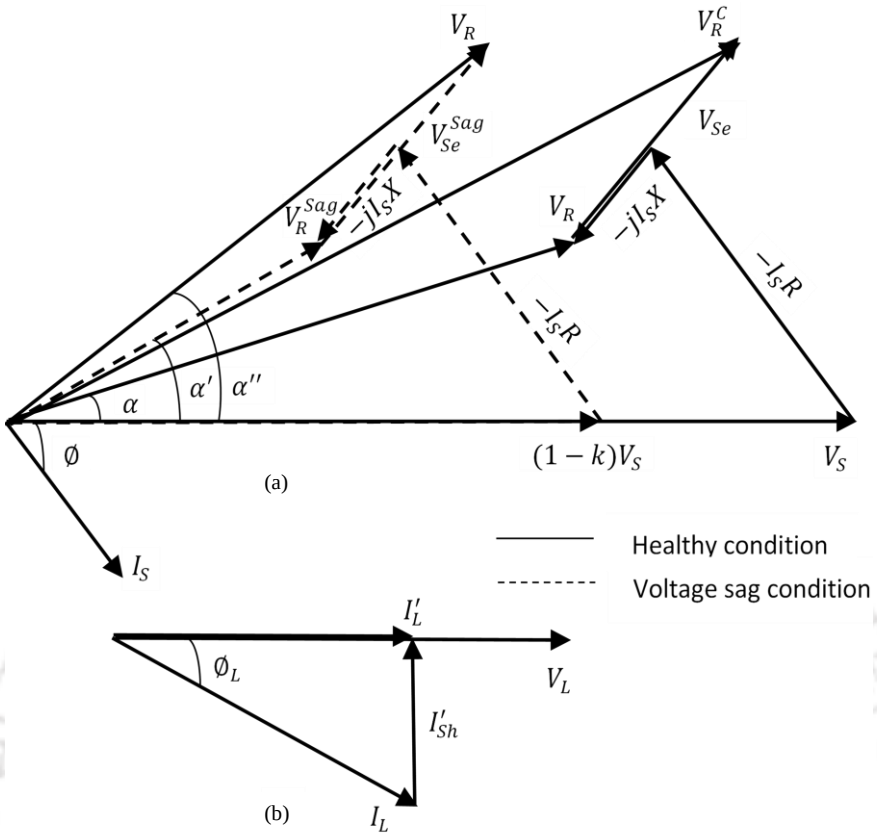

Fig. 2.4: Phasor diagrams for Model C (a) series inverter (b) shunt inverter

The RMS value of I_{Sh}' can be computed by following the similar steps as followed for the computation of $I_{Sh1}^{'RMS}$ (*Refer section 2.2.1*).

$$I_{Sh}^{'RMS} = I_L\sqrt{\sin^2\emptyset_L + {THD_L}^2} \tag{2.56}$$

The VA-rating of shunt inverter of UPQC-O-WOP is computed as:

$$S_{Sh}^{WOP} = V_L I_{Sh}^{'RMS} \tag{2.57}$$

The reactive power supplied by the shunt inverter of UPQC-O-WOP is computed as:

$$Q_{Sh}^{WOP} = V_L I_{Sh}' \tag{2.58}$$

If $Q_{Sh\_req}^{WOP}$ is found to be higher than Q_{Sh}^{WOP} then $Q_{Sh\_req}^{WOP}$ is set to Q_{Sh}^{WOP}.

The rating of battery connected to the DC link of shunt inverter of UPQC-O-WOP is computed as:

$$PB_{Sh}^{WOP} = \sum_{d\epsilon[1,2]} INVL_{Sh_d}^{WOP} t_d \tag{2.59}$$

The total VA-rating of UPQC-O-WOP is computed as:

$$S_{UPQC-O}^{WOP} = S_{Se}^{WOP} + S_{Sh}^{WOP} \tag{2.60}$$

The total rating of battery connected to the UPQC-O-WOP is computed as:

$$PB_{UPQC-O}^{WOP} = PB_{Se}^{WOP} + PB_{Sh}^{WOP} \quad (2.61)$$

2.2.4 Model D: UPQC-O-WP

The phasor diagrams of the shunt inverter is shown in Fig. 2.5. In this model, the phasor diagram of the series inverter is same as shown in Fig. 2.4(a). Thus, the VA-rating of series inverter (S_{Se}^{WP}), reactive power supplied by the series inverter (Q_{Se}^{WP}), and the rating of battery connected to the DC link of series inverter (PB_{Se}^{WP}) are same as that of the S_{Se}^{WOP}, Q_{Se}^{WOP}, and PB_{Se}^{WOP}, respectively. Hence, the reactive power required from the shunt inverter is obtained as:

$$Q_{Sh\_req}^{WP} = Q_{Comp} - Q_{Se}^{WP} \quad (2.62)$$

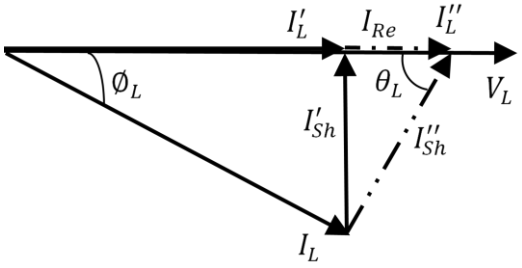

Fig. 2.5: Phasor diagram for shunt inverter of Model D

Here, the battery connected to the shunt inverter supports a fraction (K_{Re}) of line current I_L to provide the active power compensation to the network. i.e.,

$$I_{Re} = K_{Re} I_L \quad (2.63)$$

For lossless UPQC-O-WP,

$$V_L I_L'' = V_L I_L \cos \emptyset_L + V_L I_{Re} \quad (2.64)$$

From Eqs. (2.63) and (2.64),

$$I_L'' = I_L (\cos \emptyset_L + K_{Re}) \quad (2.65)$$

From Fig. 2.5, the shunt compensating current provided by the shunt inverter of UPQC-O-WP is computed as:

$$I_{Sh}'' = \sqrt{I_L''^2 + I_L^2 - 2 I_L'' I_L \cos \emptyset_L} \quad (2.66)$$

From Eqs. (2.65) and (2.66),

$$I''_{Sh} = I_L\sqrt{1 + (\cos\emptyset_L + K_{Re})^2 - 2\cos\emptyset_L\,(\cos\emptyset_L + K_{Re})} \quad (2.67)$$

The RMS value of I''_{Sh} can be computed by following the similar steps as followed for the computation of I'^{RMS}_{Sh1} (*Refer section 2.2.1*).

$$I''^{RMS}_{Sh} = I_L\sqrt{1 + (\cos\emptyset_L + K_{Re})^2 - 2\cos\emptyset_L\,(\cos\emptyset_L + K_{Re}) + THD_L{}^2} \quad (2.68)$$

The VA-rating of shunt inverter of UPQC-O-WP is computed as:

$$S^{WP}_{Sh} = V_L I''^{RMS}_{Sh} \quad (2.69)$$

The active and reactive power supplied by the shunt inverter are computed as:

$$P^{WP}_{Sh} = V_L I''_{Sh}\cos\theta_L \quad (2.70)$$

$$Q^{WP}_{Sh} = V_L I''_{Sh}\sin\theta_L \quad (2.71)$$

If $Q^{WP}_{Sh\_req}$ is found to be higher than Q^{WP}_{Sh} then $Q^{WP}_{Sh\_req}$ is set to Q^{WP}_{Sh}.

The rating of battery connected to the DC link of shunt inverter of UPQC-O-WP is computed as:

$$PB^{WP}_{Sh} = \frac{V_L I_{Re} t_1}{\eta_{INV}} + INVL^{WP}_{Sh_2} t_2 \quad (2.72)$$

The total VA-rating of UPQC-O-WP is computed as:

$$S^{WP}_{UPQC-O} = S^{WP}_{Sh} + S^{WP}_{Se} \quad (2.73)$$

The total rating of battery connected to the UPQC-O-WP is computed as:

$$PB^{WP}_{UPQC-O} = PB^{WP}_{Se} + PB^{WP}_{Sh} \quad (2.74)$$

2.3 Incorporation of UPQC/UPQC-O models into radial distribution network load flow

The load flow analysis is essentially required in finding out the operating condition/parameter of a power network, such as bus voltage, line current, line losses etc. It helps in solving the power system operation and planning problems. The conventional load flow approaches, such as, Newton Raphson, Gauss-Seidal etc., often fail to converge in distribution system power flow analysis due to the high resistance to reactance ratio of distribution line and radial topology of distribution networks [105]. Thus, the forward-backward sweep load flow (FBSLF) [106], a simple but efficient algorithm, is used to determine the voltage in each bus of a distribution network. The FBSLF algorithm and the incorporation of UPQC/UPQC-O models into FBSLF algorithm are described in subsequent subsections.

2.3.1 FBSLF algorithm

It is an iterative algorithm, in which Kirchhoff's current and voltage laws are used to determine the line current and bus voltage, respectively. The voltage in each bus in the first iteration is assumed to be $1\angle 0^o$p.u. The algorithm consists of two steps as described below.

- *Backward sweep*: In this step, line current is calculated using load currents. The load current of any bus m is calculated as:

$$\bar{I}(m) = \frac{P(m)-jQ(m)}{\bar{V}^*(m)}, \qquad m \in [2, \dots, N] \tag{2.75}$$

The line current of line 'mn' is calculated as:

$$\bar{I}(mn) = \bar{I}(n) + \sum_{i\in \aleph} \bar{I}(i), \qquad mn \in [1, \dots, N-1] \tag{2.76}$$

where, $\aleph$ is the set of all downstream buses which are beyond the bus 'n'.

- *Forward sweep:* In this step, bus voltages are determined by using Eq.(2.77)

$$\bar{V}(n) = \bar{V}(m) - \bar{I}(mn)Z(mn), \qquad mn \in [1, \dots, N-1] \tag{2.77}$$

where, 'm' and 'n' represent the sending and receiving end of the line 'mn', $\bar{I}(mn)$ and $Z(mn)$ are the line current and the line impedance of the line 'mn'.

2.3.2 Incorporation of UPQC/UPQC-O models into FBSLF algorithm

In this work, UPQC and UPQC-O models are incorporated into FBSLF algorithm to determine the network bus voltages, line current flows, and power loss. The incorporation of series and shunt inverters models of UPQC-WOP at bus 'i' modifies the voltage of bus 'i' and reactive power demand of bus 'i', respectively. i.e.,

$$\bar{V}(i) = V_{DR}\angle(\beth_i + \delta_1) \tag{2.78}$$

$$Q'(i) = Q(i) - Q_{Sh1}^{\max\prime} \tag{2.79}$$

where, $\beth_i$ is the phase angle of the voltage at bus 'i' before placement of UPQC-WOP and V_{DR} is the desired voltage magnitude at bus 'i'.

The incorporation of series inverter model of UPQC-WP at bus 'i' modifies the voltage of bus 'i' as shown in Eq. (2.78), because, the series inverter of UPQC-WP is also designed to provide only reactive power compensation to the network. However, the incorporation of shunt inverter model of UPQC-WP at bus 'i' modifies the active and reactive power demands of bus 'i' as shown in Eqs. (2.80) and (2.81), respectively.

$$P'(i) = P(i) - P_{Sh1}^{WP} \quad (2.80)$$

$$Q'(i) = Q(i) - Q_{Sh1}^{\max''} \quad (2.81)$$

After incorporation of series and shunt inverters models of UPQC-O-WOP at buses j_1 and j_2, respectively, the reactive power demand of corresponding buses are modified as:

$$Q'(j_1) = Q(j_1) - Q_{Se}^{WOP} \quad (2.82)$$

$$Q'(j_2) = Q(j_2) - Q_{Sh\_req}^{WOP} \quad (2.83)$$

After incorporation of series and shunt inverters models of UPQC-O-WP at buses j_1 and j_2, respectively, the active and reactive power demands of corresponding buses are modified as:

$$Q'(j_1) = Q(j_1) - Q_{Se}^{WP} \quad (2.84)$$

$$P'(j_2) = P(j_2) - P_{Sh}^{WP} \quad (2.85)$$

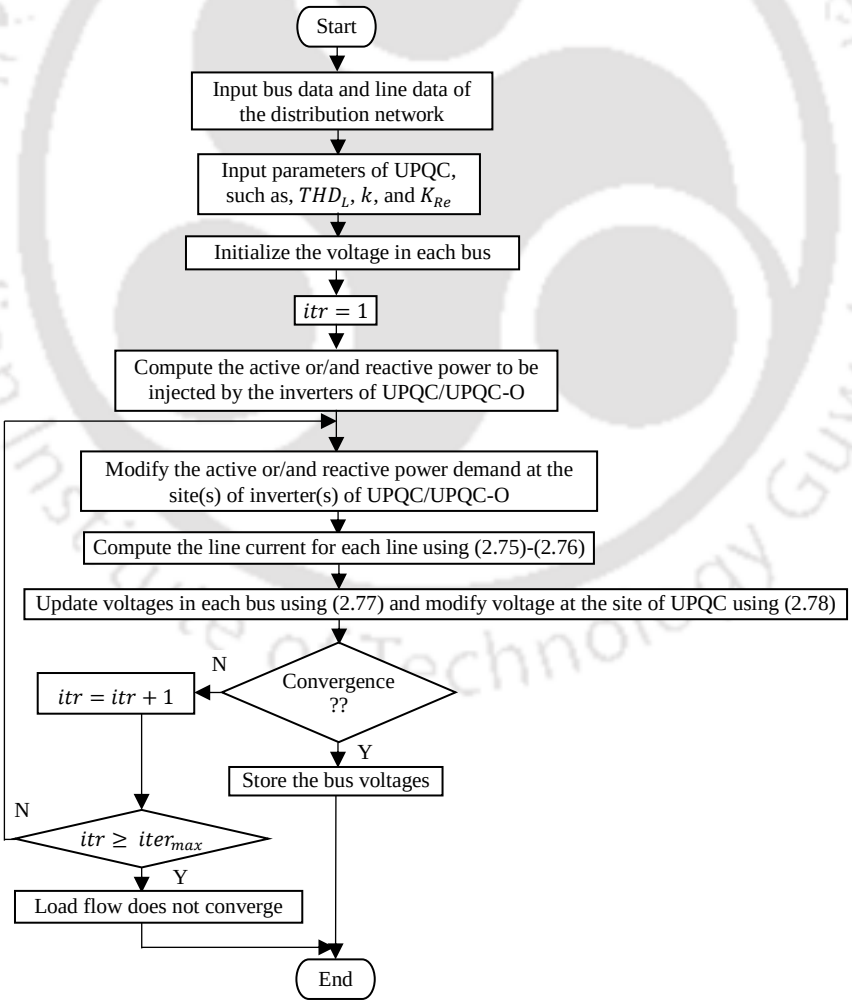

Fig. 2.6: FBSLF algorithm incorporating UPQC/UPQC-O models

$$Q'(j_2) = Q(j_2) - Q_{Sh\_req}^{WP} \tag{2.86}$$

The FBSLF algorithm is performed with the revised/modified power demand. The bus voltage is modified in forward sweep of FBSLF algorithm. Flow-chart for FBSLF algorithm with UPQC/UPQC-O model is shown in Fig. 2.6.

2.4 Planning model for the allocation of UPQC/UPQC-O in distribution network

This section describes the planning model for the allocation of UPQC/UPQC-O. The placement of UPQC/UPQC-O mitigates some of the PQ issues, such as voltage sag, current harmonics and it also provides the active and reactive power compensations to the network. However, the placement of UPQC/UPQC-O needs considerable investment by the distribution network owners. Thus, a planning optimization problem is formulated to determine the optimal locations and sizes of the inverters in a distribution network. The active power compensation to be provided by the UPQC/UPQC-O depends on the value of K_{Re}.Thus, in this optimization problem, locations for the series and shunt inverters, and K_{Re} are considered to be the optimizing variables. The objective function formulated as the minimization of the investment costs of series and shunt inverters of UPQC/UPQC-O, investment, operation, and maintenance costs for the battery, and the cost of energy loss of the network with UPQC/UPQC-O. Since the integration of UPQC/UPQC-O in a distribution network affects the network parameters, such as, voltage, current, line losses etc., the objective function is minimized under certain technical constraints. The mathematical formulation of the objective function is given in Eq. (2.87).

$$\begin{aligned} OF = {} & \textstyle\sum_{m\epsilon[2,\dots,N]}(C_m^{Se}\, S_m^{Se} + C_I^B PB_m^{Se})x_m + \sum_{m\epsilon[2,\dots,N]}(C_{O\&M}^B \frac{PB_m^{Se}}{t_b})T^h D^f x_m + \\ & 365C^E T^h D^f \textstyle\sum_{m\epsilon[2,\dots,N]}(\sum_{d\epsilon[1,2]} TFL_{md}^{Se} t_d\,)x_m + \\ & 365C^E T^h D^f \textstyle\sum_{m\epsilon[2,\dots,N]}(\sum_{d\epsilon[1,2]} INVL_{md}^{Se} t_d)x_m + \sum_{n\epsilon[2,\dots,N]}(C_n^{Sh}\, S_n^{Sh} + \\ & C_I^B PB_n^{Sh})x_n + \textstyle\sum_{n\epsilon[2,\dots,N]}(C_{O\&M}^B \frac{PB_n^{Sh}}{t_b})T^h D^f x_n + \\ & 365C^E T^h D^f \textstyle\sum_{n\epsilon[2,\dots,N]}(\sum_{d\epsilon[1,2]} INVL_{nd}^{Sh} t_d)x_n + \\ & 365C^E T^h D^f \textstyle\sum_{d\epsilon[1,2]} PL_d t_d \end{aligned} \tag{2.87}$$

The overall cost of energy loss includes the cost of line losses, inverter losses, and transformer loss. This study includes the cost of transformer losses, because the series inverter of UPQC/UPQC-O requires a transformer to connect with the distribution line. The investment cost of transformer is separately not included in the objective function, because the transformer cost is already included in the cost of UPQC/UPQC-O. The planning cost excludes the cost of communication interface for UPQC-O. The unit cost of series and shunt inverters in dollar per kVA ($\$/kVA$) is computed as in [92]. The energy loss is computed for a planning horizon considering two load levels, i.e., peak hour and off-peak hour load levels. The active power is injected in Models B and D only in peak hour. The objective function is optimized under the following constraints:

- *Active and reactive power balance constraints*: The total active/ reactive power coming at any bus 'e' should be equal to the total active/ reactive power consumed by the downstream loads, active/ reactive power losses in the downstream lines, and the load demand at bus 'e'. The mathematical expressions for active and reactive power balance are given below.

$$\sum_{oe\in\sigma} PF(oe) = \sum_{ef\in\tau} P(ef) + \sum_{ef\in\tau} PL(ef) + P(e) \qquad e \in [2,..,N] \quad (2.88)$$

$$\sum_{oe\in\sigma} QF(oe) = \sum_{ef\in\tau} Q(ef) + \sum_{ef\in\tau} QL(ef) + Q(e) \qquad e \in [2,..,N] \quad (2.89)$$

  where, $PF(oe)$ and $QF(oe)$ are the active and reactive power flow in line 'oe'; σ is the set of incoming lines connected to the bus 'e'; $\aleph$ is the set of all downstream buses which are located beyond bus 'e'; τ is set of all downstream lines which are beyond bus 'e'; $PL(ef)$ and $QL(ef)$ are the active and reactive power losses, respectively in branch 'ef'.

- *Voltage constraint*: The bus voltages of the network must lie within the specified minimum and maximum limits. i.e.,

$$V_{min} \le V(m) \le V_{max}, \qquad m \in [2,..,N] \quad (2.90)$$

- *Thermal constraint*: The current flowing through the lines must be less than its thermal limit. i.e.,

$$I(mn) \le I_{TH}(mn), \qquad mn \in [1,..,N-1] \quad (2.91)$$

  The thermal limit of a line depends on the type/specification of the line conductor.

- *Minimum reactive power compensation constraint:* A fraction (K_{comp}) of total reactive power demand of the network must be provided by the UPQC/UPQC-O. i.e.,

$$(Q_{Sh} + Q_{Se}) \geq K_{comp} \sum_{m\epsilon[2,..,N]} Q(m) \quad (2.92)$$

- *PVSML constraint*: $PVSML$ is the percentage of load protected from a given value of voltage sag by the series inverter. $PVSML$ at bus n is calculated as:

$$PVSML(n) = 100 \frac{Re\{\bar{V}(n)\bar{I}^*(mn)\}}{\sum_{i\epsilon[2,..,N]} P(i)+PL} \quad (2.93)$$

where, PL is the uncompensated network power loss. This constraint is incorporated to maintain a given desired PQ level for a distribution network in terms of voltage sag mitigation with UPQC/UPQC-O placement.

2.5 Planning algorithm for the allocation of UPQC/UPQC-O in radial distribution networks using PSO

This section describes the PSO-based planning algorithm used for the allocation of UPQC/UPQC-O.

2.5.1 PSO: Basics

This is a meta-heuristic algorithm inspired by the swarming behavior of bird flock and fish school [107]. The original algorithm is modified by considering inertia weight [108]. In this algorithm, multiple solutions are randomly generated. This set of solutions is called population and the each solution is called particle. Initially each particle starts with random initial velocity (U) and position (x). The velocity of each particle is updated iteratively by using its previous individual best position (L_{Best}) and by using previous neighborhood best position (G_{Best}) and its position is updated by using this new velocity. The value of objective function is called fitness value. The equations used to update the velocity and position for a particle (e is particle number and f is the optimizing variable) are as:

$$U_{ef}^{itr+1} = wU_{ef}^{itr} + C_1R_1\left(L_{Best}{}_{ef}^{itr} - x_{ef}^{itr}\right) + C_2R_2\left(G_{Best}{}_{f}^{itr} - x_{ef}^{itr}\right) \quad (2.94)$$

$$x_{ef}^{itr+1} = x_{ef}^{itr} + U_{ef}^{itr+1} \quad (2.95)$$

The inertia weight (w) is used to control the search space; acceleration constant C_1 is used to drive particles towards its individual best position and acceleration constant C_2 is used to drive particles towards its global best position; R_1 and R_2 are the random numbers lie between 0 to 1; 'itr' is the iteration number.

2.5.2 Planning algorithm

The pseudo codes for the overall planning algorithm is shown in Fig. 2.7. A particle of PSO encodes the locations of the series and shunt inverters and value of K_{Re}.

Begin
Input radial distribution network bus data and line data;
Calculate PVSML at each buses;
Input THD_L, itr_{max}, T^h,C_1, C_2, k, K_{Se1}, $Penalty\ Factor$, N_{Pop}, $I_{TH}(mn)$, V_{max}, V_{min}, $PVSML$, $rate\ of\ interest$, t_1, t_2, t_{Sag}, w, C^E,C_I^B, $C_{O\&M}^B$, η_{INV}, η_{TF}.
Initialize random position and velocity of the particles of size N_{Pop} for PSO;
Decode the particles and calculate fitness values;
Find initial L_{Best} and G_{Best};
For *iteration*=2: itr_{max}
  For *i*=1: N_{Pop}
    Update velocity and position of particles by (2.94) and (2.95), respectively;
    Decode particle position to obtain the locations of inverters and value of K_{Re};
    Perform the FBSLF with UPQC/UPQC-O model;
    Calculate the value of objective function OF;
    If technical constraints are not satisfying add $Penalty\ Factor$ to OF;
  End
 Find new L_{Best} and G_{Best};
End
The final G_{Best} value gives the locations of series and shunt inverters and K_{Re};
Calculate other parameters of UPQC/UPQC-O;
End

Fig. 2.7: Pseudo codes for the allocation of UPQC/ UPQC-O models in radial distribution networks

2.6 Simulation results and discussion

In this section, simulation results are discussed. The 69-bus and 33-bus test networks are used to demonstrate the proposed planning models. In both the networks, bus 1 is the substation bus and rest are load buses. The substation bus voltage magnitude is considered as 1.0 p.u. The description on these networks is given below.

- *69-bus radial distribution network* [109].: This is a single feeder radial distribution network with base VA and base voltage of 10 MVA and 12.66 kV, respectively. The total peak hour active and reactive power demand of the network are 3.8022 MW and 2.6946 MVAr, respectively. The network data are available in Appendix.
- *33-bus radial distribution network* [110]: This is also a single feeder radial distribution network with base VA and base voltage of 100 MVA and 12.66 kV, respectively. The total peak hour active and reactive power demand of the network are 3.7150 MW and 2.3 MVAr, respectively. The network data are available in Appendix.

The peak hour and off-peak hour load levels are considered to compute the daily energy loss. The peak hour and off-peak hour load level durations are considered to be 4 hours and

20 hours, respectively. Different planning parameters used in the simulation study are shown in Table 2.2. A comparative study is provided between all the four UPQC models.

Table 2.2: Different planning parameters

Planning Parameters	Cost Components
$THD_L = 0.2$, K_{Re}=0.1-0.5, $k = 30\%$	C^E =0.08 $\$/kWh$ [75]
$rate\ of\ interest = 10\%$, T^h = 10 Years, $t_{Sag} = 60$ sec	$C_U = 0.0003{S_U}^2 - 0.2691S_U + 188.2$ ($\$/kVA$) [92]
Minimum acceptable PVSML = 70%	C_I^B =300 $\$/kWh$ [111]
Ratio of the off-peak demand to the peak demand = 0.6	$C_{O\&M}^B = 10\frac{(\$/kW)}{Yr}$ [112]
$V_{min} = 0.9$ p.u, $V_{max} = 1.05$p.u.	C_I^{PV} =2025 $\$/kW$ [113]
$\eta_{INV} = 98\%$, $\eta_{TF} = 95\%$, CUF=0.2	$C_{O\&M}^{PV}$ =16 $\frac{(\$/kW)}{Yr}$ [113]

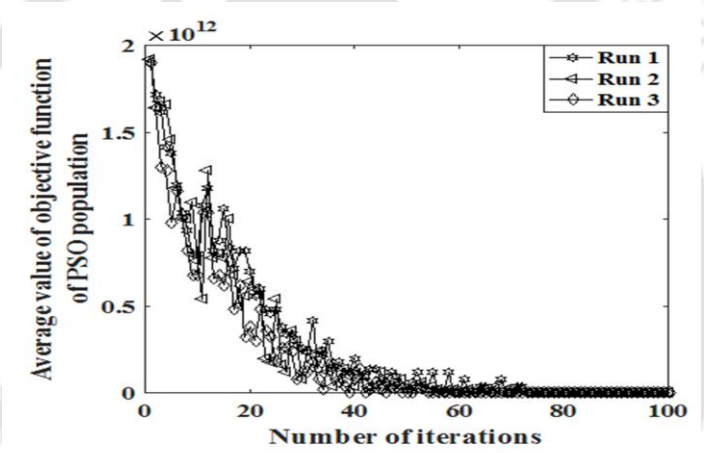

(a)

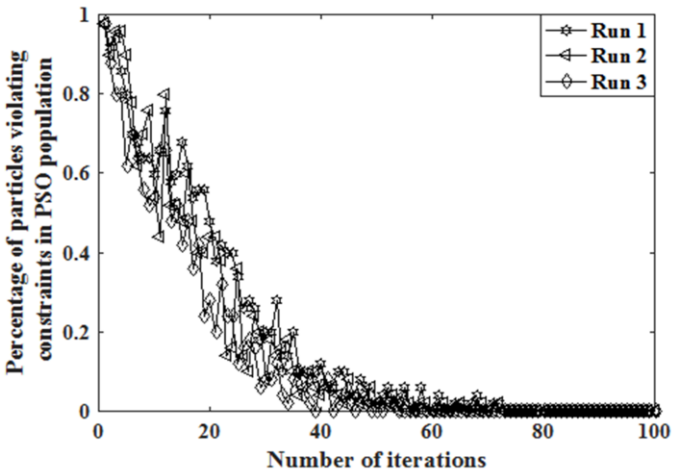

(b)

Figure 2.8: The variations of: (a) mean fitness value and (b) percentage of particles violating constraints in the PSO population with iterations as obtained with Model D for 69-bus network

The PSO parameters are optimized with repetitive runs and the optimal parameters are found to be as follows: C_1=2, C_2=2, w=0.5, population size (N_{Pop}) and maximum iteration (itr_{max}) as 100. To study the PSO convergence, the variation of the mean fitness of PSO population with iteration as obtained with the 69-bus and 33-bus networks are plotted in Figs. 2.8(a) and 2.9(a), respectively and the variation of the percentage of particles violating constraints with iteration as obtained with the 69-bus and 33-bus networks are plotted in Figs. 2.8(b) and 2.9(b), respectively. These show that the variation significantly diminishes by 50-70 iterations. The solutions obtained with PSO algorithm are given in Tables 2.3 and 2.4 for the 69-bus and 33-bus networks, respectively. The 69-bus

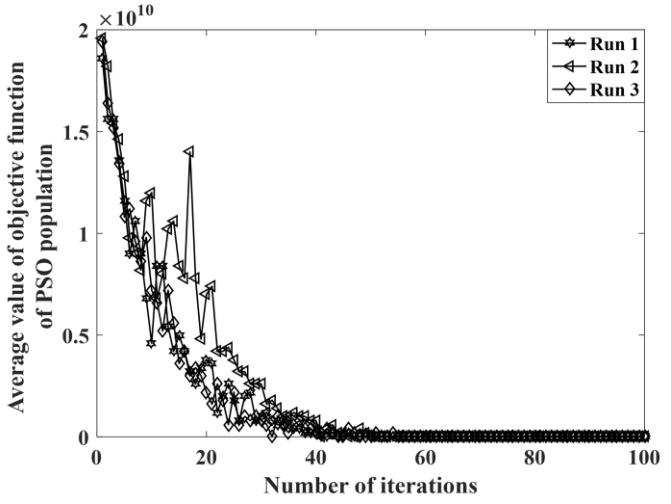

(a)

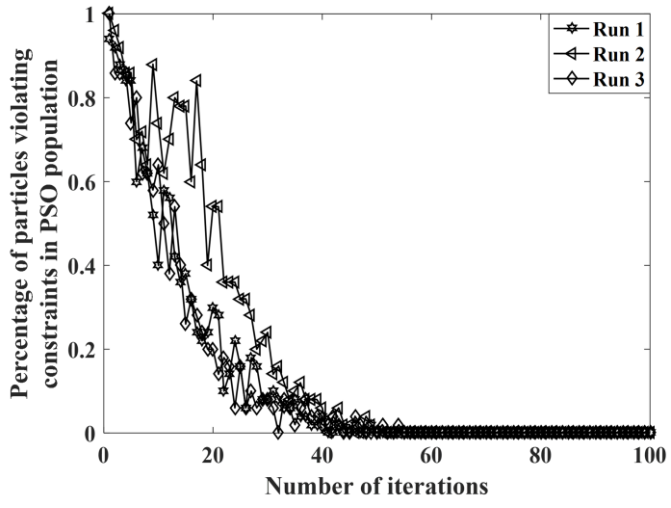

(b)

Figure 2.9: The variations of: (a) mean fitness value and (b) percentage of particles violating constraints in the PSO population with iterations as obtained with Model D for 33-bus network

and 33-bus networks with the optimal placement of UPQC and UPQC-O are shown in Figs. (2.10) and (2.11), respectively.

Table 2.3: Solutions as obtained with the 69-bus distribution network

Solution	Model A	Model B	Model C	Model D
Series inverter location	7	7	7	7
Shunt inverter location	7	7	61	61
Peak hour power loss (kW)	201.9072	197.3922	149.9359	122.0317
Off-peak hour power loss (kW)	68.2819	68.2819	51.6529	51.6529
Peak hour minimum bus voltage magnitude (p.u.)	0.9187	0.9203	0.9376	0.9443
Off-peak hour minimum bus voltage magnitude (p.u.)	0.9512	0.9512	0.9624	0.9624
Total UPQC/UPQC-O rating (MVA)	2.4863	2.4984	2.6372	2.6527
Total battery rating (MWh)	-	1.9903	0.8525	1.5419
Planning cost ($\times 10^6$ \$)	0.9362	1.5411	1.1576	1.3560
Annual energy loss reduction with respect to (*w.r.t.*) base-case network (%)	9.59	10.34	32.07	36.72

Table 2.4: Solutions as obtained with the 33-bus distribution network

Solution	Model A	Model B	Model C	Model D
Series inverter location	3	3	3	3
Shunt inverter location	3	3	30	30
Peak hour power loss (kW)	186.5512	184.5875	149.4147	138.3901
Off-peak hour power loss (kW)	63.3599	63.3599	51.1246	51.1246
Peak hour minimum bus voltage magnitude (p.u.)	0.9205	0.9221	0.9277	0.9291
Off-peak hour minimum bus voltage magnitude (p.u.)	0.9523	0.9523	0.9567	0.9567
Total UPQC/UPQC-O rating (MVA)	2.8903	2.9225	2.5895	2.5957
Total battery rating (MWh)	-	2.3263	0.8369	1.1874
Planning cost ($\times 10^6$ \$)	1.0360	1.7480	1.1678	1.2697
Annual energy loss reduction with respect to (*w.r.t.*) base-case network (%)	7.68	8.04	25.71	27.73

2.6.1 Comparison of the optimal locations as obtained with PSO

The optimal location for the connected UPQC is found to be near to the substation, since one of the design constraints is to protect minimum 70 % of total load from the possible upstream voltage sag (Eq. 2.93). In case of the UPQC-O, the series inverter is located near to the substation for the same reason. But, the shunt inverter location for UPQC-O is found to be at the bus, in which its placement results in optimal compensation for the network.

2.6.2 Comparison in view of power loss and minimum bus voltage

The power loss of 69-bus and 33-bus networks without compensation are 224.98 kW and 202.67 kW in peak hour, respectively and 75.53 kW and 68.74 kW in off-peak hour, respectively. A significant amount of loss reduction is observed with the optimal allocation of all these four models. The results also illustrate that the power loss in peak

hour can further be reduced when UPQC/UPQC-O is designed to inject active power in addition to the reactive power. The power loss reduction in both the peak hour and off-peak hour loading is found to be higher in case of UPQC-O as compared to UPQC. The reason is that the different location for the shunt inverter in UPQC-O provides compensation to the point of network which results in higher power loss reduction. The integrations of the UPQC and UPQC-O also help in the improvement of the network bus voltages. Without compensation, the minimum bus voltages for the 69-bus and 33-bus networks are 0.9092 p.u. and 0.9131 p.u., respectively in peak hour loading and 0.9476 p.u. and 0.9495 p.u. in off-peak hour loading, respectively. From Tables 2.3 and 2.4, it can be seen that the minimum bus voltage is also improved with the UPQC and UPQC-O placement.

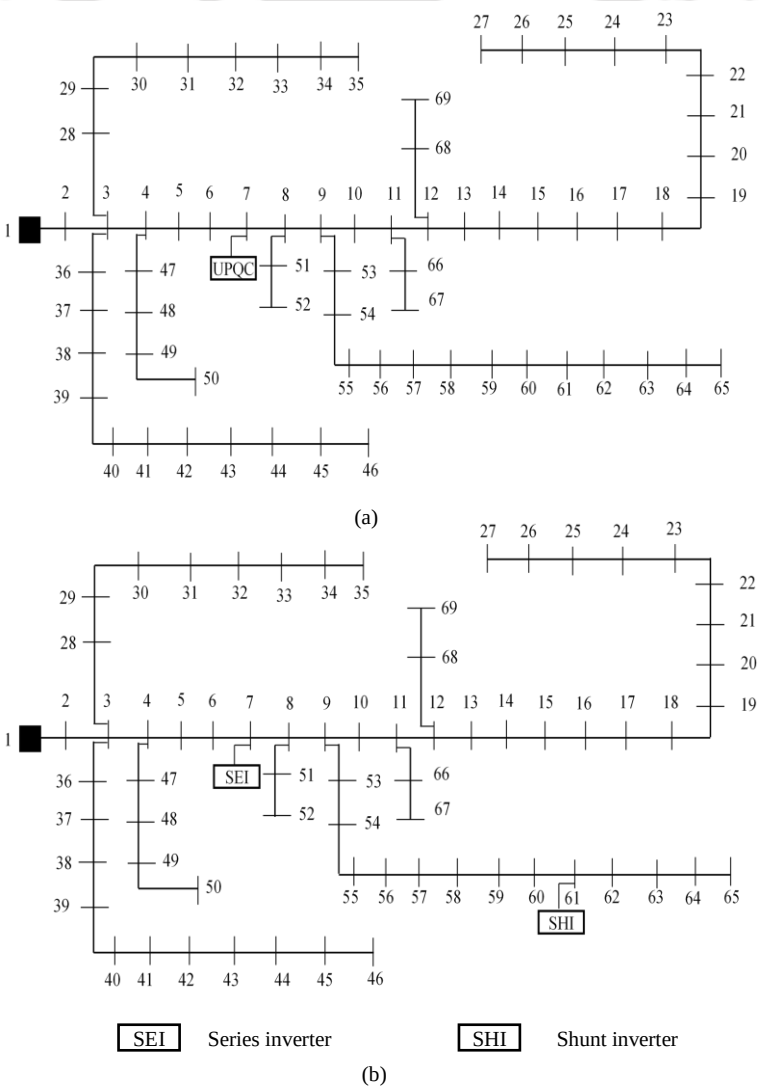

(a)

(b)

Fig. 2.10: The 69-bus network with optimal placement of (a) UPQC and (b) UPQC-O without and with active power injection

2.6.3 Comparison among the VA-rating

The VA-rating of UPQC-WP is found to be slightly higher than that of UPQC-WOP because the active power injection through the shunt inverter increases the overall VA-rating. For the same reason the VA-rating of UPQC-O-WP is also found to be slightly higher than that of UPQC-O-WOP. The VA-ratings of connected UPQC models, i.e., Models A and B are found to be lower as compared to UPQC-O models, i.e., Models C and D for the 69-bus network. However, the VA rating for the Models A and B are found to be higher than those of the Models C and D in the 33-bus network. The battery rating requirement for UPQC-O-WP model (i.e., Model D) is found to be significantly lower as compared to the UPQC-WP (i.e., Model B). It primarily depends upon the voltage and the

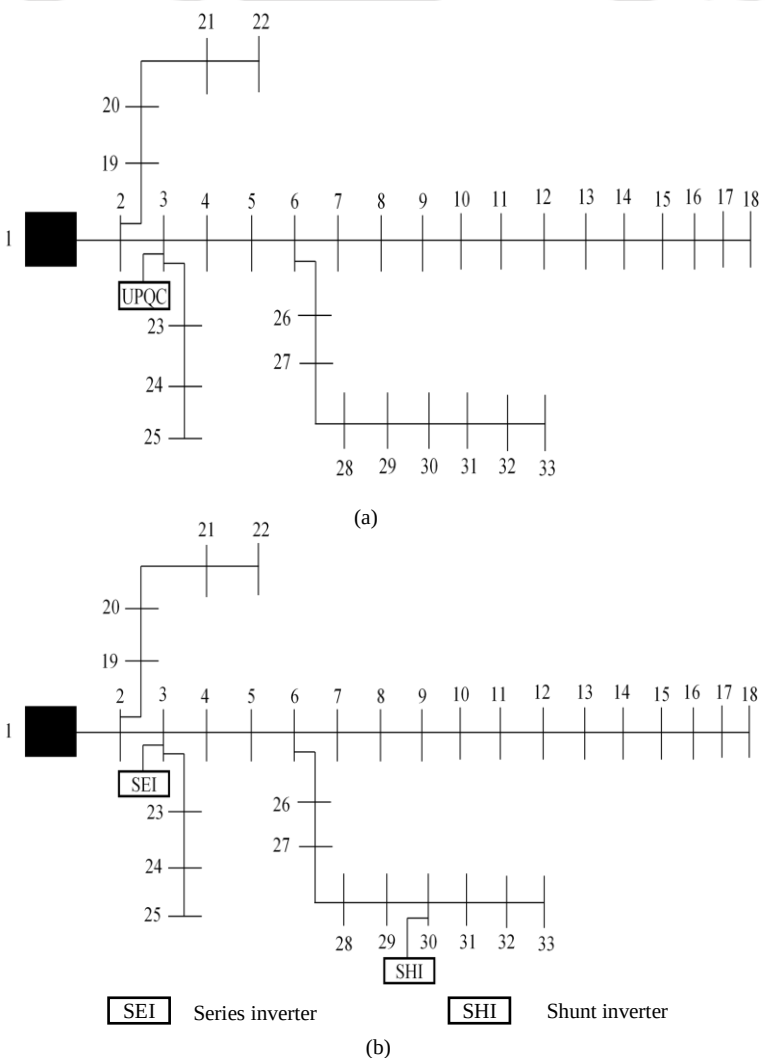

Fig. 2.11: The 33-bus network with optimal placement of (a) UPQC and (b) UPQC-O without and with active power injection

line current at the location of the shunt inverter and both these quantities are higher in case of UPQC-WP model due to the location of its inverters near to the substation.

2.6.4 Comparison among planning cost of UPQC models

The planning cost of Model B is higher as compared to Model A because of the additional investment cost for the battery. The planning cost of Model D is found to be significantly lower as compared to the Model B for both the networks. The results illustrate that the placement of UPQC-O is more economical than that of UPQC connected topology if the active power injection is to be provided. Otherwise, the placement of the UPQC connected topology is an economical option. The percentage of annual energy loss reduction obtained with UPQC-O placement (i.e., Models C and D) is found to be substantially higher than that of the UPQC placement (Models A and B). Basically, to satisfy the PVSML constraint so as to protect 70% of loads from the voltage sag, the location of the series inverter needs to be at the nearest to the substation. Since the shunt inverter location is same as the series inverter in connected UPQC, this prevents the location of the shunt inverter to the point of the network which results in maximum energy loss reduction. The battery rating requirement in Model B is also higher as compared to the Model D. This makes the Model B an expensive option as compared to the Model D.

2.6.5 The charging schemes for the battery

The battery connected to the different UPQC models needs to be charged. In this study, it is assumed to be done during off-peak hour so that the stored energy can be utilized during peak demand hour. The battery charging can be done either by consuming the equivalent amount of energy from the grid or from the local distributed generator resources, such as, PV array. Thus, the following two schemes are proposed:

- Scheme 1: Charging of battery by consuming/purchasing energy from the grid
- Scheme 2: Charging of battery with the installation of a PV array with each battery unit

The implementation of any of these two schemes for battery charging requires additional cost/investment. The implementation of Scheme 1 requires additional cost of energy purchase from the grid, which can be computed as:

$$CE_{Grid} = 8760 C^{E} T^{h} D^{f} PB_{Model} \quad (2.96)$$

where, PB_{Model} is the total battery rating requirement of individual UPQC model in kWh. The implementation of Scheme 2 requires additional installation, operational, and maintenance costs of PV array. The expression for this cost function is given below.

$$C_{PV} = C_I^{PV} PPV_{Model} + T^h D^f C_{O\&M}^{PV} PPV_{Model} \quad (2.97)$$

where, PPV_{Model} represents the size of PV array (kW) required to charge the battery of size PB_{Model} (kWh). Since the peak demand hour is assumed to be sustained during evening, the PV generation hour does not coincide with it. Hence, during operational hours of the PV array, the battery can be charged. The size of the PV array can be computed as:

$$PPV_{Model} = \frac{t_1 PB_{Model}}{24CUF} \quad (2.98)$$

The rating requirement for the PV array to be used in different UPQC models to charge the battery is provided in Table 2.5. The cost of implementation of these two schemes and their impact on the total planning cost of UPQC/ UPQC-O placement are provided in Tables 2.6 and 2.7 for 69-bus and 33-bus networks, respectively. From the Tables 2.6 and 2.7, it can be observed that the implementation of Scheme 1 requires significantly higher cost as compared to the Scheme 2. The charging of the battery for the Models C and D needs lower cost than that of the Model B.

Table 2.5: The rating requirement for PV installation for battery charging in different UPQC models for 69-bus and 33-bus networks

Systems	The rating requirement for PV installation for battery charging in MW		
	Model B	Model C	Model D
69-bus network	1.6586	0.7104	1.2849
33-bus network	1.9386	0.6974	0.9895

Table 2.6: Cost analysis for battery charging schemes for the 69-bus network

Battery charging schemes	Additional cost for battery charging ($)		
	Model B	Model C	Model D
Additional cost required for Scheme 1 ($\times 10^6$ $)	5.3776	2.3034	4.1660
Percentage of additional cost required in Scheme 1 *w.r.t.* the planning cost	348.9455	198.9806	307.2271
Additional cost required for Scheme 2 ($\times 10^6$ $)	0.8652	0.3706	0.6703
Percentage of additional cost required in Scheme 2 *w.r.t.* the planning cost	56.1417	32.0145	49.4322

Table 2.7: Cost analysis for battery charging schemes for the 33-bus network

Battery charging schemes	Additional cost for battery charging ($)		
	Model B	Model C	Model D
Additional cost required for Scheme 1 ($\times 10^6$ $)	6.2854	2.2612	3.2082
Percentage of additional cost required in Scheme 1 *w.r.t.* the planning cost	359.5766	193.6290	252.6739
Additional cost required for Scheme 2 ($\times 10^6$ $)	1.0113	0.3638	0.5162
Percentage of additional cost required in Scheme 2 *w.r.t.* the planning cost	57.8547	31.1526	40.6553

2.7 Conclusion

In this chapter, four different models for UPQC so as to improve the energy efficiency of radial distribution networks have been reported. A planning optimization model is proposed to optimally place UPQC/UPQC-O in distribution networks. The PSO is used as solution strategy. The proposed planning approach for the allocation of UPQC/UPQC-O in radial distribution networks is validated on 69-bus and 33-bus test networks. A comparative performance assessment among these four models provides the following:

- In the connected UPQC models, the series and shunt inverters locations are same and they are to be placed near to the substation to protect the given number of loads from voltage sag. But, the same can be done with UPQC-O by placing only the series inverter near to the substation. Hence, UPQC-O has the flexibility to place its shunt inverter at the location which results in higher power loss reduction.
- The battery rating requirement is significantly less in case of UPQC-O as compared to UPQC, if active power injection is to be provided.
- In peak hour, a significant amount of loss reduction and improvement in minimum bus voltage are observed due to the placement of any of the UPQC models. The placement of the UPQC-O results in significantly higher annual energy loss reduction.
- The placement of UPQC-O is found to be an economical option compared to that of UPQC, if it is designed for active power injection. Otherwise, UPQC placement is more economical option.
- The charging of the battery can be done with the installation of PV array. This needs additional investment cost. It is found to be an economical option as compared to the cost of the energy purchase from the grid for the battery charging over a planning horizon.

3

Modelling and Allocation of Open-UPQC-integrated PV Generation System to Improve Energy Efficiency and Power Quality of Radial Distribution Networks

3.1 Introduction

The optimal placement of DG unit in the distribution networks improves the energy efficiency and bus voltages by providing active power compensation. Its installation can help to meet the increasing load growth and to meet load demand in peak hour. It also helps in ensuring the uninterruptible power supply. Thus, the proper planning for DG allocation in the distribution networks is very much important. There are number of works reported on the DG allocation. The state-of-the-art review on these works can be found in [5-6, 114]. The allocation of DG in distribution networks is an optimization problem. Different objective functions are formulated for the optimal integration of DG, such as, minimizations of power loss, bus voltage deviation, carbon emission, cost of placement of DG units (investment and operational costs), cost of energy loss, and cost of energy imported from the grid etc. In some works, maximization of reliability, DG capacity, and cost of exported energy to the grid etc., are considered as the objectives. The DG allocation is done under the uncertainties of load and/or generation in [8, 18]. In [16, 23], an approach for combined planning for network expansion and DG allocation under uncertainties of load and generation is reported. A DG allocation strategy along with network reconfiguration planning is done in [11, 115]. In some of these works, multi-objective planning is done to

optimally place the DG units in distribution networks [11-12, 116]. Several solution strategies are reported to solve the DG allocation problem. These include conventional approaches, such as mixed-integer programming [9], and meta-heuristic algorithms, such as, GA [8, 11, 18, 23, 115], PSO [16, 116], honey bee mating algorithm [12] etc.

The increasing use of non-linear loads in distribution networks is responsible for PQ deterioration. As mentioned above, there are several benefits of DG integration in distribution networks. However, its integration cannot ensure a desired PQ level in terms of harmonics elimination and voltage sag mitigation. There are several measures to ensure a desired PQ level in a network. The integration of custom power devices is one of such measures. As mentioned in Chapter 2, the custom power devices are the power electronics-based devices which are designed to improve the PQ and to provide the reactive power compensation. It also helps in the improvement of bus voltages and energy efficiency of the network. Thus, the allocation of custom power device connected with PV array can be used in improving both energy efficiency and PQ of distribution networks.

The comparative study carried out in the previous chapter illustrates that the allocation of UPQC-O in distribution network can significantly improve the energy efficiency and bus voltages as compared to the UPQC. Thus, in this chapter, the study is carried out with UPQC-O. The recently reported works on UPQC-O [96-102] are briefly discussed in the introduction section of Chapter 2. The most of the UPQC-O models reported in [96-102] are developed for PQ improvement. However, the development of UPQC-O model with PV array and its optimal allocation strategy to the distribution networks to improve the energy efficiency by maintaining a pre-set PQ constraint are not reported. This is set as the theme of this chapter.

A planning optimization problem is formulated, in this work, to optimally place UPQC-O with PV array. The energy generated by the PV array can be used in two ways: (i) by storing it into storage devices during the operation hours of PV so as to utilize the stored energy during the peak hours, and (ii) by directly utilizing it during the operation hours of PV. Thus, two models for UPQC-O are formulated in this chapter. These are: (i)

UPQC-O with battery and PV array (UPQC-O-WB) (ii) UPQC-O with PV array without battery (UPQC-O-WOB). A comparative study is provided in between these two UPQC-O models. In this chapter, the series and shunt inverters of UPQC-O are also designed to communicate the information of reactive power sharing among them. PSO is used as the solution strategy to find the optimal locations and sizes of the series and shunt inverters, and the sizes of PV array and battery. The key contributions of this chapter are:

- Development of UPQC-O model with PV array and battery to act as active and reactive power compensator of radial distribution networks.
- Formulation of a planning approach to optimize the energy loss of radial distribution networks with the optimal placement of UPQC-O by maintaining a pre-set PQ criteria in terms of voltage sag mitigation and harmonic suppression.

To validate the proposed planning approach, the 69-bus and 33-bus radial distribution networks are used.

3.2 Modelling of UPQC-O with PV array for distribution networks

In this work, the functions of series and shunt inverters of UPQC-O during healthy and voltage sag conditions are considered to be same as of UPQC-O-WP (*Refer Table 2.1*). Here, the PV array is integrated in the DC side of the shunt inverter to provide the active power compensation as shown in Fig. 3.1. Two planning cases are proposed in this work, as given below.

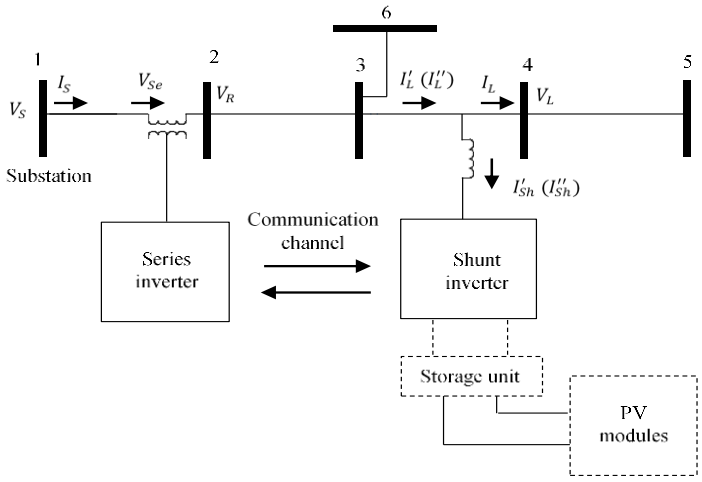

Fig. 3.1: A 6-bus radial distribution network with the placement of UPQC-O {symbol used in bracket is used for UPQC-O with PV array}

- *Case A*: In this case, the energy generated by the PV array is stored in battery during its generation hours to inject this energy during peak load demand hours. UPQC-O-WB model is used in this case.
- *Case B*: In this case, the energy generated by PV array is directly injected to the network during operation hours of PV array. Since there is no need of battery, UPQC-O-WOB model is used.

The case-study is carried out based on the following assumptions/considerations:

- The PV generation hour does not coincide with peak hour. This is true for the networks with domestic loads. If the generation hour coincides with the peak hour, there is no need of battery. This reduces the planning cost.
- The battery connected to the PV array is designed to be charged during the generation hours of the PV array and it will be discharged during the peak hours.

Hence, in planning Case A, the UPQC-O provides both active and reactive power compensations during peak hours and only reactive power compensation during off-peak hours. However, in Case B, the UPQC-O provides both active and reactive power compensations during generation hours of PV array and only reactive power compensation during rest of the time. The phasor diagrams for the operations of the series and shunt inverters of UPQC-O are same as shown in Figs. 2.4(a) and 2.5, respectively. The series inverter is mathematically modelled using Eqs. (2.46)-(2.52) to provide reactive power compensation to the network. However, the shunt inverter is mathematically modelled using Eqs. (2.63)-(2.71) to provide both active and reactive power compensations.

The active power to be injected through the DC-link of the shunt inverter is determined as:

$$P_{Sh}^{DG} = V_L I_{Re} \tag{3.1}$$

In UPQC-O-WB, the rating requirement for the battery in kWh is:

$$PB_{Sh} = P_{Sh}^{DG} t_1 \tag{3.2}$$

The size for PV-array in kW is determined as:

$$PPV_{Sh} = \frac{t_1 P_{Sh}^{DG}}{24CUF} \tag{3.3}$$

In UPQC-O-WOB, the size for PV-array is:

$$PPV_{Sh} = \frac{t_4 P_{Sh}^{DG}}{24CUF} \quad (3.4)$$

The total VA-rating of UPQC-O is determined by summing up the individual VA-ratings of series and shunt inverters. The series and shunt inverters placed in different locations of distribution networks communicate the information of reactive power compensation sharing to each other using communication channel. The mathematical Eqs. (2.1)-(2.2) are involved in the reactive power compensation sharing between the series and shunt inverters.

3.3 Placement strategy for UPQC-O in radial distribution networks

The FBSLF algorithm is used to incorporate the UPQC-O models to determine the voltage in each bus and the network power loss. The placement of the series and shunt inverters in a distribution network modifies the active and reactive power demands of the buses as shown in Eqs. (2.84)-(2.86).

3.4. Problem formulation

In this chapter, an optimization problem is formulated to find out the optimal locations and sizes for the series and shunt inverters and the optimal value for K_{Re}. The planning cost for the allocation of UPQC-O in the distribution networks is considered to be the objective function which consists of: (i) the investment costs of the series and shunt inverters, (ii) investment, operational, maintenance, and replacement costs for the battery, (iii) investment cost, operational and maintenance cost for the PV array, and (iv) cost of energy loss of the network as given below.

$$\begin{aligned} PC_{UPQC-O} = {} & \sum_{m\epsilon[2,\dots N]}(C_m^{Se} S_m^{Se}) x_m + \sum_{n\epsilon[2,\dots N]}(C_n^{Sh} S_n^{Sh} + C_I^B PB_n^{Sh} + \\ & C_I^{PV} PPV_n^{Sh}) x_n + \sum_{n\epsilon[2,\dots N]}(C_{REP}^B PB_n^{Sh}) D^{f1} x_n + \\ & \sum_{n\epsilon[2,\dots N]}(C_{O\&M}^B \frac{PB_n^{Sh}}{t_1} + C_{O\&M}^{PV} PPV_n^{Sh}) T^h D^f x_n + \\ & 365 C^E T^h D^f \sum_{mn\epsilon[1,\dots N-1]}(t_1 PL_{mn}^{t_1} + t_3 PL_{mn}^{t_3} + t_4 PL_{mn}^{t_4}) \end{aligned} \quad (3.5)$$

In UPQC-O-WOB model, the costs of battery are not included. The energy loss is computed for a planning horizon considering two load levels, i.e., peak hour and off-peak hour load levels. The objective function PC_{UPQC-O} is optimized under the active and reactive power balance constraints, bus voltage constraint, thermal constraint, PVSML constraint, and DG

penetration constraint. The mathematical expressions for active and reactive power balance constraints, bus voltage constraint, thermal constraint, and PVSML constraint are given in Eqs. (2.88-2.89), (2.90), (2.91), and (2.93), respectively. An additional constraint, i.e., DG penetration constraint is considered in this planning as given below.

- *DG penetration constraint*: DG penetration is defined as the ratio of energy supplied by the DG unit (in a day) to the total energy required by the loads (in a day). i.e.,

$$DG\ penetration = \frac{(Operation\ hours\ of\ DG)\ P_{Sh}^{DG}}{(t_1 P_{total}^{Peak}) + \{(t_3 + t_4) P_{total}^{Off-peak}\}} \tag{3.6}$$

According to the DG penetration constraint, the amount of DG penetration should be higher than a given set value.

3.5. Solution algorithm

The PSO algorithm is used as the solution approach for the optimal allocation of UPQC-O in radial distribution networks. The basics of PSO algorithm are discussed in subsection 2.5.1. The overall planning algorithm uses the FBSLF algorithm with UPQC-O model as the support subroutine. A particle of PSO consists of three segments. They are: (i) location of series inverter (ii) location of shunt inverter and (iii) the value of K_{Re}. In case of multiple shunt inverters placement, a particle carries information of location of the series inverter, locations of shunt inverters, and the values of K_{Re}. Direct encoding and decoding techniques are used. The pseudo codes for overall planning algorithm are shown in Fig. 3.2.

Begin
Input radial distribution network bus data and line data;
Calculate PVSML at each buses;
Input THD_L, itr_{max}, T^h, C_1, C_2, k, $Penalty\ Factor$, N_{Pop}, $I_{TH}(mn)$, V_{max}, V_{min}, $PVSML$, $rate\ of\ interest$, t_1, t_3, t_4, w, C^E, C_I^B, $C_{O\&M}^B$, C_{REP}^B, C_I^{PV}, $C_{O\&M}^{PV}$ and minimum DG penetration limit.
Initialize random position and velocity of the particles of size N_{Pop} for PSO;
Decode the particles and calculate fitness values;
Find initial L_{Best} and G_{Best};
For *iteration*=2: itr_{max}
  For *i*=1: N_{Pop}
    Update velocity and position of particles by (2.94) and (2.95), respectively;
    Decode particle position to obtain the locations of inverters and K_{Re};
    Perform the FBSLF with UPQC-O model;
    Calculate the fitness value for each particle;
    If any particle violates constraints, a penalty factor is added with it;
  End
  Update L_{Best} and G_{Best};
End
The final G_{Best} value provides the locations of inverters and K_{Re} ;
End

Fig. 3.2: Pseudo codes for the allocation of UPQC-O in radial distribution networks

3.6 Simulation results and discussion

The computer simulation study is carried out using 69-bus and 33-bus radial distribution networks to validate the proposed planning model. The descriptions of these networks are provided in section 2.6. The unit costs of series and shunt inverters of UPQC-O are obtained from [92]. The minimum DG penetration is set to be 5 %. The minimum allowable PVSML is set as 70%. For each case, three subcases are considered. Each subcase corresponds to different number of shunt inverter. These are:

- One series inverter and one shunt inverter (1-Se, 1-Sh)
- One series inverter and two shunt inverters (1-Se, 2-Sh)
- One series inverter and three shunt inverters (1-Se, 3-Sh)

Different planning parameters and cost components used are provided in the Table 3.1.

Table 3.1: Different planning parameters

Planning parameters	Cost components
T^h = 20 years	C^E = 0.08 \$/kWh [75]
THD_L = 0.2, k = 30%	C_I^B = 900 \$/kWh [112]
$rate\ of\ interest$ = 10 %	$C_{O\&M}^B$ = 10 $\frac{(\$/kW)}{Yr}$ [112]
t_4 = 5 hrs, K_{Re} = 0.1 − 0.5	C_{REP}^B = 244 \$/kWh [112]
t_1 = 4 hrs, t_3 = 15 hrs	C_I^{PV} = 2025 \$/kW [113]
$\frac{Off-peak\ demand}{Peak\ demand}$ = 0.6	$C_{O\&M}^{PV}$ = 16 $\frac{(\$/kW)}{Yr}$ [113]

The PSO parameters are optimized with repetitive runs and the optimal parameters are found to be: C_1 =2, C_2 =2, w =0.5, N_{Pop} =200, and itr_{max} =200. To study the PSO convergence, the variation of the mean fitness of PSO population with the iterations and the variation of the percentage of particles violating constraints with the iterations are plotted in Figs. 3.3(a) and 3.3(b), respectively for the 69-bus network and in Figs. 3.4(a) and 3.4(b), respectively for the 33-bus network. The solutions obtained with the PSO algorithm are listed in Tables 3.2 and 3.3 for the 69-bus and 33-bus networks, respectively.

3.6.1 Impact on energy loss and bus voltages

The network power losses of the 69-bus and 33-bus networks without compensation are 224.98 kW and 202.67 kW in peak hour, respectively and 75.53 kW and 68.74 kW in off-peak hour, respectively. From Tables 3.2 and 3.3, it is observed that the optimal placement of UPQC-O with PV array results in significant reduction in energy loss for both

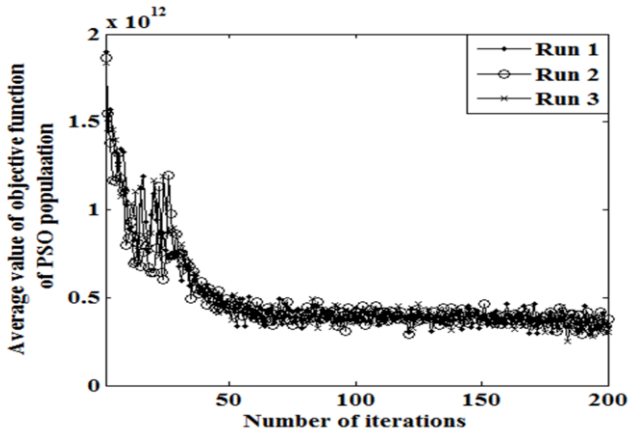

(a)

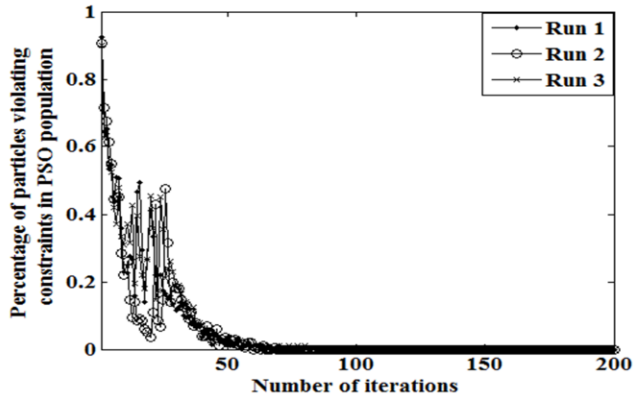

(b)

Fig. 3.3: The variations of: (a) mean fitness value and (b) percentage of particles violating constraints in the PSO population with iterations as obtained with 69-bus network Case A (1-Se, 2-Sh)

the networks. The results also illustrate that the reduction in energy loss in Case A is more as compared to Case B. Basically, the power loss in peak hour is much higher than that of the off-peak hour. Since both active and reactive power compensations are provided by UPQC-O during peak hour in Case A, it results in higher power loss reduction as compared to Case B. The network minimum bus voltages of the 69-bus and 33-bus networks without compensation are 0.9092 p.u. and 0.9131 p.u. in peak hour, respectively and 0.9476 p.u. and 0.9495 p.u. in off-peak hour, respectively. The results show that the bus voltages of the networks are also improved with the optimal placement of UPQC-O. The minimum bus voltage of the network in peak hour ($V_{min}^{t_1}$) is found to be better in Case A than that of the Case B for the same reason mentioned above. There is no difference between $V_{min}^{t_3}$ and $V_{min}^{t_4}$ in Case A because UPQC-O is designed to provide only reactive power compensation

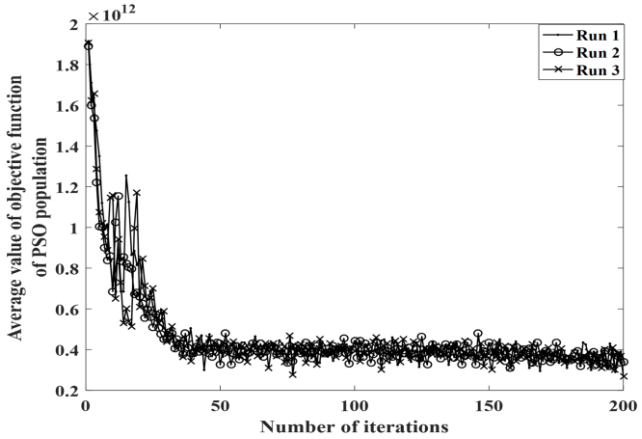

(a)

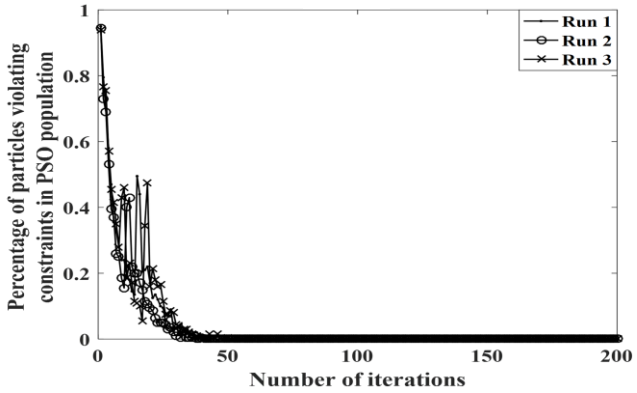

(b)

Fig. 3.4: The variations of: (a) mean fitness value and (b) percentage of particles violating constraints in the PSO population with iterations as obtained with 33-bus network Case A (1-Se, 2-Sh)

during the durations t_3 and t_4 in Case A. However, since the PV generation is directly injected into the network in Case B during the generation hour of PV array, $V_{min}^{t_4}$ is found to be better than $V_{min}^{t_3}$. For the same reason, $V_{min}^{t_4}$ in Case B is also higher than that of the Case A.

3.6.2 Locations of the series and shunt inverters

The locations of the series inverter are found to be same in all the cases. This is to satisfy the PVSML constraint, as shown in Eq. (2.93). However, locations of the multiple shunt inverters are found to be case-sensitive. It is observed that there are few buses, which are repetitively found to be the optimal locations for the shunt inverter placement, for example buses 59, 61, 69 for the 69-bus network and buses 6, 33 for the 33-bus network.

There might be various reasons for that. The first one is for the less rating requirement of the shunt inverters in these locations because these are mostly the remote terminal buses. The second reason is that there are few buses, in which the appropriate active and/or reactive power compensation results in significant power/energy loss reduction, for example bus 61 for the 69-bus network.

Table 3.2: The optimal solutions as obtained with PSO for the 69-bus radial distribution network

Solution	Case A			Case B		
	1-Se, 1-Sh	1-Se, 2-Sh	1-Se, 3-Sh	1-Se, 1-Sh	1-Se, 2-Sh	1-Se, 3-Sh
Series inverter location	7	7	7	7	7	7
Shunt inverter 1 location	61	61	61	59	69	22
Shunt inverter 2 location	-	69	69	-	59	69
Shunt inverter 3 location	-	-	35	-	-	61
K_{Re} for shunt inverter 1	0.3960	0.3942	0.3867	0.4930	0.1	0.5
K_{Re} for shunt inverter 2	-	0.1	0.5	-	0.4913	0.4791
K_{Re} for shunt inverter 3	-	-	0.1	-	-	0.5
Energy loss reduction *w.r.t.* base-case network (%)	46. 4502	46.4804	46.3796	34.6195	34.6842	40.6280
$V_{min}^{t_1}$ (p.u.)	0.9631	0.9630	0.9626	0.9353	0.9351	0.9376
$V_{min}^{t_4}$ (p.u.)	0.9624	0.9624	0.9624	0.9784	0.9783	0.9809
$V_{min}^{t_3}$ (p.u.)	0.9624	0.9624	0.9624	0.9612	0.9612	0.9613
Sum of the shunt inverter ratings (MVA)	1.4036	1.4232	1.4256	1.2674	1.2885	1.2469
Series inverter rating (MVA)	1.4574	1.4574	1.4574	1.4574	1.4574	1.4574
Total UPQC-O rating (MVA)	2.8610	2.8806	2.8830	2.7248	2.7460	2.7044
Total battery rating (kWh)	3041.752	3041.752	3041.752	-	-	-
Total PV rating (kW)	633.6983	633.6983	633.6983	633.6983	633.6983	633.6983
PC_{UPQC-O} ($\times 10^6$\$)	5.0081	5.0117	5.0123	1.9611	1.9649	1.9462
Cost reduction *w.r.t.* Case A (%)	-	-	-	60.8414	60.7937	61.1715

Table 3.3: The optimal solutions as obtained with PSO for the 33-bus radial distribution network

Solution	Case A			Case B		
	1-Se, 1-Sh	1-Se, 2-Sh	1-Se, 3-Sh	1-Se, 1-Sh	1-Se, 2-Sh	1-Se, 3-Sh
Series inverter location	3	3	3	3	3	3
Shunt inverter 1 location	6	6	33	6	6	33
Shunt inverter 2 location	-	33	26	-	33	9
Shunt inverter 3 location	-	-	15	-	-	7
K_{Re} for shunt inverter 1	0.2860	0.2832	0.4911	0.3859	0.3830	0.2166
K_{Re} for shunt inverter 2	-	0.1	0.5	-	0.1	0.5
K_{Re} for shunt inverter 3	-	-	0.1	-	-	0.5
Energy loss reduction *w.r.t.* base-case network (%)	27.1365	27.5	29.4005	23.0698	23.4039	25.0799
$V_{min}^{t_1}$ (p.u.)	0.9376	0.9376	0.9402	0.9277	0.9277	0.9310
$V_{min}^{t_4}$ (p.u.)	0.9567	0.9567	0.9577	0.9646	0.9646	0.9672
$V_{min}^{t_3}$ (p.u.)	0.9567	0.9567	0.9577	0.9567	0.9567	0.9588
Sum of the shunt inverter ratings (MVA)	1.7712	1.8113	1.3828	1.6078	1.6503	0.9686
Series inverter rating (MVA)	1.7523	1.7523	1.7523	1.7523	1.7523	1.7523
Total UPQC-O rating (MVA)	3.5235	3.5636	3.1351	3.3601	3.4026	2.7209
Total battery rating (kWh)	2972	2972	2972	-	-	-
Total PV rating (kW)	619.1667	619.1667	619.1667	619.1667	619.1667	619.1667
PC_{UPQC-O} ($\times 10^6$\$)	5.0578	5.0646	4.9811	2.0586	2.0659	1.9355
Cost reduction *w.r.t.* Case A(%)	-	-	-	59.2985	59.2090	61.1431

3.6.3 Ratings of the series and shunt inverters

The rating requirement for both the inverters depends on the respective locations, in which these are placed. Since the location of the series inverter, which depends on the satisfaction of the PVSML constraint, remains same in all the cases, the series inverter rating is found to be same in all the cases. But, the ratings of the shunt inverters are found to be varying with the planning cases depending on their locations in the network. The sum total of the ratings of the multiple shunt inverters is shown in Tables 3.2-3.3. The total rating requirement for the shunt inverters is found to be lower in Case B as compared to Case A. The total rating of the shunt inverters is found to be less if three shunt inverters are placed in the 33-bus network. However, in the 69-bus network, there is no appreciable difference in the total rating requirement if multiple shunt inverters are placed.

3.6.4 Size of the battery and PV array

The size of the battery in each sub-case is found to be same. The size of the PV array is also found to be same in all the sub-cases of Cases A and B. These two ratings are basically governed by the minimum DG penetration limit, as set in Eq. (3.6). From the results, it is observed that the total ratings of the battery and the PV array are same in all the sub-cases in spite of these are placed in different locations of the network. This happens because the different values of K_{Re} corresponding to the shunt inverters placed in different locations are such that the sum of the ratings of the PV array becomes equal in all the sub-cases in Case A and Case B, as can be seen from the Eqs. (2.63) and (3.1).

3.6.5 Comparison of the planning costs of two cases

The planning costs for all the sub-cases of Case A are found to be higher than those of the sub-cases of Case B, primarily because of the inclusion of the cost of the battery in Case A. The planning costs of all the sub-cases in Case A or Case B are found to be nearly equal in the 69-bus network. But, the planning cost for the placement of three shunt inverters is found to be significantly less due to the lower rating requirement of UPQC-O for the 33-bus network.

3.6.6 Relative merits and demerits for the deployment of Cases A and B

A distribution network owner (DNO) may opt either of these two planning cases depending on its needs and choices. There are relative merits and demerits in both the planning cases as given below:

- If the DNO is desirous in reducing its peak load demand and the energy losses, the planning Case A can be chosen. However, the planning cost of Case A is nearly 60% higher as compared to the Case B. The maintenance and periodic replacement of battery in Case A need additional efforts and costs.
- If the DNO needs to exercise the economical option, the planning Case B can be selected. However, this choice provides higher amount of energy loss as compared to the Case A. The power loss and voltage profile during peak hour will also be poor as compared to the Case A.

However, it is noteworthy that the implementation of either of the planning cases on the uncompensated networks results in significant power/energy loss reduction, improvements in voltage profile, and mitigation of two important PQ problems, i.e., voltage sag and current harmonics.

3.6.7 Performance comparison with similar approaches

The aim of this work is to simultaneously improve the energy efficiency and PQ of distribution networks with the placement of UPQC-O with PV array. There are several conventional approaches reported in the literature for power/energy loss minimization, for example, capacitor bank placement, voltage regulator placement, on-load tap changer (OLTC) placement etc. But, the PQ improvement is not set as the objective/criterion in these approaches. Hence, the objective function formulation in these approaches is different as compared to the proposed approach. Thus, the direct performance comparison of the proposed approach with these approaches would be impractical. However, to have a comparative study with similar approaches, an approach for distribution STATCOM (DSTATCOM) allocation [117] is chosen. In this approach, the 69-bus network is used. In [117], a combined approach for DSTATCOM allocation and network reconfiguration for power loss minimization is provided. In Table 3.4, the results reported in the work [117] are compared with those of the proposed approach, in which the UPQC-O-WB model with

one-series and one-shunt inverter is used. The peak-hour operational parameters are only provided in the comparison, since the objective function formulated in [117] is minimization of power loss during peak hour. The results show that the placement of UPQC-O provides higher amount of power loss reduction as compared to two approaches, studied here. The minimum bus voltage as obtained with the proposed approach is also comparable with that of the combined approach for DSTATCOM allocation and reconfiguration. The UPQC-O rating requirement is higher than that of the DSTATCOM [117] because it is designed to improve power loss by maintaining a desired PQ level. However, PQ issue is not incorporated into the planning approach in [117]. The planning cost is not shown in the comparison because the same is not provided in [117].

Table 3.4: Comparison of proposed approach with similar other approaches for power loss minimization

Solutions and the features of the planning approach	UPQC-O allocation (proposed approach)	DSTATCOM allocation along with network reconfiguration [117]	Only reconfiguration [117]
Series inverter location	7	-	-
Shunt inverter location	61	61	-
Peak hour power loss(kW)	64.4425	78.59	99.8
Network minimum bus voltage magnitude (p.u.)	0.9631	0.9632	0.9428
VA-rating of device (MVA)	2.8610	0.924	-
Does the planning approach include the PQ issues?	Yes	No	No

3.7 Conclusion

In this chapter, two UPQC-O models have been proposed with the integration of PV array so as to improve the energy efficiency and PQ of the radial distribution networks. A planning optimization problem is formulated to find the optimal placement for the series and shunt inverters of UPQC-O in the distribution networks. PSO is used in solving the planning problem. The following are the outcomes of the simulation results:

- The placement of any of the UPQC-O models can significantly improve energy loss, bus voltage profile, and PQ for the networks.
- The location of the series inverter depends on the minimum allowable value of PVSML set. This implies to the fact that the series inverter location depends on the amount of load needs to be protected from the voltage sag. However, the shunt inverter locations are found to be varying with the planning cases.

- The multiple placement of the shunt inverters significantly reduces the overall rating requirement for UPQC-O for certain type of the networks, such as the 33-bus network.
- The sizes of the PV array and battery basically depend on the minimum DG penetration limit to be set by the DNO.

4

Modelling and Allocation Planning of Inverters of Open UPQC to Improve the Rooftop PV Hosting Capacity and Energy Efficiency of Radial Distribution Networks

4.1 Introduction

The depletion of conventional energy resources, increase in load demand, and need of carbon/ pollution free power generation are the prime motivations behind the integration of renewable energy sources to distribution networks. The Ministry of New and Renewable Energy of the Government of India has taken an initiative to integrate renewable generation of 175 GW, including 100 GW of PV generation and 60 GW of wind power generation by 2022 [118]. This target shows that the PV generation has a tremendous potential in the country like India due to the availability of solar irradiation in most of the part of the country. To achieve this target, the government of India is encouraging the rooftop PV installation in different areas with a subsidized price. In the coming years, it is expected that the adoption of rooftop PV installation by the domestic customers will globally increase. This will enforce to formulate appropriate policies for the grid connected rooftop PV, in which the surplus generation can be injected into the network for the mutual benefits of owners of rooftop PV array and distribution networks. But, the increasing injection of PV generation into the network may lead to several issues, such as, over voltage problem, increase in line losses, violation of line thermal limit etc. The low voltage networks of the country like Australia are suffering from different operational issues, such as, over voltage problem,

voltage imbalance etc., due to the injection of rooftop PV in large scale [119]. Thus, the determination of total amount of DG/PV capacity that a network can accommodate without deteriorating the operational performance of the network is a matter of interest to the power systems researchers. This is called DG/PV hosting capacity (DGHC/PVHC) of the network. The researchers have started investigating different technologies which can allow the networks to accommodate higher PV capacity.

The state-of-the-art review on the impacts of high PV penetration on distribution networks and the different approaches to mitigate the problems caused by the high PV penetration can be found in [120-123]. In [124], the impacts and challenges of PV deployment in the remote Australian networks are reported along with the different control strategies used for the enhancement of PV penetration. The active network management technologies, such as, reactive power compensation, bus voltage control, power factor correction, network reconfiguration, generation curtailment, etc., are mostly used approaches to enhance the DGHC/PVHC of a network [120-123, 125]. The reactive power compensation using static VAr compensator and bus voltage control using OLTC are used in [34] to maximize the DGHC of the distribution network considering the uncertainties in the generation of DG units and load demand. In [126], the reactive power compensation, wind energy curtailment, and bus voltage control using OLTC are used to maximize the wind power hosting capacity of a distribution network considering the individual benefits of the owners of the wind farm and the distribution network. In [32], a multi-objective optimization model is formulated to optimally place the BESS in a distribution network to improve the DGHC of the network. In this work, BESS is utilized for three purposes: bus voltage control, power loss reduction, and peak demand reduction. In [127], a mixed-integer nonlinear type of planning problem is formulated to maximize the PVHC of distribution networks using the optimal controls of capacitor switching, voltage regulator, branch switches, and smart PV inverters. The investigation of the impact of PV location and PV operating power factor on the PVHC of distribution networks is also carried out. A multistage and stochastic mathematical model is presented in [128] to maximize the DGHC of distribution networks. The ESSs, reactive power sources, and network reinforcement are used to maximize the DGHC. The part II of this work [129] provides the numerical

results and merits of the proposed model. In [130], the PVHC of a distribution network is determined by considering the daily variations in PV generation and load demand. It considers different scenarios of PV location and size to determine the PVHC of a network. Furthermore, the estimation of percentage of accuracy of PVHC and the impact of different network and simulation parameters on the PVHC are studied. In [131], a control scheme is proposed for the control of reactive power output of the main PV inverters and some auxiliary converters. The controllable range of reactive power compensation mitigates the large voltage variations and increases the PVHC of a network. In [132], the static network reconfiguration at the planning stage and dynamic network reconfiguration using controllable switches are used to enhance the DGHC of a network. In [133], the operation of OLTC is controlled based on the PV generation forecast to enhance the PV penetration in a distribution network. In [134], a multi-period multi-objective planning problem is formulated to simultaneously maximize the DGHC and to minimize the energy loss of a network. The modelling of load and generation uncertainties, co-ordinated operation of OLTCs and voltage regulators, generation curtailment, and reactive power control of DG unit are the key features of this approach. In [135], a centralized battery storage system (BSS), which consists of batteries and converter units, is used for the control of both active and reactive power in the network to improve the hosting capacity of a network. The different combination of the sizes of BSS and converter units are used to maximize the PVHC. In [136], DSTATCOM along with ESS, OLTC, and PV inverter are used for the voltage management to increase the rooftop PVHC along with the reduction in voltage unbalance factor, and the maximum and minimum voltage limits violation. All these works are mostly focused on the determination of DGHC and the development of different types of technologies or control schemes to enhance the DGHC of distribution networks. The motivations behind this research proposal are the following research gaps seen in the above-mentioned literature:

- Although the total power loss is an important performance index for the distribution networks, none of the above-mentioned works considers it as a constraint in defining the hosting capacity.

- The roof-top PV generation can be installed in every location of a network. Thus, it is of interest to determine the optimal PV generation capacity in each bus of a network for the maximization of the hosting capacity.
- The different types of converter/inverter can be used as sources of reactive power compensation to increase PVHC as shown in [135-136]. But, this needs an appropriate modelling and allocation planning. Although the allocation planning of converter/inverter is reported in [135-136], the modelling of the converter/inverter unit to determine the size/rating requirement is not done. Rather, the converter/inverter size is chosen from an available set of sizes. Moreover, the potential of series inverter allocation in maximizing PVHC is not investigated in any work.
- As mentioned above, the injection of DG/PV beyond a certain limit deteriorates the network performance and it causes increase in energy loss. Hence, there needs to have a simultaneous optimization approach for the maximization of PVHC and minimization of energy loss. In none of these works, it is done.
- The PQ is an important issue for the distribution networks. Hence, there needs to have an approach which can capable of maintaining a desired PQ level as well.

Thus, in this chapter, mono- and multi-objective planning approaches are developed to improve PVHC and energy efficiency of distribution networks. These two planning approaches are separately shown in two sections of this chapter. For mono-objective planning approach, the hosting capacity is firstly defined considering the power loss as a performance index. Then, the modelling of two different types of inverters of UPQC-O, i.e., series and shunt inverters is done. The series inverter is designed to provide the reactive power compensation by injecting a series voltage into a network. The shunt inverter is designed to provide both harmonic compensation and reactive power compensation by injecting a shunt compensating current into a network. A planning optimization model is formulated to optimally place these inverters of UPQC-O to maximize the PVHC of a network. The worst-case scenario, i.e., minimum load demand and maximum PV generation is considered to determine the PVHC of a network. The usage of these inverters in any other loading condition also results in power loss reduction of the network. The PSO is used as the solution approach. However, in multi-objective planning approach, a multi-

objective planning problem is formulated for the simultaneous optimization of PVHC and energy loss of distribution networks. The inverters of UPQC-O are used to simultaneously provide the reactive power compensation and PQ mitigation. In this approach, the series inverter is designed to mitigate voltage sag during voltage sag condition and to provide reactive power during healthy condition. However, the functions of shunt inverter are same as mentioned for the mono-objective planning. The MOPSO-based planning algorithm is chosen as the solution strategy, in which Pareto-dominance principle [137] is used to find out a set of non-dominated solutions called Pareto-approximation set. The strength Pareto Evolutionary algorithm-2 (SPEA2) [138] is used in MOPSO for fitness assignment and archiving of solutions. The highlights of the contribution of this work are:

- Formulation of a mono-objective planning problem to maximize the PVHC of a distribution network considering the network power loss as one of the operational constraints.
- Modelling of series and shunt inverters for reactive power compensation of radial distribution networks.
- Development of mono-objective planning approach to optimally place the series and shunt inverters of UPQC-O, and to determine the maximum PV generation capacity in each bus, except the substation bus, for the maximization of PVHC of a network.
- Development of multi-objective planning approach for the simultaneous optimization of PVHC and energy loss of distribution networks.
- Modelling and allocation of UPQC-O, which can be used to improve the energy loss and PQ of distribution networks.

The proposed planning approaches are validated on 33-bus and 69-bus radial distribution networks.

4.2 Mono-objective planning for the maximization of PVHC

In this section, a study is carried out with the mono-objective optimization problem formulated for the maximization of PVHC of a distribution network. The simulation results obtained with this approach are presented and discussed in this section.

4.2.1 Determination of the DGHC

The maximum amount of DG that can be accommodated by a distribution network without deteriorating the operational performance of the network is known as the DGHC of the network [139]. The injection of DG into a network initially results in improvement in the operational performance of the network in terms of power loss reduction, improvement in bus voltages, reduction in line current flow etc. But, after a certain value of DG injection, the operational performance of the network starts deteriorating, i.e., it increases the network power loss and it also causes over voltage problem to the buses and/or thermal limit violation of the lines etc. The operational performance of a network with respect to increment in the amount of DG injection is shown in Fig. 4.1. It is seen from the figure that, the DGHC can either be set at the point above which the network performance starts deteriorating, or at the point above which the deterioration in the operational performance of the network is unacceptable. For mono-objective planning, network power loss is considered to be the performance index to determine the rooftop PVHC of a distribution network. Each bus of a distribution network is chosen as the potential sites to install the rooftop PV array, as shown in the 7-bus radial distribution network in Fig. 4.2, in which the bus 1 is the substation bus and remaining all buses are load buses.

The following are the assumptions and features of this work:

- All the PV arrays are operating at unity power factor.
- The series and shunt inverters are designed to provide the reactive power compensation to the network irrespective of the loading and generation conditions.
- The rating requirements for the series and shunt inverters are determined at peak load demand so that these can also be operated during the peak load demand.
- The peak load demand and the maximum PV generation do not coincide with each other.

Based on these, the following planning cases are proposed:

- *Case A*: In this planning case, the PVHC of a network is maximized without placement of inverters of UPQC-O considering the minimum load and maximum generation scenario under the constraint of no deterioration in the power loss with respect to the base-case network, i.e., without PV array.

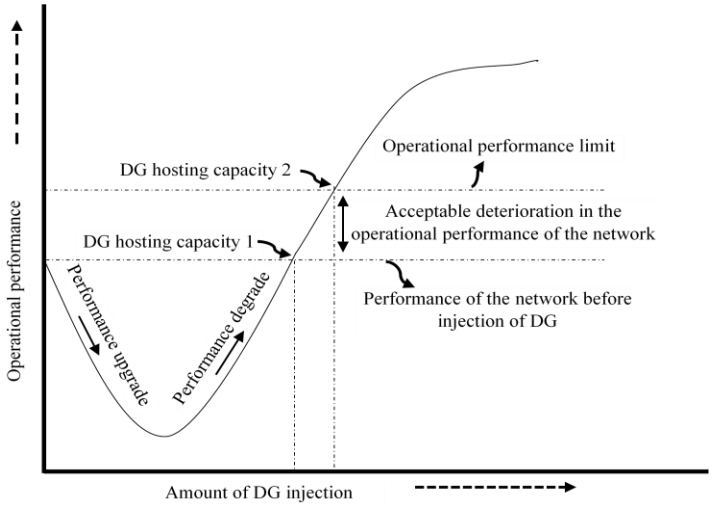

Fig. 4.1: Plot of operational performance of a distribution network with respect to amount of DG injection used for the determination of DGHC

- *Case B*: In this planning case, the series and shunt inverters are to be optimally placed to maximize the PVHC of a network considering the minimum load and maximum generation scenario under the constraint of no deterioration in the power loss with respect to the base-case network.

The acceptable power losses in planning Cases A and B are modified by considering 10% deterioration with respect to the power loss of the base-case network to obtain the new planning cases and these are named as Case A(a) and Case B(a), respectively. To understand the effect of inverter placement during the peak load with no PV generation, a separate case study is provided.

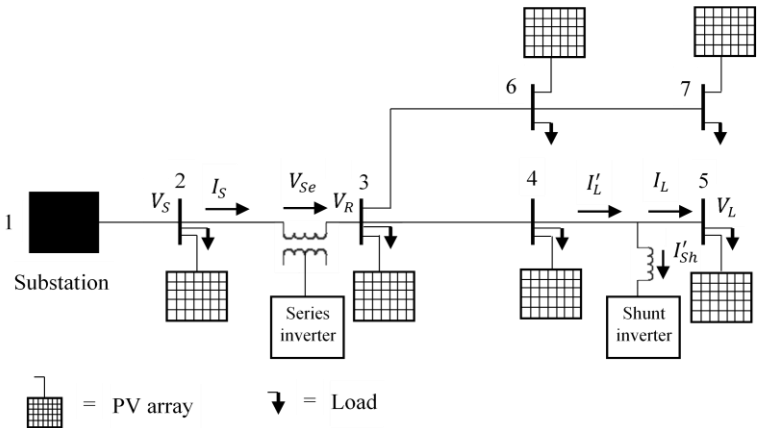

Fig. 4.2: A 7-bus radial distribution network with the placement of PV arrays and series and shunt inverters

4.2.2 Modelling of series and shunt inverters

This section describes the mathematical modelling of the series and shunt inverters for distribution networks. The series inverter is designed to inject the series voltage V_{Se} to maintain the receiving end voltage magnitude at 1.0 p.u. by providing the reactive power compensation. However, the shunt inverter is designed to inject the shunt compensating current I'_{Sh} to eliminate the current harmonics present in the line current I_L and to provide the reactive power compensation. The phasor diagrams of series and shunt inverters are shown in Figs. 4.3 (a) and (b), respectively.

4.2.2.1 Modelling of the series inverter

The amount of series voltage injected by the series inverter can be calculated as:

$$V_{Se} = \sqrt{{V_R^C}^2 + {V_R}^2 - 2V_R^C V_R \cos(\delta'_2 - \delta_2)} \tag{4.1}$$

From Fig. 4.3(a),

$$V_R^C \cos\delta'_2 = V_R \cos\delta_2 + V_{Se}\cos(90° - \emptyset) \tag{4.2}$$

$$V_R^C \sin\delta'_2 = V_R \sin\delta_2 + V_{Se}\sin(90° - \emptyset) \tag{4.3}$$

From Eqs. (4.2) and (4.3),

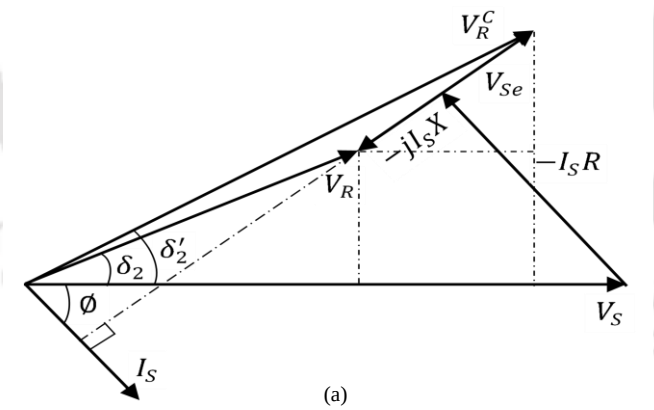

(a)

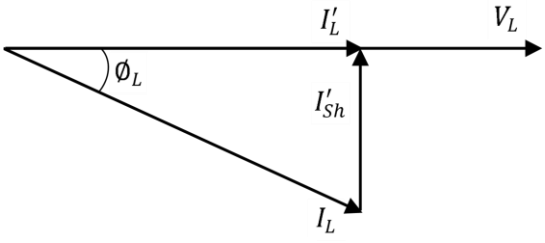

(b)

Fig. 4.3: Phasor diagrams for: (a) series and (b) shunt inverters

$$V_R^C \cos(\delta_2' + \emptyset) = V_R \cos(\delta_2 + \emptyset) \quad (4.4)$$

From Eq. (4.4), the phase angle δ_2' can be calculated as:

$$\delta_2' = \cos^{-1}\left(\frac{V_R}{V_R^C}\cos(\delta_2 + \emptyset)\right) - \emptyset \quad (4.5)$$

The VA-rating of series inverter is computed as:

$$S_{Se} = V_{Se} I_S \quad (4.6)$$

Here, the phase angle between V_{Se} and I_S is to be maintained at 90° to provide reactive power compensation. The amount of reactive power supplied by the series inverter is,

$$Q_{Se} = S_{Se} \quad (4.7)$$

4.2.2.2 Modelling of the shunt inverter

In this work, the function of shunt inverter is same as that of the shunt inverter of UPQC-O-WOP. The shunt inverter can be mathematically modelled by using Eqs. (2.55)-(2.58). The total amount of VAr injected by the inverters of UPQC-O can be computed by summing up the individual VAr injection capacities of series and shunt inverters.

4.2.3 Incorporation of PV generation and inverters models into FBSLF

The PV generation and inverters models are incorporated into the FBSLF algorithm [74] to determine the network bus voltages, line current flows, and power loss. The algorithmic steps of the FBSLF algorithm are discussed in subsection 2.3.1. If the PV array injects active power at load bus l and the series (shunt) inverter injects reactive power at load bus m (n) the active and reactive power demands of corresponding buses are to be modified as:

$$P'(l) = P(l) - P_{PV}(l) \quad (4.8)$$

$$Q'(m) = Q(m) - Q_{Se} \quad (4.9)$$

$$Q'(n) = Q(n) - Q_{Sh} \quad (4.10)$$

where, $P_{PV}(l)$ is the maximum PV generation capacity of bus 'l'. Q_{Se} and Q_{Sh} are the rated VAr injected by the series and shunt inverters, respectively.

The load flow analysis is carried out with the modified active and reactive power demands.

4.2.4 Mono-objective optimization problem for the maximization of PVHC

This section describes the optimization problem formulated for the maximization of PVHC of a network. In this optimization problem, the locations of series and shunt inverters, and the PV generation capacity in each bus except the substation bus are determined by maximizing the PVHC, i.e., total PV generation capacity. The objective function is given below.

$$\max\{PVHC\} = \sum_{i=2}^{N} P_{PV}(i) \tag{4.11}$$

This objective function is to be maximized under the active and reactive power balance constraints, bus voltage magnitude constraint, thermal constraint, and network power loss constraint. The active and reactive power balance constraints, bus voltage magnitude constraint, and thermal constraint are mathematically expressed as shown in Eqs. (2.88-2.89), (2.90), and (2.91), respectively. However, the network power loss constraint is defined below.

- *Network power loss constraint*: According to this constraint, the power loss of a network with the PV generation (PL_{PV}) during minimum loading condition should not be more than a pre-set acceptable power loss during minimum loading condition. The mathematical expression for this constraint is given below.

  $$PL_{PV} \leq \vartheta PL_{base} \tag{4.12}$$

  where, ϑ is a constant factor. In the planning Cases A and B, the value of ϑ is set to be 1. This means that the maximum acceptable power loss with PV integration is considered to be the power loss of the base-case network (PL_{base}) during minimum loading condition. In planning Cases A (a) and B (a), the value of ϑ is set to be 1.1. This implies to fact that the maximum acceptable power loss of the network with PV is considered to be 1.1 time of the power loss of the base-case network during minimum loading condition.

4.2.5 Solution approach for mono-objective planning

The PSO algorithm [107-108] is used as the solution approach to optimally place the series and shunt inverters of UPQC-O in a distribution network, and to obtain the optimal PV generation capacities in all the buses, except the substation bus. The PSO algorithm is discussed in subsection 2.5.1. The FBSLF algorithm incorporating the PV

generation and inverters models is used as the supporting subroutine of the PSO algorithm. A particle of PSO consists of the information of location of series inverter, location of shunt inverter, and PV generation capacity in each load bus. The pseudo codes for the overall planning algorithm are shown in Fig. 4.4.

Begin
Input radial distribution network bus data and line data;
Input THD_L, itr_{max}, C_1, C_2, $Penalty\ Factor$, N_{Pop}, $I_{TH}(mn)$, V_{max}, V_{min}.
Initialize random position and velocity of the particles of size N_{Pop} for PSO;
Decode the particles and calculate fitness values;
Find initial individual best position (L_{Best}) and neighbourhood best position (G_{Best});
For *iteration*=2: itr_{max}
  For *i*=1: N_{Pop}
    Update velocity and position of particles;
    Decode particle position to obtain the locations of inverters and PV generation capacities at all the load buses;
    Perform FBSLF algorithm with PV generation and inverters models;
    Calculate the fitness value for each particle;
    If any particle violates constraints, a penalty factor is added with it;
  End
  Update L_{Best} and G_{Best};
End
The final G_{Best} value provides the locations of series and shunt inverters and PV generation capacities at all the load buses;
End

Fig. 4.4: Pseudo codes for the maximization of PVHC of a distribution network using PSO

4.2.6. Simulation results of mono-objective planning

This section presents the results obtained with the proposed mono-objective planning approach for the maximization of PVHC constrained by a permissible network power loss. The proposed mono-objective planning cases are validated on 33-bus and 69-bus radial distribution networks. The description on these test networks is provided in section 2.6. In this work, the shunt inverter is designed to compensate 20% of line current THD and series inverter is designed to maintain the receiving end voltage magnitude at 1.0 p.u. The maximum acceptable deterioration in the performance index (i.e., network power loss at minimum load demand) is considered to be 10%. The minimum load demand of the network is considered to be 20% of peak load demand of the network [34]. The minimum and maximum voltage limits for load bus are considered to be 0.95 p.u. and 1.05 p.u., respectively. The thermal limit for each line of the 33-bus network is considered as 300 A as given in [34]. The thermal limit for each line of the 69-bus network is taken from [109]. The maximum capacities for the PV generation in any bus are judiciously set as 115 kW

and 70 kW, for the 33- and 69-bus, respectively. The PSO parameters are optimized with repetitive runs and the optimal parameters are found to be: C_1=2, C_2=2, and w=0.2. The population size for 33-bus and 69-bus networks are found to be 200 and 500, respectively. The maximum iteration for 33-bus and 69-bus networks are found to be 100. The solutions as obtained with the PSO algorithm are listed in Tables 4.1 and 4.2 for the 33-bus and 69-bus networks, respectively.

4.2.6.1 PVHC

The PVHC of the planning Cases B and B(a) are found to be more as compared to the planning Cases A and A(a), respectively as shown in Tables 4.1 and 4.2. This happens because the reactive power compensation provided by the series and shunt inverters in Cases B and B(a) results in network power loss reduction. Thereby, it helps in accommodating more PV generation by satisfying the power loss constraint. The PV hosting capacities in Cases A(a) and B(a) are found to be more as compared to the Cases A and B, respectively. This happens because of the higher value of the acceptable power loss set in Cases A(a) and B(a) as compared to those of the Cases A and B, respectively. It is imperative that a network can accommodate more PV injection if the acceptable power loss is set with the higher values.

4.2.6.2 Bus voltages of the network

The plots of bus voltages for the 33-bus and 69-bus networks for different planning cases are shown in Figs. 4.5(a) and (b), respectively. From these plots, it is observed that the voltages in each bus is almost equal to the substation voltage, i.e., 1.0 p.u. In planning Cases B and B(a), the voltages in some of the buses are found to be slightly higher as compared those obtained with planning Cases A and A(a), respectively. It happens because of the higher injection of PV generation in Cases B and B(a).

4.2.6.3 Maximum line current flow

From Tables 4.1 and 4.2, it is observed that the maximum line current flows in both the networks are higher in planning Cases A (a) and B (a) than those obtained with planning Cases A and B, respectively. This happens because the total PV penetration is higher in

planning Cases A (a) and B (a) due to the increase in the maximum allowable power loss set.

Table 4.1: Solutions of different planning cases for the 33-bus radial distribution network

Solution	Case A	Case A (a)	Case B	Case B (a)
Maximum line current flow (A)	58.8332	61.0790	61.4370	63.3236
Maximum bus voltage (p.u.)	1.0043	1.0043	1.0092	1.0099
PVHC (MW)	1.9538	2.0070	2.0870	2.1273
Location of series inverter	-	-	7	8
Location of shunt inverter	-	-	32	32
VA rating of series inverter (kVA)	-	-	144.5730	128.2288
VA rating of shunt inverter (kVA)	-	-	152.6638	152.6638
Total VA rating of UPQC-O (kVA)	-	-	297.2368	280.8926
Percentage of PV penetration	52.5922	54.0242	56.1777	57.2624
Increase in PVHC as compared to Case A/ Case A(a) (%)	-	-	6.3824	5.6550

Table 4.2: Solutions of different planning cases for the 69-bus radial distribution network

Solution	Case A	Case A (a)	Case B	Case B (a)
Maximum line current flow (A)	110.4726	113.9755	116.3917	120.4878
Maximum bus voltage (p.u.)	1.0048	1.0051	1.0085	1.0083
PVHC (MW)	3.1289	3.2084	3.3121	3.4012
Location of series inverter	-	-	61	61
Location of shunt inverter	-	-	23	69
VA rating of series inverter (kVA)	-	-	294.0741	294.0741
VA rating of shunt inverter (kVA)	-	-	42.3096	21.1509
Total VA rating of UPQC-O (kVA)	-	-	336.3837	315.2250
Percentage of PV penetration	82.2918	84.3827	87.1101	89.4535
Increase in PVHC as compared to Case A/ Case A(a) (%)	-	-	5.5312	5.6686

4.2.6.4 VA-rating of inverters of UPQC-O

The VA-rating requirements for the series and shunt inverters in planning Cases B and B(a) are provided in Tables 4.1 and 4.2 for 33-bus and 69-bus networks, respectively. The total VA-rating requirement for inverters of UPQC-O is found to be higher in Case B as compared to Case B(a). It happens because the higher allowable power loss limit set in Case B(a) requires less amount of VAr support as compared to Case B. Basically, the higher value of VAr injection into the network at appropriate locations results in higher value of power loss reduction and vice-versa. Hence, the Case B(a) requires less VAr support as compared to Case B.

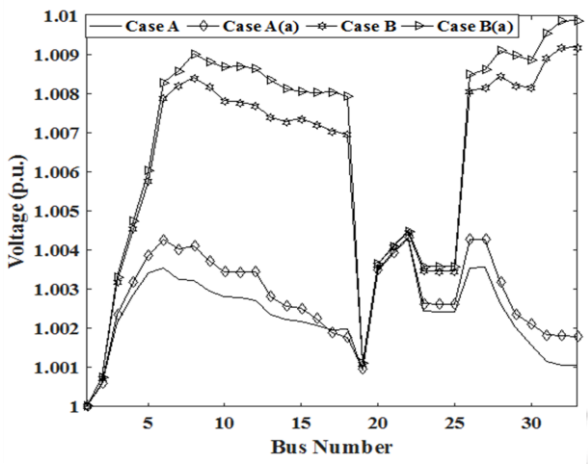

(a)

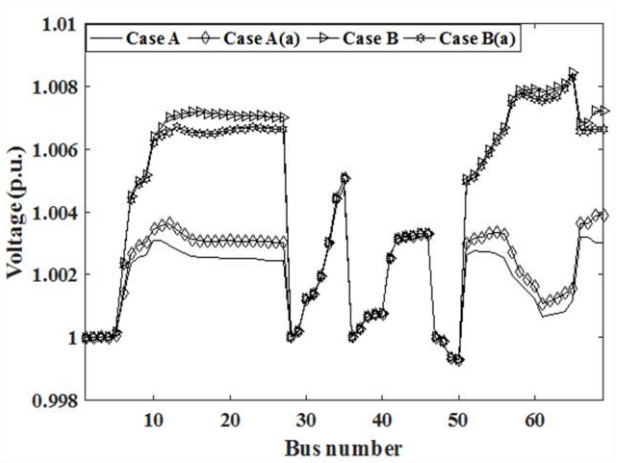

(b)

Fig. 4.5: Voltage profile for: (a) 33-bus and (b) 69-bus neworks as obtained with PSO

4.2.6.5 Effect of placement of inverters of UPQC-O on network power loss and bus voltages during peak load and no PV generation

The series and shunt inverters can also be used to provide VAr support to the network during other loading conditions, as well. To have a case study, the same rated series and shunt inverters, as obtained with the planning Cases B and B(a), are integrated in peak load and no PV generation scenario to show their impact on the network operational parameters. The results are shown in Table 4.3. The results indicate that the placement of inverters reduces the network power loss and it also improves the bus voltages of the network as compared to uncompensated base-case network. Similarly, the same inverters can also be deployed in any other loading conditions to reduce the power loss of the network

and thereby, to improve the energy efficiency of the network. This shows that the deployment of series and shunt inverters of UPQC-O in distribution networks can simultaneously improve the hosting capacity and energy efficiency.

Table 4.3: Power loss as obtained with PSO for the networks with the placement of inverters during peak load and no PV generation

Operational parameters of the network due to the inverter placement during the peak load and no PV generation	33-bus network			69-bus network		
	Base-case network	With Solutions of Case B	With Solutions of Case B(a)	Base-case network	With Solutions of Case B	With Solutions of Case B(a)
Location of series inverter	-	7	8	-	61	61
Location of shunt inverter	-	32	32	-	23	69
VA rating of series inverter (kVA)	-	144.5730	128.2288	-	294.0741	294.0741
VA rating of shunt inverter (kVA)	-	152.6638	152.6638	-	42.3096	21.1509
Minimum bus voltage (p.u.)	0.9131	0.9167	0.9168	0.9092	0.9144	0.9143
Network power loss (kW)	202.6762	181.7134	181.6691	225.0021	193.9810	195.1501
Reduction in power loss compared to base-case network power loss (%)	-	10.3430	10.3648	-	13.7870	13.2674

4.2.6.6 The optimal PV generation capacities as obtained with PSO

Since PSO is a meta-heuristic optimization algorithm, the solutions obtained with its different simulation runs may differ. Hence, to determine the optimal sizes for the PV array in each bus of the network, 30 independent simulation runs are taken. The PV generation capacity in each bus as obtained with PSO in different runs are shown with boxplots in Figs. 4.6 and 4.7 for the 33-bus and 69-bus networks, respectively. From the boxplots, it is observed that the buses near to substation are capable of accommodating the maximum capacity for the PV generation set. However, this is not happening in case of the buses located distant away from the substation. The result is found to be consistent in both the planning cases and in both the test networks. For example, the optimal values for PV capacity as obtained with PSO in buses 2-9 and 28-53 of the 69-bus network are found to be 70 kW, which is the maximum capacity for the PV array set in any location. It can be seen from the Fig. 2.10(b) that these are the buses located near to the substation. Similarly, in the 33-bus network, the optimal values for PV capacity as obtained with PSO in buses 2-6 and 19-25 are found to be the maximum capacity for the PV array set. These buses are also located near to the substation, as seen in Fig. 2.11(b). The optimal PV capacity as obtained with PSO in other than these buses varies between zero to the maximum capacity set. It is also noteworthy that the optimal locations of the inverters, as obtained with PSO,

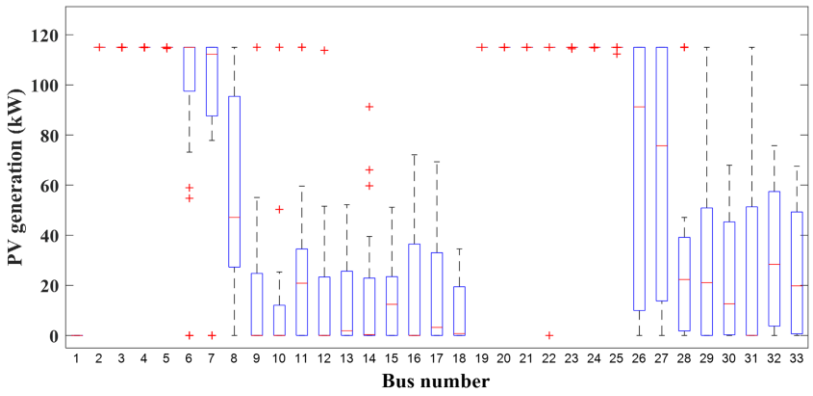

(a)

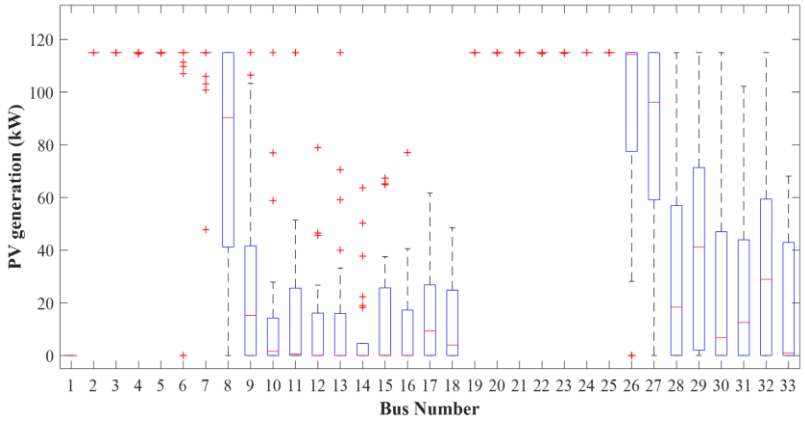

(b)

Fig. 4.6: Boxplot for the PV generation capacities in each bus of the 33-bus network as obtained with PSO: (a) Case A and (b) Case B

are found to be the buses located distant away from the substation. This shows that these buses need VAr support so as to enhance the overall hosting capacity of the network.

4.2.6.7 Impact of placement of single series and single shunt inverter on PVHC

In this section, a comparative case-study considering two planning cases are shown to study the PVHC with the placement of: (i) a series inverter and (ii) a shunt inverter by fixing the location in each bus of a distribution network, one at a time. The 33-bus network is used for this case-study. The PVHC as obtained with the placement of single inverter is shown in Fig 4.8(a). The result shows that the placement of either series or shunt inverter results in similar PVHC in some of the buses. The PVHC obtained with the placement of a shunt inverter at bus 31 is found to be the best solution with single inverter. The placement of single series inverter provides the highest PVHC at bus 6. The rating requirement of

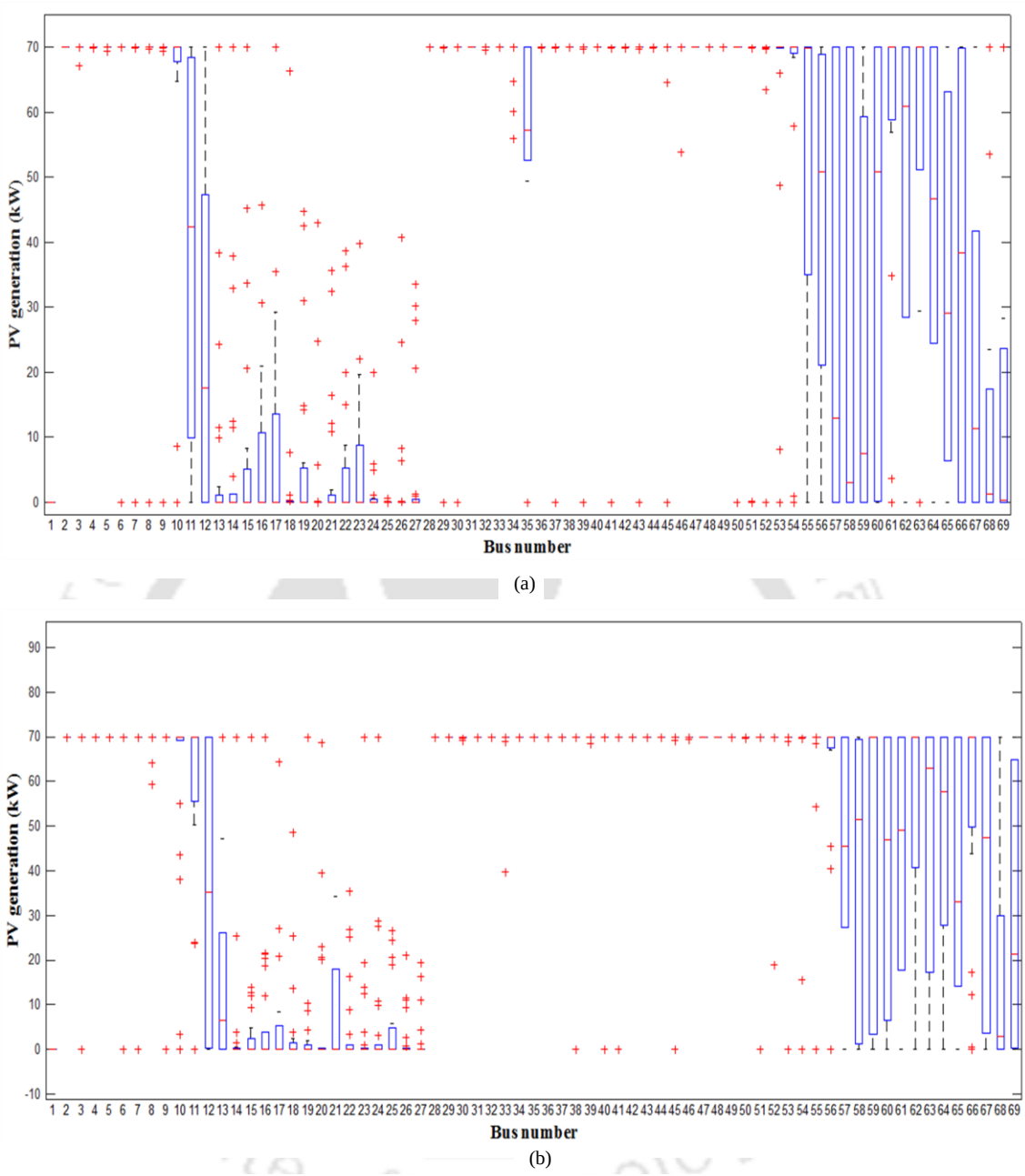

Fig. 4.7: Boxplot for the PV generation capacities in each bus of the 69-bus network as obtained with PSO: (a) Case A and (b) Case B

inverter, the network power loss, and the minimum bus voltage due to the placement of inverter are also shown in Figs. 4.8(b)-(d), respectively. No feasible solutions are obtained for the shunt inverter placement in some of the locations, for example buses 3-6 and 26-30. The VA rating requirement of the series inverter is found to be less as compared to the shunt inverter. The lower VA-rating requirement for the series inverter placement is advantageous, but its placement effects the reliability of the network, since the addition of a series element

deteriorates the reliability of a network. Fig. 4.8 (c) shows that the placement of a shunt inverter is more effective in the reduction of network power loss than the placement of a series inverter. The placement of higher rated shunt inverter provides higher reactive power compensation. This results in higher power loss reduction. For the same reason, the network minimum bus voltage magnitude obtained with the placement of a shunt inverter is found to be relatively better as compared with the placement of a series inverter. The best solutions obtained with single series and single shunt inverter placement in view of PVHC are compared with the best solution obtained with the placement of both types of inverter in Table 4.4. The results show that the combined placement provides better PVHC as compared to the placement of single shunt inverter or single series inverter. The individual rating requirements of the inverters of the solution obtained with the placement of both types of inverters of UPQC-O are also less.

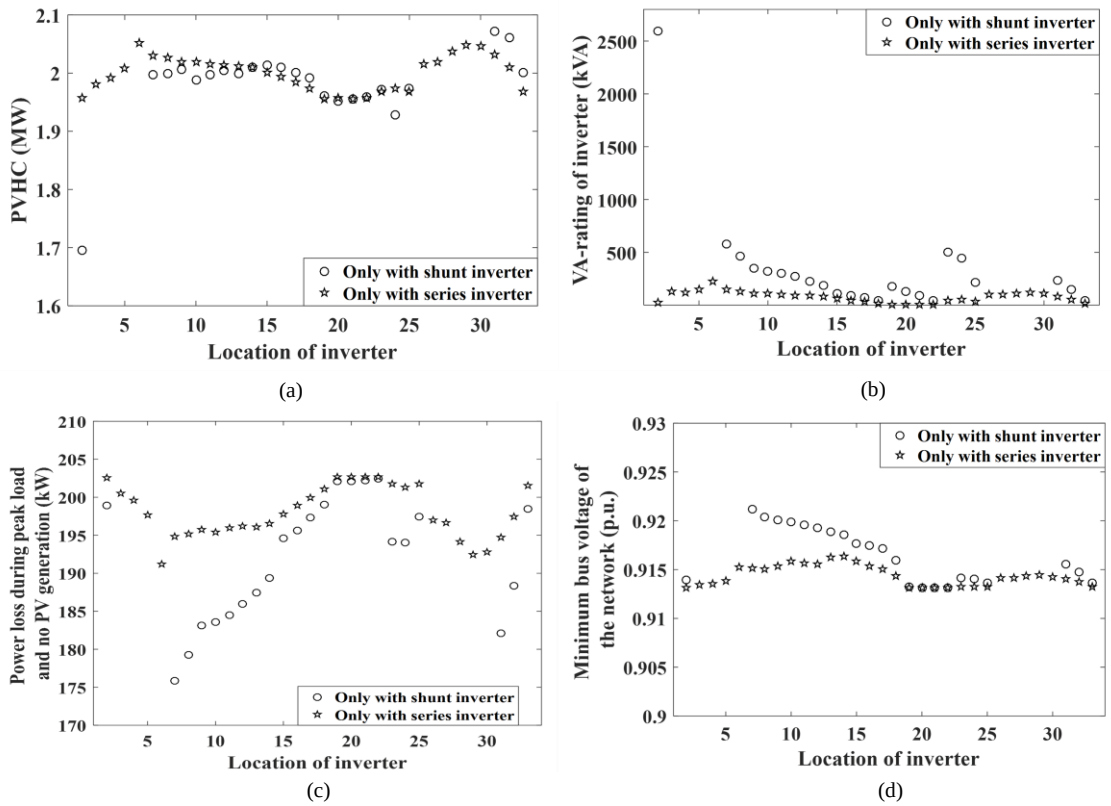

Fig. 4.8: The effect of a single inverter placement in each load bus of the 33-bus network on: (a) PVHC, (b) VA-rating requirement of inverter, (c) power loss during peak load and no PV generation, and (d) minimum bus voltage of the network as obtained with PSO

Table 4.4: The best solution obtained in view of PVHC in planning Case B for 33-bus network

Solution	With series and shunt inverters	Only with shunt inverter	Only with series inverter
Location of series inverter	7	-	6
Location of shunt inverter	32	31	-
VA rating of series inverter (kVA)	144.5730	-	224.8068
VA-rating of shunt inverter (kVA)	152.6638	230.3154	-
Total VA rating of inverters (kVA)	297.2368	230.3154	224.8068
PVHC (MW)	2.0870	2.0714	2.0511
Network power loss (kW)	181.7134	182.0773	191.1631

Table 4.5: Qualitative comparison of proposed approach with the approaches reported in [134-135]

Planning tasks	Proposed approach	Approach reported in [134]	Approach reported in [135]
Objective function	Maximization of PVHC	1. Maximization of total installed DG capacity 2. Minimization of energy loss and energy consumption of voltage dependent loads	Maximization of PVHC
Optimizing variables	Locations for the placements of series and shunt inverters, and PV generation capacity in each load bus	Tap positions of voltage regulators and OLTCs, sizes of DG units, generation curtailment, and reactive power injected by DG units	Active and reactive power output of central BSS
Solution tool	PSO	Mixed integer programming	*fmincon* function of MATLAB
Type of DG units	PV	Wind turbine and synchronous generator	PV
Type of compensator	Series and shunt inverters	No compensator is used	Shunt converter
Modelling of compensator	Sizes of series and shunt inverters are determined based on the modelling provided in subsections 4.2.2.1 and 4.2.2.2, respectively	---	No modelling of converter is done. The size of shunt converter is selected from a set of given sizes
Special features/ contributions	PVHC constrained with an allowable power loss and the design of shunt inverter to provide both harmonics and reactive power compensations	Probability based modelling of load and generation uncertainties	Control of the active and reactive power with centralized battery based storage system

4.2.6.8 Comparison of proposed mono-objective planning approach with similar approaches

In the proposed mono-objective planning approach, the series and shunt inverters are used to improve the PVHC and energy efficiency of radial distribution network. There are several approaches reported in the literature for the maximization of PVHC of distribution networks, such as, network reconfiguration, line conductor replacement, reactive power control etc. However, only two approaches [134-135] are found, in which the maximization of DGHC/PVHC along with energy/power loss minimization is considered in the optimization problem. Since the problem formulation, the optimizing variables, and the planning tasks reported in [134-135] are completely different than the

proposed work, the quantitative performance comparison is not possible. Hence, a qualitative performance comparison with [134-135] is shown in Table 4.5. The contribution of each approach is summarized in the last row of the table.

4.3 Multi-objective planning for simultaneous optimization of PVHC and energy loss of distribution network

In this section, the multi-objective optimization problem formulated for the simultaneous optimization of PVHC and energy loss of distribution networks is discussed. The simulation results obtained with the proposed multi-objective optimization approach are also presented and discussed in the subsequent subsections.

4.3.1 Multi-objective optimization problem

The objectives of proposed multi-objective optimization problem are: (i) maximization of PVHC and (ii) minimization of energy loss of distribution networks. These two objectives are optimized to determine the PV generation capacity in each bus, except substation bus, and the locations of inverters of UPQC-O to provide reactive power compensation. These two objectives are mathematically expressed as:

Objective 1: $\max\{PVHC\} = \sum_{i=2,\ldots,N} P_{PV}(i)$ (4.13)

Objective 2: $\min\{EL\} = \sum_{c\in\psi} PL_c t_c$ (4.14)

where, N is the total number of buses in the network; $P_{PV}(i)$ represents the PV generation capacity of bus 'i'; EL represents the total energy loss of network with PV during a day; ψ is the set of different load and generation scenarios; PL_c represents the total line losses in the network during load and generation scenario 'c'; and t_c is the duration of load and generation scenario 'c'.

These objectives are optimized under the active and reactive power balance constraints, bus voltage magnitude constraint, thermal constraint, PVSML constraint, and PV capacity constraint. The active and reactive power balance constraints, bus voltage magnitude constraint, thermal constraint, and PVSML constraint are mathematically expressed as shown in Eqs. (2.88-2.89), (2.90), (2.91), and (2.93), respectively. However, the PV capacity constraint is discussed below.

- *PV capacity constraint*: The PV generation capacity in each bus is restricted in between minimum and maximum set values, i.e.,

$$(P_{PV})_{min} \leq P_{PV}(i) \leq (P_{PV})_{max}, \qquad i \in [2,..,N] \qquad (4.15)$$

where, $(P_{PV})_{min}$ and $(P_{PV})_{max}$ are the minimum and maximum set values of PV capacity.

The DG/PV integration beyond a certain value leads to increase in power loss, as explained in section 4.2.1. Hence, the maximization of PVHC results in higher power/energy loss [139]. Thus, the maximization of PVHC and minimization of energy loss are two conflicting objectives and this needs a multi-objective optimization approach so as to simultaneously optimize these two objectives. This yields a set of non-dominated solutions, in which none of the solutions is superior to other [137]. Finally, a solution can be selected from the set of non-dominated solutions according to the requirement of a utility. For example, if a utility desires to implement the solution corresponding to the lowest energy loss, it can select the solution corresponding to the lowest PVHC and vice-versa. There are different multi-objective optimization approaches [137], for example weighted aggregation, Pareto-based approach, lexicographic ordering etc. In this work, the Pareto-based approach is used.

4.3.1.1 Pareto-dominance principle

The Pareto-dominance principle [137] states that, for an M-objective optimization problem, a solution 'a' dominates a solution 'b' if the following two conditions satisfy.

i. The solution 'a' is no worse than solution 'b' in all objectives, i.e.,

$\forall_e, f_e(a) \leq f_e(b)$ for minimization of objective

$\forall_e, f_e(a) \geq f_e(b)$ for maximization of objective

where, $e = 1,2,..,M$

ii. The solution 'a' is strictly better than solution 'b' in at least one objective, i.e.,

$f_h(a) < f_h(b)$ at least for one $h \in \{1,2,..,M\}$ for minimization objective

$f_h(a) > f_h(b)$ at least for one $h \in \{1,2,..,M\}$ for maximization objective

The set of the optimal non-dominated solutions is called the Pareto-optimal set.

4.3.2 Modelling of UPQC-O

In this work, the UPQC-O is designed to support the reactive power demand of the system and thereby, it helps in reduction in energy loss. The functions of series and shunt inverters during voltage sag and healthy conditions are same as that of the functions of inverters of UPQC-O-WOP model (*Refer Table 2.1*). Thus, the same phasor diagrams, as shown in Figs. 2.4(a) and 2.4(b), are used to model the series and shunt inverters of UPQC-O, respectively. The series inverter can be mathematically modelled by using Eqs. (2.46)-(2.52). However, the shunt inverter is mathematically modelled by using Eqs. (2.55)-(2.58). The total VA-rating of UPQC-O is determined by summing up the individual VA-ratings of series and shunt inverters.

4.3.3 SPEA2-MOPSO based solution approach

This section describes the MOPSO-based multi-objective planning algorithm to determine the optimal PV generation capacity in each bus, except the substation bus and the optimal locations for the series and shunt inverters of UPQC-O. The basics of PSO algorithm are discussed in subsection 2.5.1. The SPEA2-based MOPSO is described in the subsequent section.

4.3.3.1 Assumptions

The following assumptions/considerations are used for the operation of rooftop PV and UPQC-O in the proposed model:

- All rooftop PV arrays are always operating at unity power factor. Thus, they are capable of injecting only active power into the network during the operational hour.
- The PV generation hours and the peak demand hours do not coincide with each other. The peak demand takes place during evening 6 to 10 PM and this duration is named as peak hour. The rest of the time is treated as off-peak hour. The peak and off-peak demand refer to the average load demand during the peak and off-peak hours, respectively.
- The PV generation is directly injected into the network during operational hours of PV arrays. There is no provision for storage.

4.3.3.2 SPEA2-MOPSO

MOPSO is a version of PSO algorithm which is used to solve the multi-objective optimization problems. In this algorithm, multiple fitness values corresponding to the multiple objectives are assigned to each particle. In literature, many MOPSO variants are found. The state-of-the-art review on MOPSO is available in [140]. The most of the MOPSO approaches are based on the Pareto-dominance principle. All these approaches are used to find out a set of non-dominated solutions. The plot of the non-dominated solutions is called Pareto approximation front (PAF). In SPEA2-MOPSO, the non-dominated solutions obtained with the MOPSO algorithm are stored in an elite archive. This elite archive is utilized to assign fitness to each member of the archive itself and the current population undergoing evolution according to the fitness assignment scheme of SPEA2 [138]. Single fitness value is assigned to each particle according to its non-domination rank and solution density [137, 141].

4.3.3.3 MOPSO based planning algorithm

The overall MOPSO-based planning algorithm uses the FBSLF subroutine incorporating UPQC-O and PV models. A particle of MOPSO consists information of maximum PV generation capacity in each bus, except the substation, and the locations for series and shunt inverters. The flow chart for the overall planning algorithm is shown in Fig. 4.9. In this work, each particle consists of two fitness values corresponding to the following functions,

$$\textit{Fitness 1}: \max\{\mathcal{F}_1\} = \frac{\sum_{i=2,\ldots,N} P_{PV}(i)}{\sum_{i=2,\ldots,N} P(i)} \tag{4.16}$$

$$\textit{Fitness 2}: \min\{\mathcal{F}_2\} = \frac{\sum_{c\in\psi} PL_c t_c}{TEL_{base}} \tag{4.17}$$

The two objective functions as shown in Eqs. (4.13) and (4.14) are normalized with the total peak active power demand of base-case network and the total energy loss of base-case network in a day (TEL_{base}), respectively to obtain Eqs. (4.16)-(4.17). TEL_{base} is determined by summing up the energy loss of a distribution network during peak demand hours and off-peak demand hours without any compensation. The maximization of first fitness function provides the information of total PV generation capacity that a network can accommodate with respect to the total peak active power demand of the base-case network.

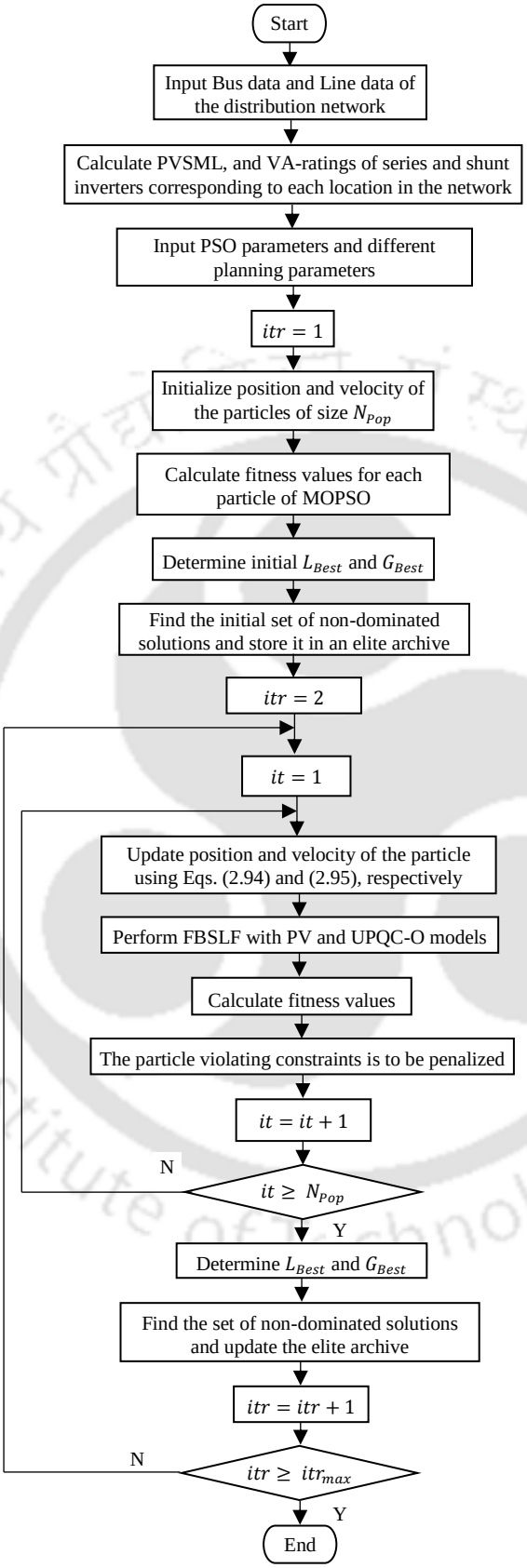

Fig. 4.9: Flow chart for the SPEA2-MOPSO-based multi-objective planning algorithm

The minimization of second fitness function results in the energy loss of network with PV in a day with respect to the energy loss of the base-case network in a day. These objectives are optimized under the constraints shown in Eqs. (2.88-2.89), (2.90), (2.91), (2.93), and (4.15).

4.3.3.4 FBSLF subroutine incorporating the PV generation and inverters models

In this approach, the FBSLF algorithm is also used incorporating the PV generation and inverters models to determine the network operational parameters, such as, bus voltage, line current flow [74] etc. The algorithmic steps of FBSLF are given in subsection 2.3.1. The incorporation of PV generation model at any bus modifies the active power demand of that bus, as shown in Eq. (4.8). However, the incorporation of series and shunt inverters models modifies the reactive power demand of corresponding buses, as shown in Eqs. (4.9-4.10). The amount of hourly average PV generation at bus 'i' during the PV operational hours is computed by using Eq. (4.18),

$$CUF = \frac{P_{PV}^{Avg}(i)t_4}{24P_{PV}(i)} \tag{4.18}$$

where, CUF is the capacity utilization factor of PV; t_4 is the operation hours of PV; $P_{PV}^{Avg}(i)$ and $P_{PV}(i)$ are the hourly average PV generation and the maximum PV generation capacity at bus 'i', respectively. The CUF is defined as the ratio of actual PV energy generation to the total PV energy generation capacity over a year. It is used to determine the hourly average PV generation $\{P_{PV}^{Avg}(i)\}$ which is to be used to compute the energy loss.

4.3.4 Simulation results of multi-objective planning

The proposed multi-objective planning approach for the simultaneous optimization of PVHC and energy loss of the network is validated on 69-bus and 33-bus radial distribution networks. In the proposed design of UPQC-O, the series inverter is designed to mitigate 30% of voltage sag during voltage sag condition and the shunt inverters are designed to compensate 20% of line current THD_L. The minimum amount of load to be protected from the voltage sag by the series inverter is set as 70%. The capacity utilization factor of the PV is considered to be 20%. The PVHC of the network is determined by

considering the minimum load and maximum PV generation scenario, i.e., the worst-case scenario. The following three different load-generation scenarios are considered for the determination of energy loss of the network:

- Scenario 1: peak load demand and no PV generation
- Scenario 2: off-peak demand without PV generation
- Scenario 3: off-peak demand with PV generation

The off-peak load demand and minimum load demand of the network are considered as 60% and 20 % [34] of the peak load demand of the network, respectively. The durations of load generation scenarios 1, 2, and 3 are considered as 4 hours, 15 hours, and 5 hours, respectively. The MOPSO parameters are optimized with repetitive runs and the optimal parameters are found as follows: $C_1 = 2.5$, $C_2 = 2$, $w_{min} = 0.1$, and $w_{max} = 0.4$. The maximum iteration and population size for the 69-bus and 33-bus networks are found to be 200 and 500, respectively. Two planning cases are considered in this work:

- *Case A*: multi-objective planning without placement of UPQC-O for the simultaneous optimization of PVHC and energy loss of distribution network.
- *Case B*: multi-objective planning with the placement of UPQC-O for the simultaneous optimization of PVHC and energy loss of distribution network.

4.3.4.1 Impact of maximum PV capacity on PAF

To analyze the impact of set value of maximum PV capacity $\{(P_{PV})_{max}\}$ in each bus on the PAF, different PAFs obtained with different simulation runs by setting different values of $(P_{PV})_{max}$ in Case B are shown in Figs. 4.10(a) and 4.10(b) for the 69-bus and 33-bus networks, respectively. From these plots, it is observed that the increment in the set value of $(P_{PV})_{max}$ in each bus increases the spread of the PAFs in both the axes. It can also be observed that some of the solutions obtained with the higher set value of $(P_{PV})_{max}$ dominate the some of the solutions obtained with the lower set value of $(P_{PV})_{max}$. For the set values of 230 kW and 310 kW maximum PV capacity, no solutions are obtained for the 69-bus and 33-bus networks, respectively. This shows that the network has some capacity limit for accommodating generation beyond which the operational parameters of the networks deteriorate.

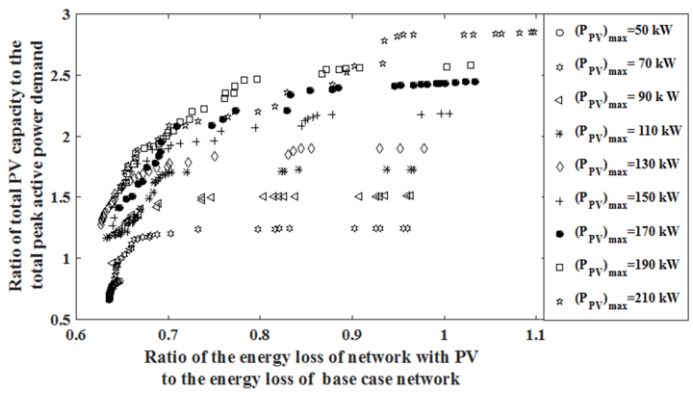

(a)

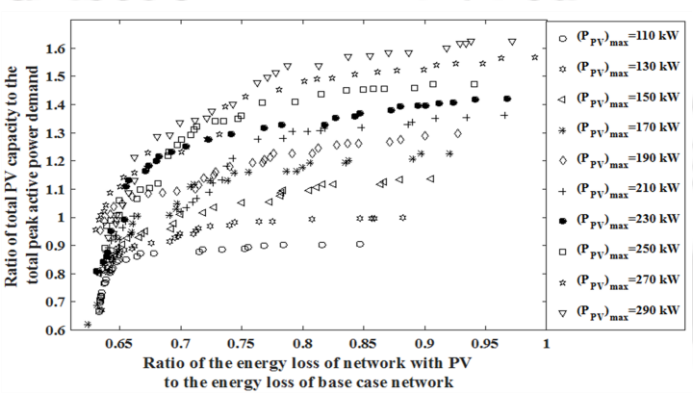

(b)

Fig. 4.10: PAFs obtained with planning Case B for different set values of maximum PV capacity for: (a) 69-bus and (b) 33-bus distribution networks

4.3.4.2. Impact of placement of UPQC-O on PAF

The PAFs obtained with planning Case A and Case B are shown in Figs. 4.11(a) and 4.11(b) for the 69-bus and 33-bus networks, respectively. The PAFs corresponding to the $(P_{PV})_{max}$ of 70 kW and 150 kW are shown. The Figs. 4.11(a) and 4.11(b) show that the most of the solutions of PAF obtained in planning Case B are dominating most of the solutions of PAF obtained with Case A for both the networks. The spread of the solutions of the PAFs as obtained with Case B is more for both the networks. Two solutions located in the extreme ends in PAF in both the cases are marked as solutions 1 and 3. The solution 1 corresponds to the solution with the highest PVHC. But, it incurs highest energy loss, as well. The solution 1 of Case B provides approximately 15-20% higher PVHC as compared to the Case A. The implementation of solution 3 can result in least energy loss. The energy loss corresponding to solution 3 of Case B is 25-30% lesser than that of the Case A. The reason behind this is the reactive power compensation provided by the UPQC-O in Case B.

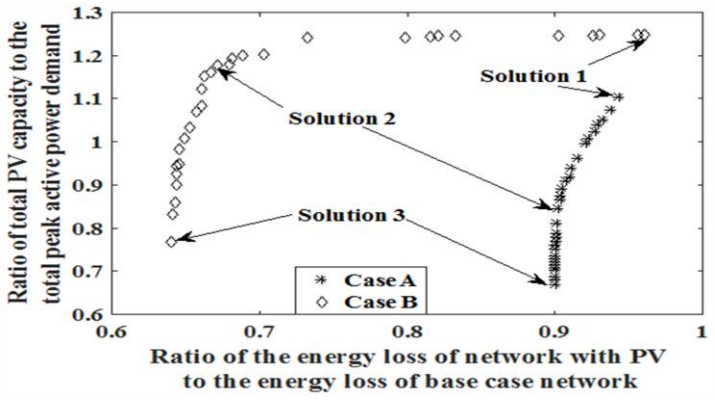

(a)

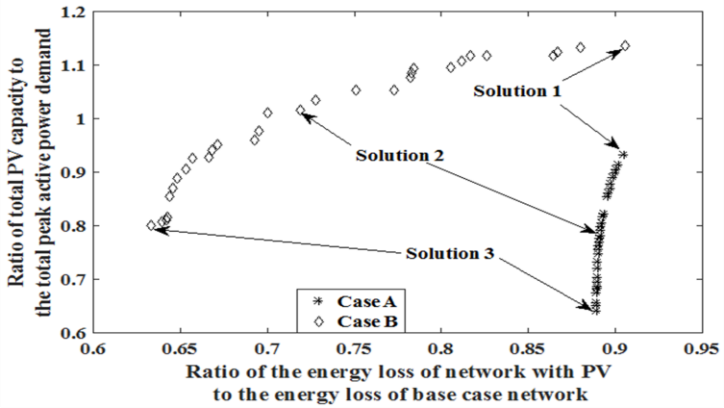

(b)

Fig. 4.11: PAFs obtained with SPEA2-MOPSO for: (a) 69-bus and (b) 33-bus networks

An intermediate solution which provides a trade-off between PVHC and energy loss is marked as solution 2. It is seen that the solution 2 of Case B dominates the solution 2 of Case A. This indicates that the solution 2 of Case B is having better PVHC and lower energy loss. For the same amount of PVHC, the energy loss of the network corresponding to the solution of Case B is lower than that of the Case A. This is also due to the reactive power compensation provided by the UPQC-O in Case B. The solutions 1-3 are quantitatively shown in Tables 4.6 and 4.7 for 69-bus and 33-bus networks, respectively. The optimal PV generation capacities in each bus of the 69-bus and 33-bus networks, as obtained with SPEA2-MOPSO, are shown in Figs. 4.12 and 4.13, respectively. It can be observed that the buses located nearer to the substation are capable of accommodating higher PV generation capacity than the buses located distant away from the substation, particularly in solution 3. The optimal locations of series inverter for all the selected solutions of PAFs are found to be same in Case B for both the networks. This happens due to the inclusion of PVSML

constraint in the planning problem. The total VA-rating of UPQC-O corresponding to the solution 1 is found to be less which results in comparatively higher energy loss. For the same reason, the total VA-rating requirement of UPQC-O in solution 3 is found to be higher. The minimum bus voltage magnitudes for the solutions obtained with Case B are found to be slightly superior to those of the Case A. In Case A, the minimum bus voltage magnitudes for all the selected solutions are found to be same for both the networks, since there is no PV generation during time durations 't_1' and 't_3'. During the period of 't_4', the improvement in minimum bus voltage magnitude is observed in Case A with the increase in total PV generation capacity of the network.

Table 4.6: The solutions 1, 2, and 3 for the 69-bus network

Solution	Case A			Case B		
	Solution 1	Solution 2	Solution 3	Solution 1	Solution 2	Solution 3
Location of series inverter	-	-	-	2	2	2
Locations of shunt inverters	-	-	-	52, 37, 35	37, 20, 61	17, 61, 49
VA-rating of series inverter (MVA)	-	-	-	2.0539	2.0539	2.0539
Total VA-rating of shunt inverters (MVA)	-	-	-	0.1243	1.4293	1.9683
Total VA-rating of UPQC-O (MVA)	-	-	-	2.1782	3.4832	4.0222
Minimum bus voltage during 't_1' (p.u.)	0.9092	0.9092	0.9092	0.9170	0.9340	0.9343
Minimum bus voltage during 't_3' (p.u.)	0.9476	0.9476	0.9476	0.9502	0.9675	0.9677
Minimum bus voltage during 't_4' (p.u.)	0.9793	0.9765	0.9758	0.9831	0.9970	0.9899
Maximum bus voltage in worst-case scenario (p.u.)	1.0409	1.0151	1.0118	1.0500	1.0494	1.0326
PVHC of the network (MW)	4.1958	3.2139	2.5486	4.7477	4.4769	2.9209
Energy loss of the network (MWh)	2.2846	2.1861	2.1825	2.3080	1.6139	1.5380

Table 4.7: The solutions 1, 2, and 3 for the 33-bus network

Solution	Case A			Case B		
	Solution 1	Solution 2	Solution 3	Solution 1	Solution 2	Solution 3
Location of series inverter	-	-	-	2	2	2
Locations of shunt inverters	-	-	-	22, 33, 33	27, 33, 33	15, 25, 30
VA-rating of series inverter (MVA)	-	-	-	2.0028	2.0028	2.0028
Total VA-rating of shunt inverters (MVA)	-	-	-	0.1296	1.0654	1.1649
Total VA-rating of UPQC-O (MVA)	-	-	-	2.1324	3.0682	3.1682
Minimum bus voltage during 't_1' (p.u.)	0.9131	0.9131	0.9131	0.9209	0.9295	0.9323
Minimum bus voltage during 't_3' (p.u.)	0.9495	0.9495	0.9495	0.9530	0.9617	0.9644
Minimum bus voltage during 't_4' (p.u.)	0.9940	0.9851	0.9831	0.9994	0.9997	0.9995
Maximum bus voltage in worst-case scenario (p.u.)	1.0285	1.0211	1.0196	1.0498	1.0487	1.0432
PVHC of the network (MW)	3.4692	2.9068	2.3861	4.2239	3.7769	2.9747
Energy loss of the network (MWh)	1.9847	1.9553	1.9501	1.9446	1.5230	1.3344

4.4 Conclusion

In this chapter, PSO-based mono- and multi-objective planning approaches have been developed to improve the PVHC and energy efficiency of distribution networks. In

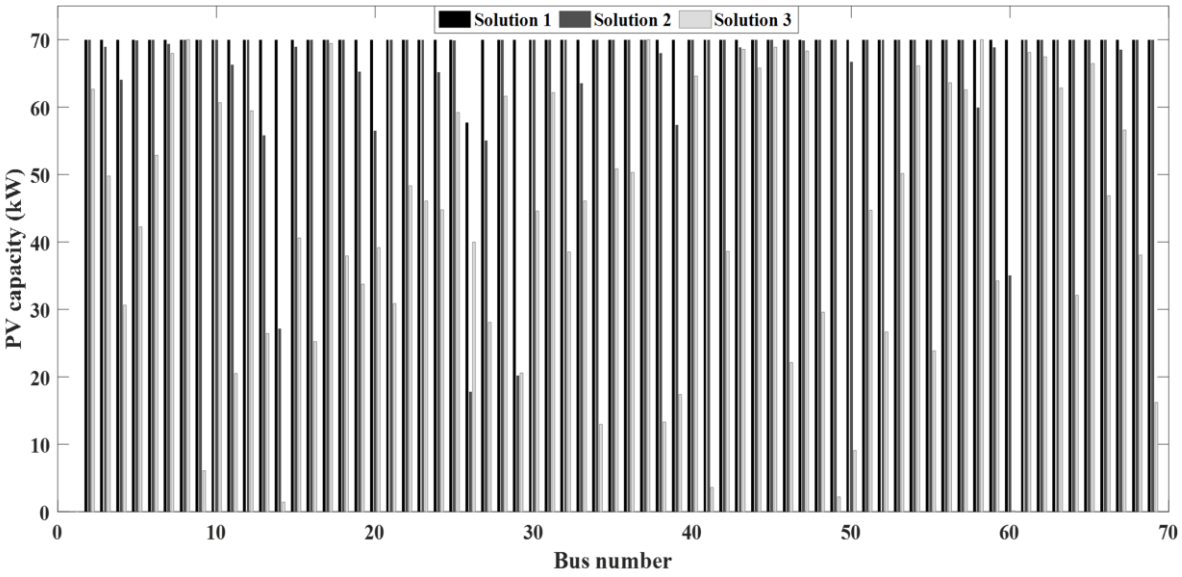

Fig. 4.12: Bar chart for the PV generation capacities in each bus for solutions 1, 2, and 3 of the 69-bus network in Case B

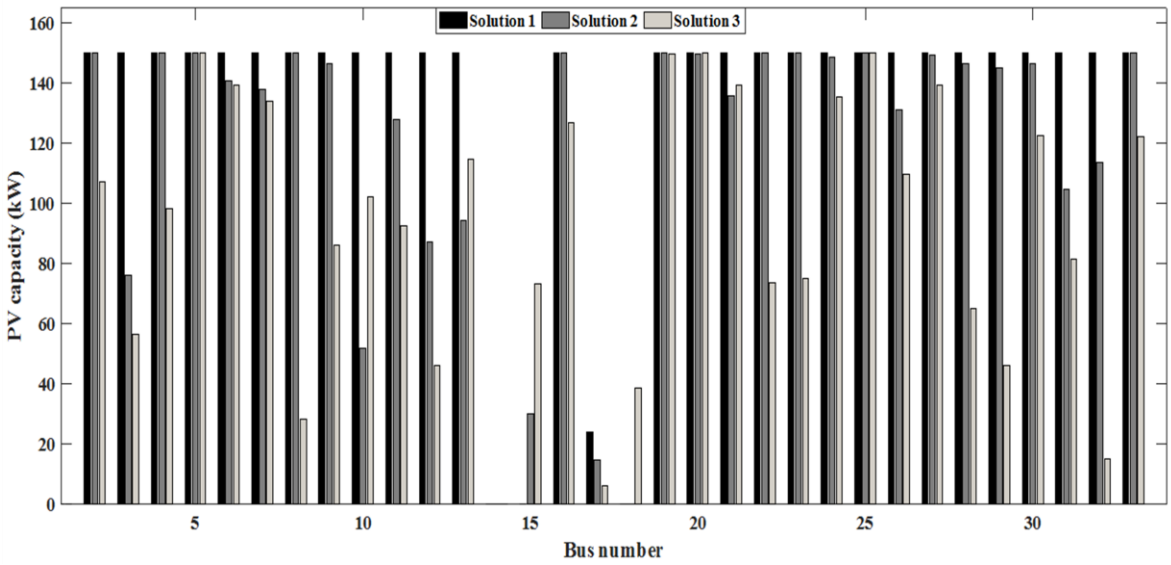

Fig. 4.13: Bar chart for the PV generation capacities in each bus for solutions 1, 2, and 3 of the 33-bus network in Case B

mono-objective planning, the PVHC of a distribution network is maximized with the placements of inverters of UPQC-O under the constraint of a maximum permissible network power loss. The modelling of series and shunt inverters has been formulated to provide reactive power compensation. PSO is used to solve the proposed mono-objective planning optimization problem. In multi-objective planning, the PVHC and energy loss of a distribution network are simultaneously optimized without and with the placement of

UPQC-O. MOPSO is used to solve the multi-objective planning optimization problem. In both the approaches, the optimal PV generation capacity in each bus, except substation bus, and the optimal locations of the placement of inverters of UPQC-O are determined. The simulation results with the proposed planning approaches provide the following:

- The appropriate placement of series and shunt inverters increases the hosting capacity of a network constrained by a permissible power loss.
- The PVHC of a distribution network can be of higher values if the permissible limit of the network power loss is set to increase.
- The inverters placed in a network can also provide reactive power compensation in different loading conditions and thereby, these improve the energy efficiency and bus voltages of the network. This is specifically useful when there is no PV generation available.
- The buses located near to the substation is capable of accommodating higher capacity of PV generation as compared to the buses located distant away from the substation. Hence, the remote buses could be the potential locations for the inverter placement to enhance the overall hosting capacity of a network.
- The placement of both series and shunt inverters provides better PVHC as compared to the placement of single shunt inverter or single series inverter.
- The PAF obtained with the proposed multi-objective optimization approach shows that the maximization of the PVHC and the energy loss minimization do conflict with each other. Hence, the benefit of PV deployment in terms of energy loss reduction gets diminishing with higher and higher values of PV capacity integration.
- The PAF, as obtained with MOPSO, provides variety of choices to an electric utility, from which it can decide the amount of PV generation that can be accommodated in each bus corresponding to the desired levels of PVHC and energy loss.
- The placement of UPQC-O simultaneously improves the PVHC and energy loss of the distribution networks. It also ensures a desired PQ level in terms of current harmonics and voltage sag mitigations. But, the placement of UPQC-O requires additional investment cost.

5

Multi-objective Planning for the Allocation of PV-BESS Integrated Open UPQC for Peak Load Shaving of Radial Distribution Networks

5.1 Introduction

The increasing competition in electricity market and the variations in load demand and generation influence the pricing of electrical energy during a day. Due to the variation in energy pricing, the electric utilities devise time-of-use (TOU)–based tariff plan. The development of smart meters helps the utilities in the implementation of TOU-based tariff plans. According to the two-level TOU-based tariff plan, the electrical energy price during peak demand hours is much more as compared to off-peak demand hours [142]. To avoid/reduce the high payment towards electrical energy purchase from the grid during peak demand hours, the DNOs are adopting different technologies, such as peak power curtailment, integration of BESS, integration of EV to grid, and demand side management etc. [143]. In the peak power curtailment approach, the BESS is used to store the energy during high penetration of renewable DG and the stored energy can be utilized for peak load shaving. In case of BESS integration, the BESS is charged during off-peak hours by taking energy from the grid and the stored energy is utilized during peak load demand hours for peak load shaving. The stored energy in EVs can also be utilized for peak load shaving, if these can be integrated with the network. In case of demand side management, the

customers' electricity consumption pattern is changed with the price of energy over time. For this, the different demand response programs are used. Although all these technologies can help in the peak load shaving, there are significant challenges in the deployment of these technologies. The integration of BESS requires high investment, operational, and maintenance costs and appropriate charging-discharging mechanism. In the integration of EV to grid, the charging-discharging of battery and the coordinating of large number of EVs are quite challenging. In the demand side management, customers' comfort might be affected by shifting the load to some other time or by shedding the load. It also requires advanced meters, communication systems [143] etc. The main advantages of using peak power curtailment strategy over other above-mentioned strategies are as: (i) it can help in mitigating overvoltage problem and (ii) it can help in reducing energy loss and line current flow during high DG penetration hours.

Several works are reported on the peak load shaving considering different issues and different technologies. In [144], a study is done using different storage technologies for the residential peak shaving. In [145], a strategy for the peak shaving using energy storage is presented considering different factors, such as, storage capacity, charging and discharging rates, size of household, and penetration of heat pump and PV. In [146], the cost-benefit analysis for the use of BESS in distribution networks is studied under high PV penetration. The annual installation cost of BESS is determined for the peak load shaving and voltage regulation considering the annual benefits obtained from the peak load shaving, load shifting, and reduction in work stress on OLTC and voltage regulator. In [147], the BESS is used for two services, i.e., peak shaving and frequency regulation. In [148], BESS is used for the peak load shaving and power smoothing of a distribution network by storing energy during the high penetration of renewable energy and by providing energy during the peak demand hours. In [149], a load shaping strategy is developed using energy storage and dynamic pricing. In this work, the energy storage is charged by consuming energy from the grid at low price and discharged during the peak demand hours. It reduces the payment towards the energy purchase and also helps in load shaping. In [150], a prediction-based real-time pricing approach is reported to control some residential appliances for the simultaneous minimization of the payment towards the electricity purchase and the waiting

time for the operation of these household appliances. In [151], an approach for the siting and sizing of BESS is developed to maximize the benefits of distribution networks in terms of system reliability improvement, deferral of system up-gradation, and advantage due to price arbitrage. The load points which are to be shed are also determined. A similar work is reported in [152], in which the siting and sizing of BESSs and their optimal operation are determined in order to minimize the cost of energy loss, deferral of the system upgrades, and to maximize the benefit from price arbitrage. In [153], the siting, sizing, and charging-discharging strategy for the distributed storage (DS) systems are optimized for the benefit of smart distribution networks in terms of price arbitrage gain, reduction in power loss, improvement in system resilience, reduction in renewable generation curtailment, and peak shaving.

In this chapter, a new proposal for the peak load shaving of radial distribution network is provided, in which a desired PQ can also be maintained with the optimal allocation of PV-BESS integrated open UPQC (PV-BESS-UPQC-O). The UPQC-O-WB model presented in Chapter 3 is used for this. Hence, the proposed PV-BESS-UPQC-O model has multiple functionalities:

- It can mitigate voltage sag and protect all the downstream load from the voltage sag. It can also eliminate harmonics present in the line current.
- It can provide active and reactive power support to distribution networks during peak hours. It can also be designed to provide reactive power compensation during off-peak hours, as well.

In this work, the PV-BESS-UPQC-O model is deployed for the peak load shaving in distribution networks. This work considers the following issues:

- The cost/rating of the devices, such as, BESS increases with the increasing level of the peak shaving.
- The injection of active/ reactive power in a large-scale for the peak load shaving may cause deterioration of the operational performance of a network in terms of increase in line losses.
- The increasing use of non-linear loads deteriorates the PQ by injecting harmonics into

a network.

Considering these issues, a multi-objective planning problem is formulated. The optimization objectives are: (i) maximization of peak load shaving for radial distribution networks with the placement of PV-BESS-UPQC-O, (ii) minimization of cost of placement of PV-BESS-UPQC-O, and (iii) minimization of total power loss during peak load demand with the placement of PV-BESS-UPQC-O. These objectives are optimized subject to the active and reactive power balance constraints, bus voltage magnitude constraint, thermal constraint, and minimum reactive power compensation constraint. The PSO-based multi-objective planning algorithm is used to solve the problem. The Pareto-dominance principle [137] is used to find out a set of non-dominated solutions called Pareto-approximation set. There are many variants of Pareto-based multi-objective evolutionary algorithms, out of which the SPEA2 [138] is an efficient approach and it is extensively used in solving various multi-objective optimization problems including the power system optimization problems. The Pareto-based MOPSO is used in various applications for solving optimization problems, for example, distribution network planning [141], design of stand-alone micro-grid system considering wind, PV, and fuel cell [154-155], design of UPQC for energy loss minimization of distribution networks [73], design of controller for microgrid system [156] etc. In this work, SPEA2-MOPSO is chosen as the solution tool to solve the proposed planning optimization problem. The contribution of this work is the development of multi-objective planning approach for the peak load shaving of radial distribution networks keeping a desired PQ level intact with the optimal allocation of PV-BESS-UPQC-O in distribution networks. The simulation study is performed using 33-bus and 69-bus radial distribution networks.

5.2 Modelling of PV-BESS-UPQC-O for peak load shaving of distribution networks

A schematic diagram for a 5-bus radial distribution network with the placement of PV-BESS-UPQC-O is shown in Fig. 5.1. The bus 1 is the substation bus and rest are load buses. The functions of series and shunt inverters of UPQC-O during healthy and voltage sag conditions are same as that of the UPQC-O-WP (*Refer Table 2.1*). The series inverter is mathematically modelled using Eqs. (2.46)-(2.52) for reactive power compensation and

voltage sag mitigation. However, the shunt inverter is mathematically modelled using Eqs. (2.63)-(2.71) to provide active power, reactive power, and harmonic compensations. These inverters share a common communication link to decide the respective set points as shown with the dotted lines. The respective VAr set points are decided using Eqs. (2.1) and (2.2). The BESSs connected to the series and shunt inverters are used to maintain the dc-link voltage constant and to provide the active power to the network, respectively. Each BESS is charged with a PV system as shown in Fig. 5.1. These all constitute PV-BESS-UPQC-O system. The phasor diagrams for the series and shunt inverters are shown in Figs. 2.4(a) and 2.5, respectively. The determination of the rating requirements of PV and BESS to be connected to the series and shunt inverters of PV-BESS-UPQC-O is explained in the subsequent section.

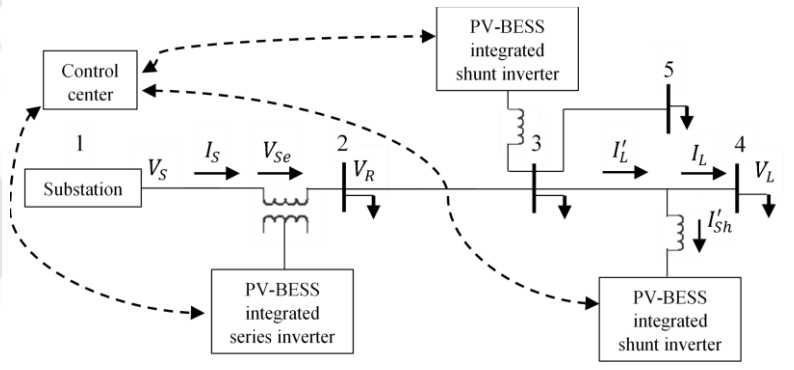

Fig. 5.1: Schematic diagram for the placement of PV-BESS-UPQC-O in a 5-bus radial distribution network (*dotted line represents communication link*)

5.2.1 PV and BESS rating requirements

The rating of BESS is computed considering the maximum depth of discharge of BESS ($\%DOD_{max}$). The depth of discharge (DOD) of BESS at any instant of time is complement of the state of charge (SOC) of BESS. SOC provides the information of present available BESS capacity at any instant of time in terms of percentage of total/actual BESS capacity [157]. The PV generation in a day is usually interminent in nature. Thus, in this work, the PV rating requirement for charging the BESS is computed considering the CUF of PV system. CUF is defined as the actual output of PV to the maximum/peak output of PV in a day/year. Since the BESS connected to the series inverter is to supply the compensating energy required in sag mitigation and inverter losses, its rating depends upon

the amount of voltage sag to be mitigated and the inverter loss to be compensated. The amount of energy required for this is computed as:

$$E_{Se} = \left(\frac{kt_{Sag}\sum_{i\epsilon[2,..,N]}P(i)}{3600} + INVL_{Se}^{Peak}t_1\right) \quad (5.1)$$

where, $INVL_{Se}^{Peak} = \gamma_{loss}S_{Se}$ (5.2)

The first part of Eq. (5.1) shows the amount of energy required to mitigate the k amount of voltage sag for maximum duration of t_{Sag}. However, second part shows the amount of energy required to compensate the inverter losses during peak demand hours. The actual rating of BESS connected to the series inverter is computed as:

$$PB_{Se} = E_{Se}\left(\frac{100}{\%DOD_{max}}\right) \quad (5.3)$$

The PV rating requirement for the charging of BESS connected to the series inverter is computed as:

$$PPV_{Se} = \left(\frac{E_{Se}}{24CUF}\right) \quad (5.4)$$

where, E_{Se} is the actual energy required for the charging of BESS connected to the series inverter.

The rating of BESS connected to the shunt inverter is determined based on the amount of active power to be supplied during peak hours and the inverter loss to be compensated. The total amount of energy required by the shunt inverter for this is computed as:

$$E_{Sh} = \left(\frac{P_{Sh}t_1}{\eta_{INV}}\right) \quad (5.5)$$

where, the numerator shows the active power to be supplied through the shunt inverter during peak load demand hours and denominator shows the efficiency of shunt inverter. The actual rating of BESS to be connected to the shunt inverter is computed as:

$$PB_{Sh} = E_{Sh}\left(\frac{100}{\%DOD_{max}}\right) \quad (5.6)$$

The PV rating requirement for the charging of BESS connected to the shunt inverter is computed as:

$$PPV_{Sh} = \left(\frac{E_{Sh}}{24CUF}\right) \quad (5.7)$$

where, E_{Sh} is the actual energy required for the charging of BESS connected to the shunt inverter.

The total BESS and PV rating requirements of PV-BESS-UPQC-O are computed as:

$$PB_{Tot} = PB_{Se} + PB_{Sh} \quad (5.8)$$

$$PPV_{Tot} = PPV_{Se} + PPV_{Sh} \quad (5.9)$$

5.2.2 Assumptions/consideration

The following assumptions are considered in this planning:

- The distribution networks are assumed to be balanced and radial.
- It is assumed that the operational hours of PV and peak demand hours do not coincide to each other. This is true for the network with domestic loads, in which the peak demand usually occurs during evening time.
- BESS is to be fully charged during operational hours of PV so that it can be discharged during peak hours.
- BESS is to be charged and discharged only once in a day.
- The series inverter location is fixed at bus 2 so as to protect all the downstream loads from the voltage sag.

5.3 Multi-objective optimization problem

In this chapter, a three-objective optimization problem is formulated for the allocation of PV-BESS-UPQC-O in distribution networks. The locations for the placement of shunt inverters and the values of K_{Re} are determined by optimizing the following objectives: (i) maximization of peak load shaving of distribution networks (ii) minimization of cost of placement of PV-BESS-UPQC-O, and (iii) minimization of total power loss during peak load demand with the placement of PV-BESS-UPQC-O. The total power loss during peak load demand includes the line loss, inverter loss, and series inverter transformer power loss. The objective function 1 is formulated as the percentage of total peak active power demand to be supplied by the PV-BESS-UPQC-O. The objective function 2 is the cost of placement of PV-BESS-UPQC-O which includes the investment costs of the inverters, investment and maintenance costs of the BESS and PV, and the replacement cost

of BESS. The cost of communication link is not included, since its value is much lesser than the cost of inverters/BESS. The objective function 3 is the ratio of total power loss during peak load demand with the placement of PV-BESS-UPQC-O to the power loss of the base-case network (i.e., without PV-BESS-UPQC-O). The mathematical expressions of these objective functions are given below.

Objective Function 1:

$$\max\{f_1\} = 100\left(\frac{\sum_{l\epsilon\xi} P_{Sh}(l)}{\sum_{m\epsilon\rho} P(m)}\right) \tag{5.10}$$

Objective Function 2:

$$\begin{aligned}\min\{f_2\} = {} & C_{Se}S_{Se} + C_I^B PB_{Se} + C_{REP}^B PB_{Se}D^{f1} + \frac{C_{O\&M}^B PB_{Se}}{t_1}T^h D^f + \\ & C_I^{PV} PPV_{Se} + C_{O\&M}^{PV} PPV_{Se}T^h D^f + \sum_{l\epsilon\xi}\Big(C_{Sh}(l)S_{Sh}(l) + \\ & C_I^B PB_{Sh}(l) + C_{REP}^B PB_{Sh}(l)D^{f1} + \frac{C_{O\&M}^B PB_{Sh}(l)}{t_1}T^h D^f + C_I^{PV} PPV_{Sh}(l) + \\ & C_{O\&M}^{PV} PPV_{Sh}(l)T^h D^f\Big)\end{aligned} \tag{5.11}$$

Objective Function 3:

$$\min\{f_3\} = \frac{\sum_{mn\epsilon\mu} PL_{HS}(mn) + \gamma_{loss}S_{Tot} + \gamma_{TF}S_{Se}}{\sum_{mn\epsilon\mu} PL(mn)} \tag{5.12}$$

These objective functions are optimized under the active and reactive power balance constraints, bus voltage magnitude constraint, thermal constraint, and minimum reactive power compensation constraint. All these constraints can be mathematically represented as shown in Eqs. (2.88-2.89), (2.90), (2.91), and (2.92), respectively. The maximization of peak load shaving requires higher amount of active power supply through the PV-BESS-UPQC-O. This results in higher rating requirement of PV-BESS-UPQC-O and higher installation cost. Hence, the maximization of peak load shaving and the cost of placement of PV-BESS-UPQC-O are two conflicting objectives. The large amount of active power injection through the PV-BESS-UPQC-O increases the total power loss during peak load demand, as well. Hence, this needs simultaneous optimization of these objectives. This is done by using the Pareto-based multi-objective optimization approach. This provides a set of non-dominated solutions, in which none is superior/ inferior to others [137]. A DNO can chose a solution from this set according to its requirement. The Pareto dominance principle [137] is discussed in section 4.3.1.1.

5.4 SPEA2-MOPSO based solution approach

In this work, PSO-based multi-objective planning algorithm is used to determine the optimal locations for the placement of shunt inverters and values of K_{Re}. The basic PSO algorithm and SPEA2-based MOPSO algorithm are briefly described in subsections 2.5.1 and 4.3.3.2, respectively. The Eqs. (2.84)-(2.86) are used to incorporate the PV-BESS-UPQC-O model into FBSLF algorithm. The algorithmic steps of the FBSLF are given in subsection 2.3.1. The MOPSO-based overall planning algorithm is discussed below.

5.4.1 MOPSO-based planning algorithm

The overall MOPSO based planning algorithm uses the FBSLF subroutine incorporating the PV-BESS-UPQC-O model. A particle of MOPSO is encoded with the information of locations of the shunt inverters and values of K_{Re}. The pseudo codes for the overall planning algorithm are shown in Fig. 5.2.

5.5 Simulation results and discussion

This section presents the computer simulation study of the multi-objective planning approach for the optimal allocation of PV-BESS-UPQC-O. The 33-bus and 69-bus radial

Begin
Input radial distribution network bus and line data;
Calculate VA-rating of the series inverter by locating it at bus 2;
Input THD_L, itr_{max}, C_1, C_2, k, $Penalty\ Factor$, N_{Pop}, V_{max}, V_{min}, t_1, t_{Sag}, w_{max}, w_{min}, C_I^B, C_I^{PV}, C_{REP}^B, $C_{O\&M}^B$, $C_{O\&M}^{PV}$, T^h, η_{INV}, γ_{loss}, γ_{TF}, $I_{TH}(mn)$, $\%DOD_{max}$.
Initialize random position and velocity of the particles of size N_{Pop} ;
Decode the particles and perform the FBSLF to determine the values of the objective functions;
Find out the non-dominated solutions and store them in the Elite Archive;
Assign fitness to each particle according to the SPEA2 fitness assignment scheme;
For *iteration*=2: itr_{max}
  For *it*=1: N_{Pop}
    Update velocity and position of particles;
    Decode the particle position to obtain the locations of placement of shunt inverters and values of K_{Re};
    Perform the FBSLF with PV-BESS-UPQC-O model;
    Calculate the values of the objective functions;
    If any particle violates constraints, a penalty factor is added with it;
  End
  Find out non-dominated solutions and update the Elite Archive;
  Assign single fitness value to each particle according to the SPEA2 fitness assignment scheme;
End
Elite Archive consists of the set of the Pareto-approximate solutions with the locations of the shunt inverters and values of K_{Re};
End

Fig. 5.2: Pseudo codes for SPEA2-MOPSO-based multi-objective planning algorithm

distribution networks are chosen for this study. The descriptions of these networks are provided in Appendix. In this work, the bus 2 is considered for the placement of series inverter to protect all the downstream loads from voltage sag. Hence, all the buses, except the substation bus and bus 2, are selected as the candidate buses for the placement of the shunt inverters. The unit cost of the inverters is taken from [92]. Different other planning parameters and cost coefficients, used in this work, are provided in Table 5.1. The values of MOPSO parameters are set by taking repetitive runs with different combination. The best performance is found to be corresponding to: $C_1 = 2.5$, $C_2 = 2$, $w_{min} = 0.1$, and $w_{max} = 0.4$. The maximum iteration and population size are found to be 300 and 200, respectively. A case-study considering the three shunt inverters is carried out to find the non-dominated solutions for the proposed multi-objective optimization problem.

Table 5.1: Different planning parameters

T^h = 20 Years, K_{Re}=0.1-0.5	C_I^B=900 $/kWh [112]
THD_L= 0.2, k= 0.3, CUF= 0.2	C_{REP}^B=244 $/kWh [112]
t_1 =4 hours, t_{Sag}= 60 sec,	$C_{O\&M}^B$=10 $/(kW-Year) [112]
V_{min}=0.9 p.u., V_{max}=1.05 p.u.	C_I^{PV}=2025 $/kW [113]
η_{INV}=98%, γ_{loss}=2%, γ_{TF}=5%	$C_{O\&M}^{PV}$=16 $/(kW-Year) [113]
$\%DOD_{max} = 80\%$	$C_{UPQC-O} = 0.0003{S_{Tot}}^2 - 0.2691S_{Tot} + 188.2$ ($/kVA) [92]

5.5.1 PAF obtained with MOPSO

The PAFs along with the Pareto-approximation surface obtained with MOPSO are shown in Figs. 5.3(a) and 5.3(b) for the 33-bus and 69-bus networks, respectively. The two-dimensional plots with the values of the objective functions 1 and 3 of the non-dominated solutions obtained with MOPSO are shown in Figs. 5.4(a) and 5.4(b) for the 33-bus and 69-bus networks, respectively. From these figures, it is seen that the total power loss with the placement of PV-BESS-UPQC-O initially decreases with the increasing value of peak load shaving. But, it starts increasing beyond approximately 25-30% of peak load shaving. This shows that the injection of active/reactive power into a network up to a certain limit improves the network power loss and then, it starts deteriorating. The case study provides number of solutions with different objective function values.

5.5.2 Technical details of three extreme solutions of PAFs

Three extreme solutions corresponding to the maximum value of peak load shaving, minimum value of cost of placement of PV-BESS-UPQC-O, and minimum value of total

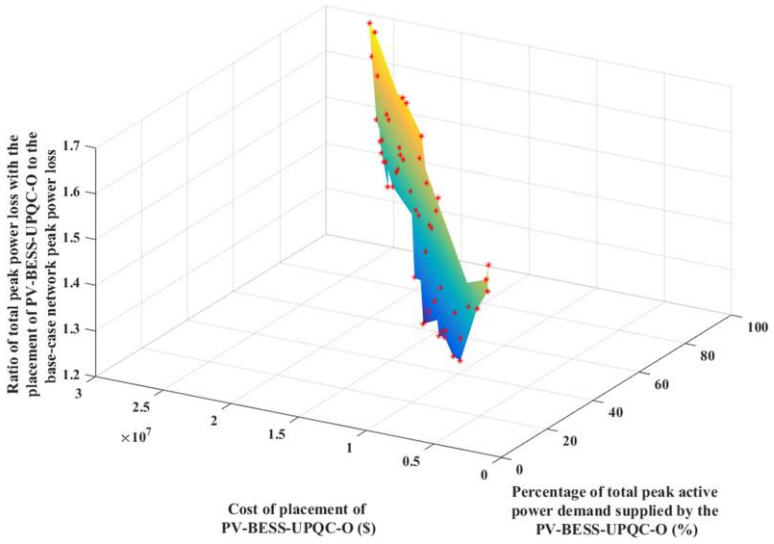

(a)

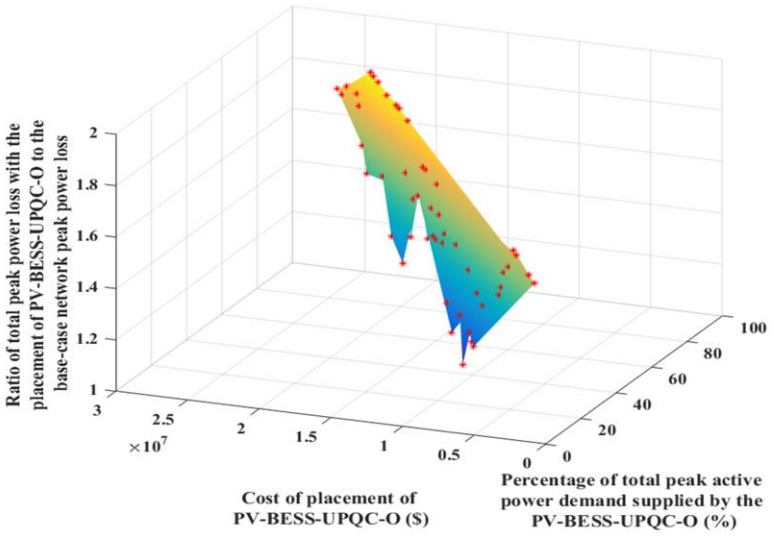

(b)

Fig. 5.3: PAFs along with Pareto-approximation surface obtained with (a) 33-bus and (b) 69-bus networks with the placement of PV-BESS-UPQC-O

power loss during peak load demand with the placement of PV-BESS-UPQC-O are selectively chosen from the PAF and named as solutions 1, 2, and 3, respectively. These are shown in Table 5.2 for 33-bus and 69-bus networks. Basically, the solutions 1, 2, and 3 are the best solutions of the PAF in view of objectives 1, 2, and 3, respectively. The cost of the placement of PV-BESS-UPQC-O and total power loss with the placement of PV-BESS-UPQC-O are found to be more in solution 1 as compared to solutions 2 and 3 because higher value of peak load shaving needs placement of higher rated inverters, BESS, and PV. This results in higher investment cost. Since the solution 2 corresponds to the lowest cost of

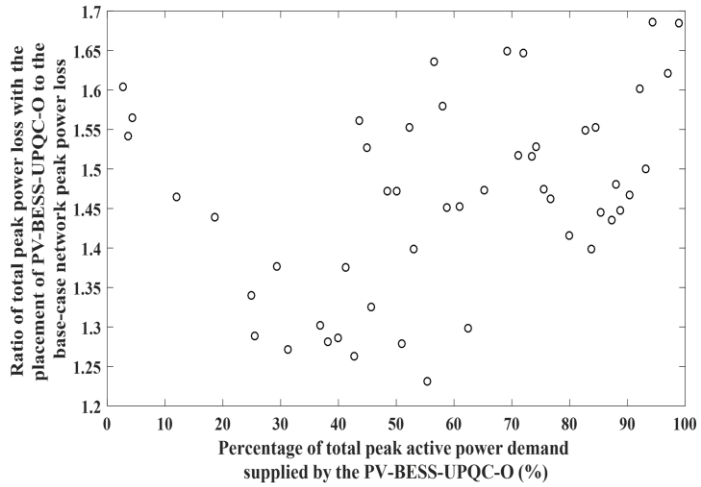

(a)

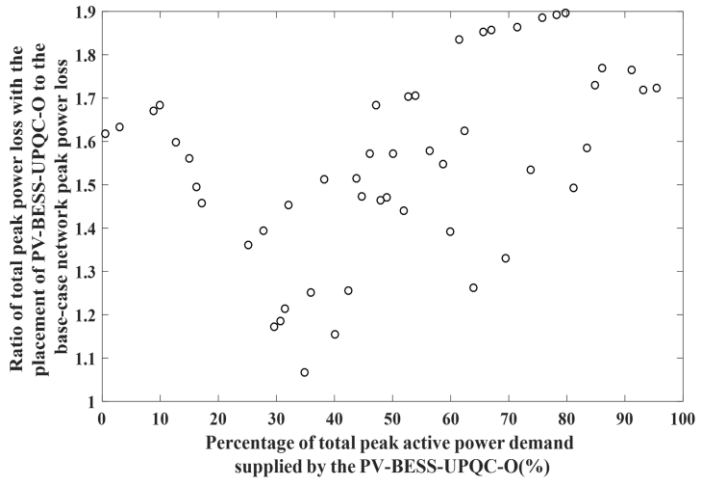

(b)

Fig. 5.4: The two-dimensional plot of the values of the objective functions 1 and 3 of the non-dominated solutions obtained with (a) 33-bus and (b) 69-bus networks

placement of PV-BESS-UPQC-O, its implementation would result in the lowest peak load shaving. Similarly, the implementation of solution 3 would provide moderate values of peak shaving and cost of placement of PV-BESS-UPQC-O along with the least total power loss among all the solutions in PAF.

5.5.3 Qualitative comparison of proposed work with other similar works

In this chapter, PV-BESS-UPQC-O is used for the peak load shaving, energy efficiency improvement, and PQ improvement of radial distribution networks. In the literature, several works have been reported on the use of BESS for the peak load shaving of distribution networks [142, 145-153]. However, all these works do not include any PQ

issue, such as, voltage sag, current harmonics etc. Very few works [151-153] consider the power/ energy loss in the objective function(s). Thus, the direct performance comparison of the proposed work with all these works would be impractical. However, the works presented in [151-153] are chosen for the qualitative comparison with the proposed work. In all these works [151-153], the BESS is charged during off-peak hour and discharged during peak hour for the peak load shaving. Table 5.3 provides a qualitative comparison of proposed work with the works presented in [151-153].

Table 5.2: The selected solutions obtained with the 33-bus and 69-bus distribution networks

Solution	33-bus network			69-bus network		
	Solution 1	Solution 2	Solution 3	Solution 1	Solution 2	Solution 3
Objective function 1 (%)	98.9031	2.7560	55.3305	95.5077	0.5331	34.8691
Objective function 2 ($\times 10^7$\$)	2.6613	0.1412	1.5190	2.6337	0.0841	1.0081
Objective function 3	1.6845	1.6043	1.2308	1.7244	1.6170	1.0667
Locations of shunt inverters	25, 3, 4	18, 33, 22	30, 13, 6	47, 3, 55	52, 27, 69	63, 15, 59
VA-rating of series inverter (MVA)	2.0028	2.0028	2.0028	2.0539	2.0539	2.0539
Total VA-rating of shunt inverters (MVA)	3.6863	0.1682	2.0775	3.6958	0.0403	1.4752
Total VA-rating of PV-BESS-UPQC-O (MVA)	5.6891	2.1709	4.0803	5.7497	2.0942	3.5292
Total active power to be injected through the shunt inverters (MW) using BESS	3.6743	0.1024	2.0555	3.6314	0.0203	1.3258
Total reactive power compensation by the shunt inverters (kVAr)	297.2313	131.6946	297.2313	640.6748	34.5724	640.6748
Total rating of BESS (MWh)	18.9697	0.7459	10.7109	18.7566	0.3326	6.9934
Total rating of PV (MW)	3.1616	0.1243	1.7851	3.1261	0.0554	1.1656

Table 5.3: Qualitative comparison of the proposed work with the works reported in [151-153]

Planning tasks	Proposed work	Work presented in [151]	Work presented in [152]	Work presented in [153]
Objectives	(i) Maximization of total peak active power demand supplied by PV-BESS-UPQC-O (ii) Minimization of cost of placement of PV-BESS-UPQC-O (iii) Minimization of network total power loss with the placement of PV-BESS-UPQC-O	Capital power and energy costs of DS unit, net present value (NPV) of replacement cost of DS unit, annual operation and maintenance cost of DS unit, and NPV of arbitrage benefit, system upgrade costs, energy loss cost, and interruption cost	Capital power and energy costs of DS unit, annual operation and maintenance cost of DS unit, and NPV of replacement cost of DS unit, arbitrage benefit, system upgrade costs, and energy loss cost	Investment cost of DS unit, arbitrage gain, economic gain due to reduction in active power loss and renewable energy curtailment, improvement in voltage profile and system resilience, and system upgrade deferral
Optimizing variables	Locations of placement of shunt inverters and the values of K_{Re}	Location and size of DS units, and load points to be shed during contingencies	Location and size of DS units	Number, location, power rating, and capacity of DS units, and charging-discharging strategy for DS units
Type of DG	PV	Wind and natural gas based DG units	Wind and diesel based DG units	PV and wind based DG units
Solution tool	SPEA2-based MOPSO	GA and linear programming	GA and linear programming	Mixed integer convex programming (branch and bound algorithm)
Special features	Ensures a minimum PQ level in terms of voltage sag and current harmonic mitigation	Control strategy for the operation of all allocated DS units	Control strategy for the operation of all allocated DS units	Linearized power flow is used for DS planning to optimize the charging-discharging strategy for each storage unit

5.6 Conclusion

In this chapter, a new proposal for the simultaneous improvement of peak load shaving, PQ, and power loss of radial distribution networks using PV-BESS-UPQC-O has been provided. A multi-objective planning approach is developed for the simultaneous maximization of peak load shaving of distribution network with PV-BESS-UPQC-O, minimization of the cost of placement of PV- BESS-UPQC-O, and minimization of total power loss during peak load demand with the placement of PV-BESS-UPQC-O. The SPEA2-MOPSO-based multi-objective optimization algorithm is used to solve the proposed planning problem. This study provides the following outcomes:

- The PAFs obtained with the proposed planning approach provides a variety of choices to a DNO, from which it can decide the amount of peak load shaving to be obtained with the placement of PV-BESS-UPQC-O according to its capital expenditure budget and energy economy.
- In addition to the peak shaving, the placement of PV-BESS-UPQC-O in distribution networks provides multiple benefits, such as, PQ improvement, power loss reduction in other loading conditions, investment deferral for network reinforcement etc.
- The deployment of solution corresponding to the higher peak load shaving requires higher investment and incurs higher power loss.

6

Operational Optimization Approach for Open UPQC with Time Varying Load Demand and PV Generation for Energy Loss Minimization in Radial Distribution Networks

6.1 Introduction

The optimal operation of power systems under time varying load demand and PV generation is a challenging research problem. In practical power systems, there are many compensating devices deployed so as to improve the steady-state operational performance, for example, capacitor bank, OLTC, voltage regulators etc. The determination of the optimal set points of these devices under time-varying load demand and PV generation needs the formulation of an on-line optimization approach. The power/energy loss reduction is one of the important objective functions used in the determination of the set points for these compensators. An UPQC-O is a type of compensator which can provide reactive power compensation and can mitigate PQ issues. In literature, there are many works reported on UPQC-O [96-102]. All these works [96-102] are briefly discussed in the introduction section of the Chapter 2. Most of these works [96-102] are reported on the development of control schemes for the inverters and the development of new model for PQ improvement of distribution networks. However, the time varying VAr compensation capability of UPQC-O for the time varying load demand and PV generation is not studied in any of these works. This is the motivation behind the proposed approach.

In this chapter, an operational optimization approach for the determination of VAr compensation/injection set points for UPQC-O for time varying load demand and PV generation is proposed. A two-stage optimization problem is formulated for this. The first stage optimization problem provides the optimal PV generation capacity in each bus by maximizing the PVHC of the network. In the second stage, the energy loss minimization in each time step is formulated as the objective function. Different operational constraints, such as, load and generation balance, bus voltage magnitude constraint, thermal capacity constraint of the lines, maximum VAr support capacity constraint for the inverters, and maximum PV generation capacity constraint for each bus, except the substation bus, are considered in the optimization problem. The optimization problem is modelled to fit into the General Algebraic Modelling System (GAMS) software. The CONOPT solver is used to solve the proposed non-liner optimization problem. The determination of the optimal operating set points for UPQC-O under time varying load demand and PV generation requires the information of real-time aggregated load demand and PV generation, high speed communication networks to send and receive information, advanced control systems to control the operation of the inverters etc. Thus, this work also provides the outline of the infrastructure required for the real-time implementation of the proposed approach. The cost-benefit analysis of proposed methodology in view of saving due to the energy loss reduction is also provided. The contributions of this work are:

- Formulation of a two-stage operational optimization approach to determine the time varying VAr compensation set points for the UPQC-O with time varying load demand and PV generation
- Investigative study to bring out the impact of the placement of UPQC-O with time varying set points on the energy loss reduction of distribution networks

The simulation study is carried out using a 33-bus radial distribution network.

6.2 Steady-state models of radial distribution network and UPQC-O

This section provides the steady-state models of radial distribution network and UPQC-O for reactive power compensation.

6.2.1 Steady-state model of radial distribution network

A 3-bus radial distribution network, as shown in Fig. 6.1, is considered to illustrate the steady-state operation model of a radial distribution network [158]. The active and reactive power flow in any line, say, 'ef' can be computed by applying the load balance at bus 'f' as:

$$P_{ef} = \sum_{fg\in\tau} P_{fg} + P_f + \sum_{fg\in\tau} L_{fg} \qquad \forall f \in \rho \qquad (6.1)$$

$$Q_{ef} = \sum_{fg\in\tau} Q_{fg} + Q_f + \sum_{fg\in\tau} M_{fg} \qquad \forall f \in \rho \qquad (6.2)$$

The receiving end bus voltage magnitude (V_f) of any line, say, 'ef' can be computed by using Eq. (6.3),

$$V_e^2 = V_f^2 + 2\left(R_{ef}P_{ef} + X_{ef}Q_{ef}\right) + Z_{ef}^2 I_{ef}^2 \qquad \forall ef \in \mu \qquad (6.3)$$

The magnitude of current flow in any line, say, 'ef' can be computed by using Eq. (6.4),

$$I_{ef}^2 = \frac{P_{ef}^2 + Q_{ef}^2}{V_f^2} \qquad \forall ef \in \mu \qquad (6.4)$$

The different operational parameters of a distribution network, such as, bus voltage magnitude, line current flow, network power loss can be computed by using Eqs. (6.1)-(6.4).

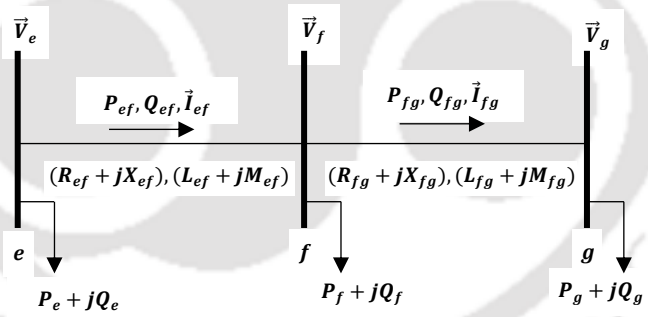

Fig. 6.1: Illustrative example for the steady-state operation of radial distribution network

6.2.2 Steady-state model of UPQC-O

In this chapter, the UPQC-O-WOP model presented in Chapter 2 is used to provide reactive power compensation, to mitigate voltage sag, and to eliminate harmonics. The functions of series and shunt inverters during healthy and voltage sag conditions are same as that of the UPQC-O-WOP model (*Refer Table 2.1*). The series inverter is mathematically modelled by using Eqs. (2.46)-(2.52). The shunt inverter is modelled by using Eqs. (2.55)-

(2.58). A typical 5-bus radial distribution network with PV generation sources and UPQC-O is shown in Fig. 6.2.

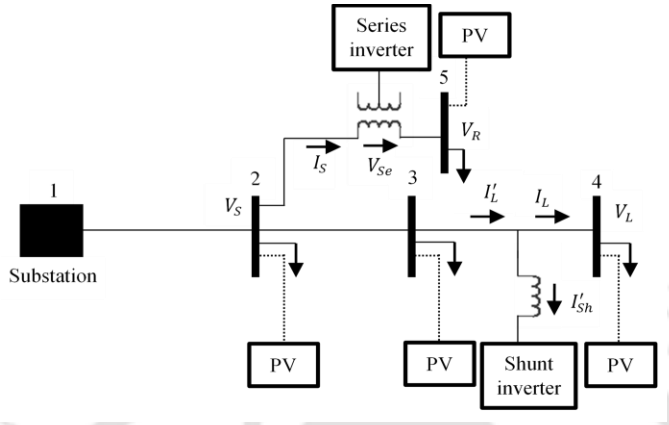

Fig. 6.2.: Schematic diagram of a 5-bus radial distribution network with UPQC-O and PV generation sources

6.3 Operation of UPQC-O during time varying load demand and PV generation

In this section, the operation of UPQC-O under the time varying load demand and PV generation is described.

6.3.1 Time varying load demand PV generation

The seasonal hourly average load demand data of IEEE reliability test system [159] is considered to add the daily variation in load demand. The PV generation data of three different months of a year are considered to have the seasonal variation in PV generation. The seasonal hourly average PV generation data can be found in [160]. The load curves and PV generation profiles for different seasons of a year are shown in Figs. 6.3 and 6.4, respectively. The mathematical expressions used to get the load demand and PV generation in a bus, say 'f' at a particular instant of time 't' are given below.

$$P_f(t) = K_L(t)P_{Lf} \tag{6.5}$$

$$Q_f(t) = K_L(t)Q_{Lf} \tag{6.6}$$

$$P_f^{PV}(t) = K_{PV}(t)P_f^{PVGEN} \tag{6.7}$$

where, $K_L(t)$ and $K_{PV}(t)$ are the percentages of peak load and peak PV generation, respectively. These values can be obtained from the Figs. 6.3 and 6.4, respectively.

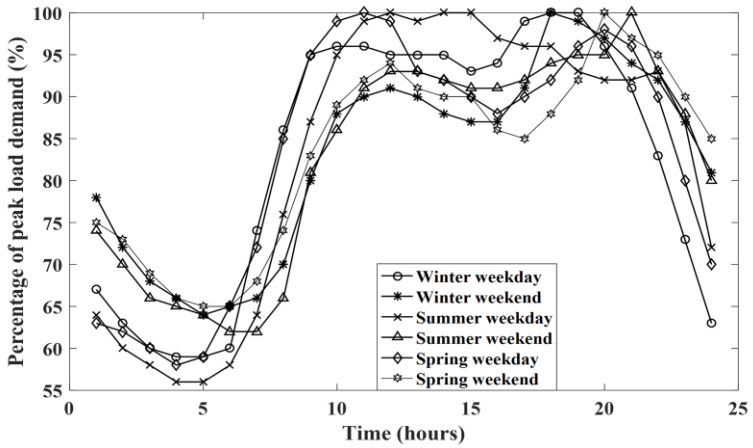

Fig. 6.3: Load curves for the different seasons of a year

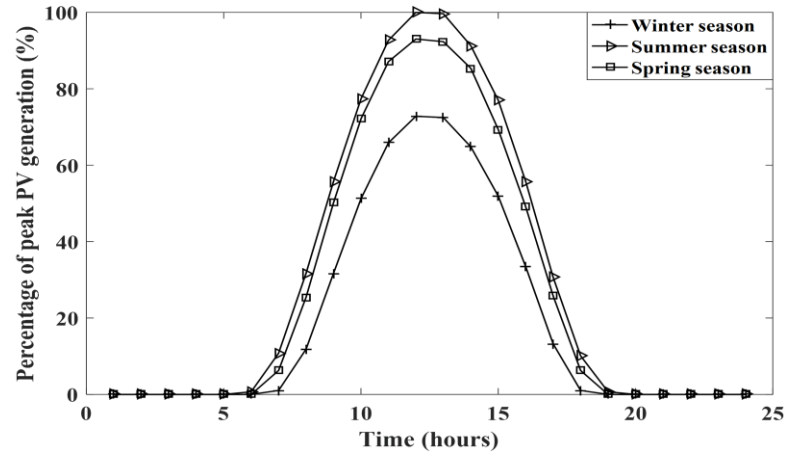

Fig. 6.4: Typical PV generation profiles for the different seasons in a year

6.3.2 Operation of UPQC-O during time varying load demand and PV generation

The load demand and PV generation variations in a network create changes in the line currents and bus voltages. The operation of UPQC-O under time varying load demand and PV generation is described below.

- *Operation of series and shunt inverters during healthy condition*: The series inverter injects a fraction $\{K_{Se}(t)\}$ of rated series voltage V_{Se}^{Hel} and shunt inverter injects a fraction $\{K_{Sh}(t)\}$ of rated shunt current (I'_{Sh}) in all the load and PV generation scenarios to provide the VAr compensation to a network. i.e.,

$$V_{Se}^{Hel}(t) = K_{Se}(t)V_{Se}^{Hel} \quad (6.8)$$

$$I'_{Sh}(t) = K_{Sh}(t)I'_{Sh} \quad (6.9)$$

The VAr compensation provided by the series and shunt inverters in buses, say 'f' and 'g' at a particular instant of time 't' can be determined as:

$$Q_f^{Se}(t) = V_{Se}^{Hel}(t) I_S(t) \tag{6.10}$$

$$Q_g^{Sh}(t) = V_L(t) I'_{Sh}(t) \tag{6.11}$$

Since both the inverters of UPQC-O are designed to inject only reactive power to a network, the phase angle between $V_{Se}^{Hel}(t)$ and $I_S(t)$ is exactly maintained at 90° for the series inverter in all the loading conditions. For the shunt inverter, the phase angle between the $V_L(t)$ and $I'_{Sh}(t)$ is also maintained at 90° for the same reason.

- *Operation of series inverter during voltage sag condition*:

  One of the functions of series inverter is to mitigate the voltage sag occurring at the upstream network. The series voltage to be injected is function of the amount of voltage sag and it can be calculated using Eqs. (2.49)-(2.50). The maximum amount of series injected voltage is limited by the rating of series inverter as shown in Eq. (6.12).

$$V_{Se}^{Sag}(t) = \frac{S_{Se}}{I_S(t)} \quad s.t. V_{Se}^{Sag}(t) \leq V_{Se}^{Hel} \tag{6.12}$$

6.4 Optimization problem

This section describes the proposed two-stage optimization problem.

6.4.1 Stage 1: Determination of PV capacity in each bus

In this stage, the PV generation capacity in each bus of a network, except the substation bus, is determined by maximizing the PVHC of the network. As mentioned earlier, PVHC is the total amount of PV capacity that a network can accommodate without deteriorating the operational performance of the network. The minimum load and maximum PV generation scenario is used to determine the PVHC of a network. The PV generation capacities of all load buses are the optimizing variables. The mathematical formulation for the first stage optimization problem is given below.

$$\max\{PVHC\} = \sum_{f \in \rho} P_f^{PVGEN} \tag{6.13}$$

subjected to the following constraints:

$$P_{ef} + P_f^{PVGEN} = \sum_{fg \in \tau} P_{fg} + P_f + \sum_{fg \in \tau} L_{fg} \qquad \forall f \in \rho \tag{6.14}$$

$$Q_{ef} = \sum_{fg \in \tau} Q_{fg} + Q_f + \sum_{fg \in \tau} M_{fg} \qquad \forall f \in \rho \tag{6.15}$$

$$V_e^2 = V_f^2 + 2\left(R_{ef}P_{ef} + X_{ef}Q_{ef}\right) + Z_{ef}^2 I_{ef}^2 \qquad \forall ef \in \mu \qquad (6.16)$$

$$I_{ef}^2 = \frac{P_{ef}^2 + Q_{ef}^2}{V_f^2} \qquad \forall ef \in \mu \qquad (6.17)$$

$$V_{min} \leq V_f \leq V_{max} \qquad \forall f \in \rho \qquad (6.18)$$

$$I_{ef} \leq I_{TH} \qquad \forall ef \in \mu \qquad (6.19)$$

$$(P_{PV})_{min} \leq P_f^{PVGEN} \leq (P_{PV})_{max} \qquad \forall f \in \rho \qquad (6.20)$$

$$PL_{PV} \leq \vartheta PL_{base} \qquad (6.21)$$

Eq. (6.13) represents the objective function. Eqs. (6.14)-(6.15) are used for active and reactive power balance at each bus of a network, except the substation bus. Eqs. (6.16) and (6.17) are used for the computation of bus voltage magnitude in each bus and line current flow in each line, respectively of a network. Eqs. (6.18) and (6.19) represent the bus voltage magnitude constraint and thermal capacity constraint, respectively. The constraint (6.20) is used to limit the PV generation capacity in each load bus. According to Eq. (6.21), the network power loss should not be more than a preset acceptable network power loss.

6.4.2 Stage 2: Operational optimization problem for energy loss minimization

In this stage, an optimization problem is formulated to determine the VAr set points for the inverters of UPQC-O in each load and PV generation scenario. The minimization of energy loss in each time step is the optimization objective. In this stage, $K_{Se}(t)$ and $K_{Sh}(t)$ of inverters are the optimizing variables. The PV capacities obtained in the first stage are used to determine the hourly PV generation of each bus. The mathematical formulation for the second stage optimization problem is given below.

$$\min\{EL\} = \sum_{ef\in\mu} I_{ef}^2 R_{ef} \qquad (6.22)$$

subjected to the following constraints:

$$P_{ef} + P_f^{PV} = \sum_{fg\in\tau} P_{fg} + P_f + \sum_{fg\in\tau} L_{fg} \qquad \forall f \in \rho \qquad (6.23)$$

$$Q_{ef} + Q_f^U = \sum_{fg\in\tau} Q_{fg} + Q_f + \sum_{fg\in\tau} M_{fg} \qquad \forall f \in \rho \qquad (6.24)$$

where, Q_f^U is the amount of VAr support to be provided by the series inverter (Q_f^{Se}) or shunt inverter (Q_f^{Sh}) located at bus 'f'.

$$V_e^2 = V_f^2 + 2\left(R_{ef}P_{ef} + X_{ef}Q_{ef}\right) + Z_{ef}^2 I_{ef}^2 \qquad \forall ef \in \mu \qquad (6.25)$$

$$I_{ef}^2 = \frac{P_{ef}^2 + Q_{ef}^2}{V_f^2} \qquad \forall ef \in \mu \qquad (6.26)$$

$$V_{min} \leq V_f \leq V_{max} \qquad \forall f \in \rho \qquad (6.27)$$

$$I_{ef} \leq I_{TH} \qquad \forall ef \in \mu \qquad (6.28)$$

$$Q_f^{Sh} \leq Q_{Sh} \qquad \forall f \in \xi \qquad (6.29)$$

$$Q_f^{Se} \leq Q_{Se} \qquad \forall f \in \Lambda \qquad (6.30)$$

Eq. (6.22) represents the objective function for the energy loss minimization. Eqs. (6.23)-(6.26) represent the steady-state operational constraints of a radial distribution network with UPQC-O and PV generation. Eqs. (6.23)-(6.24) are used for active and reactive power balance at each bus of a network, except the substation bus. Eq. (6.25) is used for the computation of bus voltage magnitude in each bus of a network. Eq. (6.26) is used for the computation of line current flow in each line of a network. Eqs. (6.27) and (6.28) represent the bus voltage magnitude constraint and thermal capacity constraint, respectively. The constraints (6.29) and (6.30) are used to limit the VAr injection below the respective capacities of shunt and series inverters, respectively.

6.5 Infrastructure for the real-time implementation of proposed methodology and solution strategy

This section briefly describes the solution approach along with the infrastructure required for the real-time implementation of the proposed methodology. A 5-bus radial distribution network with smart grid technologies, as shown in Fig. 6.5, is used. Smart-grid technologies, such as, smart meters (SMs), communication network (CN), advance control systems etc., are required for the implementation of proposed methodology. The respective functions of these technologies are explained below.

- *Smart meter (SM)*: It is required to measure the time varying load demand and PV generation under a distribution transformer (DT) and to send the information to distribution network control center (DNCC). For the proposed methodology, all the DTs located in a network should be equipped with the SMs.
- *Communication network (CN)*: It is required to send the load demand and PV generation injection data from each SM to DNCC. It would also be used to send the VAr injection

set points from the DNCC to each inverter after performing the operational optimization. The type of CN used for the communication of information can be decided based on the geographical area of network, distance between the load centers and DNCC, operating range of CN, data transfer rate of CN etc. Optical fibers or wireless communication can be used.

- *Control infrastructure*: It is used to control/regulate the behavior of devices/systems. In this work, it is used to receive the VAr injection set points from the DNCC and to tune the operations of the series and shunt inverters.
- *Other accessories*: The information of load demand and PV generation injection recorded by a SM, is, firstly encoded using an encoder to transmit the information to the DNCC. The information received by the receiver at the DNCC is, then, decoded by a decoder. The data aggregator unit collects the information of hourly average load demand and PV generation injection of all the buses. The load and PV generation data can also be obtained for a user defined time interval. These informations are transferred to the computer for determination of optimal VAr injection set points for the inverters of UPQC-O. The information of VAr injection set points are again encoded with an encoder to transmit the information to the respective control units of the inverters. The information received at the control unit is again decode with a decoder to tune the set points, i.e., $K_{Se}(t)$ and $K_{Sh}(t)$ of inverters.

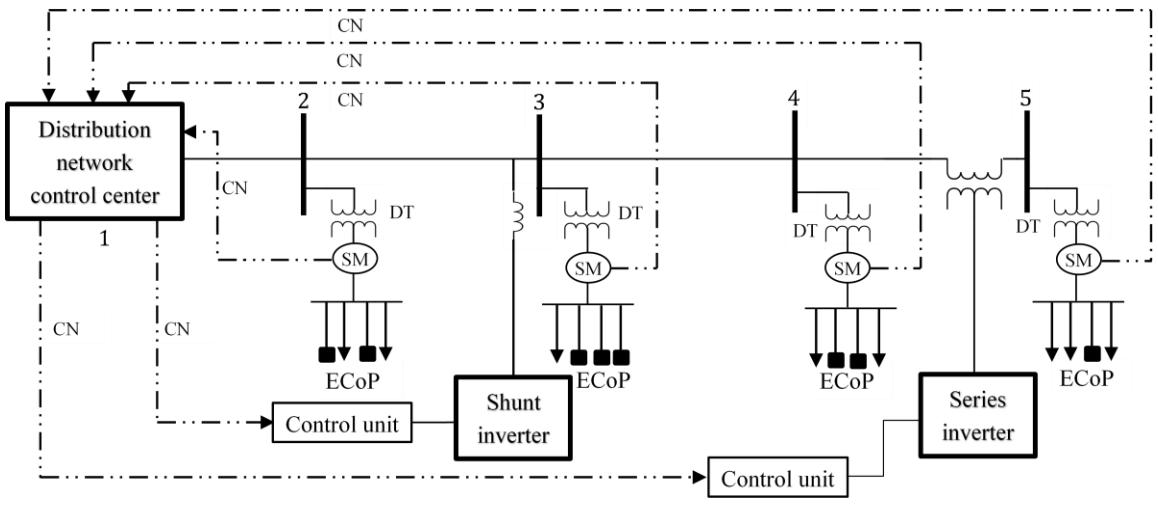

DT- Distribution transformer, SM- Smart meter, CN- Communication network, ECoP- Electricity consumers or prosumers

Fig. 6.5: Schematic diagram for the real-time implementation of proposed methodology

- *Solution strategy*: The proposed optimization model is fitted into GAMS, a high level modelling software used to solve different kind of optimization problems. Since the problem is a kind of non-linear optimization problem, CONOPT solver of GAMS is used. It takes less than two seconds to solve the proposed optimization problem. Hence, it can reliably be used in solving the problem online for real distribution networks. The determination of set points for the inverters of UPQC-O using GAMS is pictorially shown in Fig. 6.6. The set points obtained for series and shunt inverters of UPQC-O are sent to the respective control units. The snapshot for a solution obtained with GAMS-CONOPT solver is shown in Fig. 6.7.

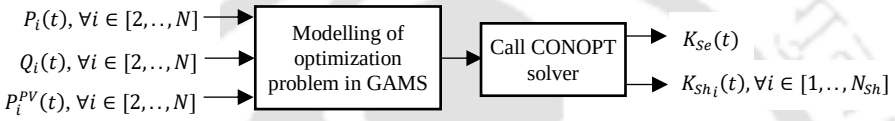

Fig. 6.6: Pictorial representation of set point determination in GAMS

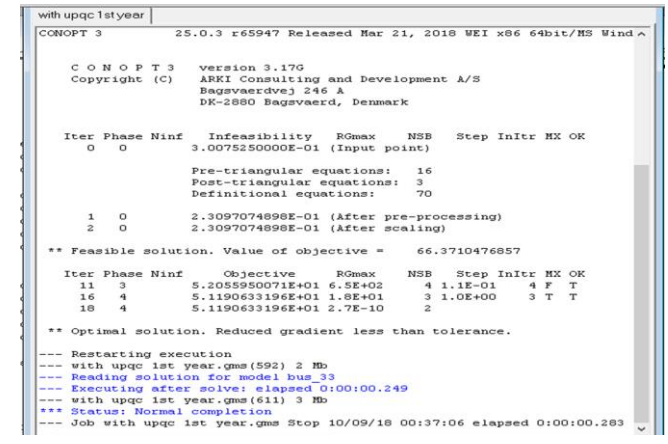

Fig. 6.7: Snapshot for a solution obtained with CONOPT solver of GAMS

6.6 Simulation results and discussion

The proposed methodology of the operational optimization of UPQC-O for the time varying load demand and PV generation is validated on a 33-bus radial distribution network. The bus data and line data of the network are provided in Appendix. It is a single feeder network as shown in Fig. 6.8. The circled area in the Fig. 6.8 is considered to be an industrial area. The voltage sag occurred in upstream network may severely affect the

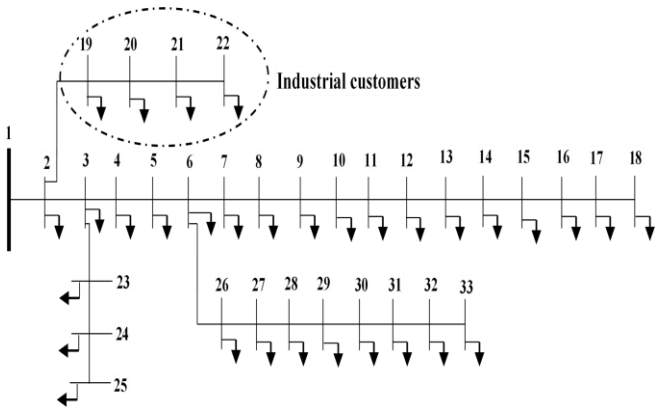

Fig. 6.8: Single line diagram of the 33-bus radial distribution network

performance of many adjustable speed drives used in industries [161]. Hence, a series inverter is judiciously located at bus 19 to protect all the industrial loads from voltage sag. Two case studies are provided as shown below.

- *Case A*: In this case, the energy loss in the network is minimized with the operational optimization of UPQC-O considering time varying load demand. This does not need the first stage of optimization. This is applicable only in passive networks.

The planning Case A consists of three subcases:

- Case A(1): Base-case network without compensation
- Case A(2): Base-case network with single-point compensation using a shunt inverter which is assumed to be located at bus 6
- Case A(3): Base-case network with three-point compensation using three shunt inverters located at buses 7, 8, and 9

- *Case B*: In this case, the energy loss in the network is minimized with the operational optimization of UPQC-O considering time varying load demand and PV generation.

The planning Case B consists of three subcases:

- Case B(1): Base-case network without UPQC-O and PV generation
- Case B(2): Base-case network with PV generation
- Case B(3): Base-case network with UPQC-O and PV generation

The VA-ratings of inverters are computed by considering the 30% voltage sag, 20% THD in line current, and peak load demand of the base-case network. The modelling

provided in subsection 2.2.3 is followed to set the VA-ratings of the inverters. It is assumed that the same amount of THD is present in all the loading conditions. The minimum load demand of the network is considered to be 20% of the peak load demand of base-case network [34]. The maximum limit of PV generation capacity $\{(P_{PV})_{max}\}$ in Eq. (6.20) is considered to be 300 kW. The rate of annual load growth and energy price growth are assumed to be 6% [57] and 4% [162], respectively. The unit cost of energy is assumed to be 0.08$/ kWh [75]. The planning horizon for the cost benefit analysis is considered to be 5 years. The minimum and maximum bus voltage magnitude limits are considered to be 0.9 p.u. and 1.05 p.u., respectively. The maximum line current flow limit for all lines are set as 300 A [34]. The CONPOT solver of GAMS is used to solve the problem. The simulation study is performed on Intel® Core™ i5-4570 CPU @ 3.2 GHz processor.

6.6.1 Simulation results with planning Case A

In this subsection, the simulation results obtained with planning Case A are discussed. An annual load growth is also considered. The load curves for different seasons of the 1st and 5th years are shown in Fig. 6.9. The planning Case A does not require Stage 1 optimization due to the consideration of no PV generation. The flow chart for the determination of the locations and sizes of shunt inverters for single-point and multi-point compensations is shown in Fig. 6.10. It is to be noted that the locations of the shunt inverters for multi-point compensation are chosen such that the sum total of the size of all inverters

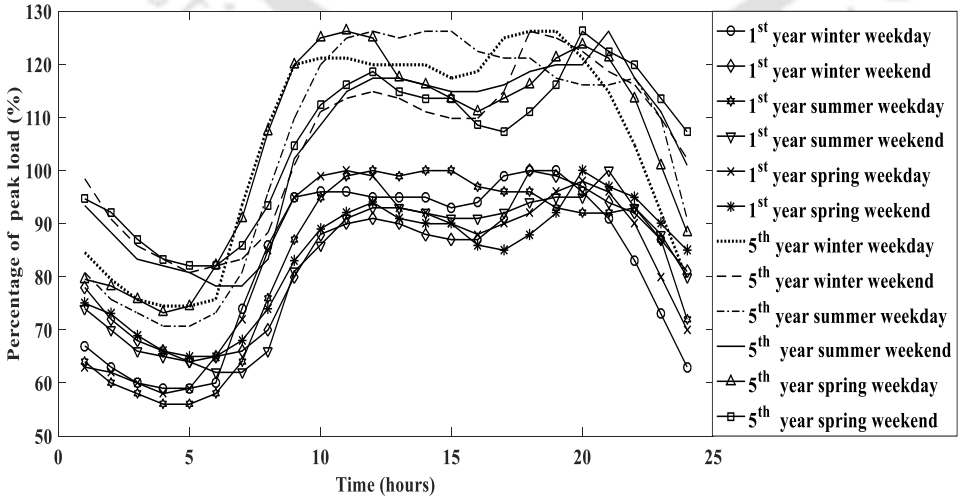

Fig. 6.9: Load curves for different seasons in the1st and 5th years of planning horizon

does not exceed the size of the inverter obtained in single point compensation. This is to have a fair comparison in between the single and multi-point compensations.

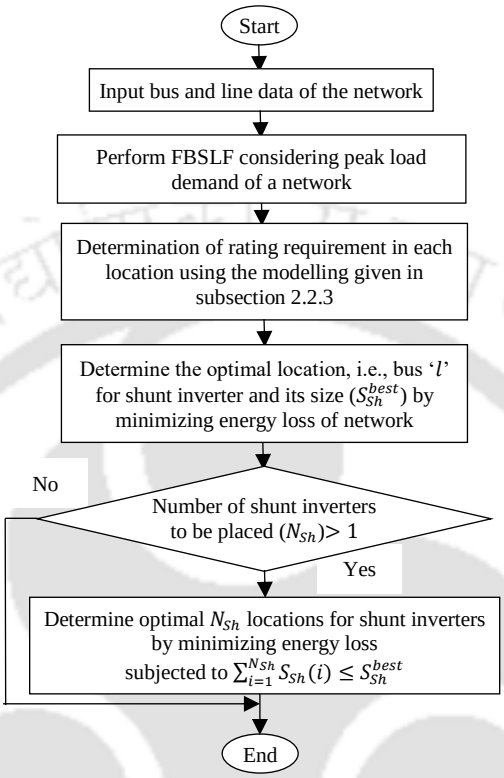

Fig. 6.10. Flow chart for the determination of locations and sizes of shunt inverters for single-point and multi-point compensations

6.6.1.1 Optimal VAr injection set point obtained for the inverters of UPQC-O in Case A(2) and Case A(3)

The optimal VAr injection set points obtained with CONOPT for the shunt inverters during 24-hour load variation are shown in Fig. 6.11 and Figs. 6.12(a) and 6.12(b) for the planning Cases A(2) and A(3), respectively. These show that the optimal VAr injection set points obtained for the shunt inverters are varying with the variation in load demand, except the one placed at bus 7 which is found to be same irrespective of different loading conditions (not shown in the figure). This illustrates that different amount of VAr injection is required in different loading condition to minimize the overall energy loss. The results also show that higher amount of VAr injection is required at higher load demand so as to minimize the overall energy loss. Thus, the shunt inverters need to set at the respective rated VAr

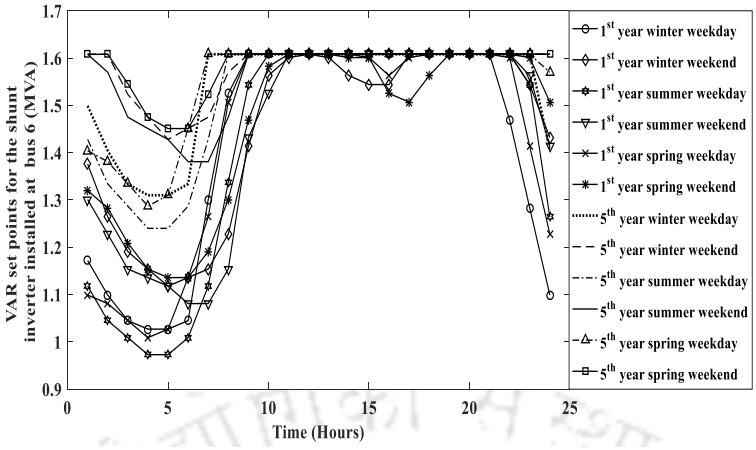

Fig. 6.11: Optimal VAr set points for the shunt inverter located at bus 6 in different seasons in the1st and 5th years

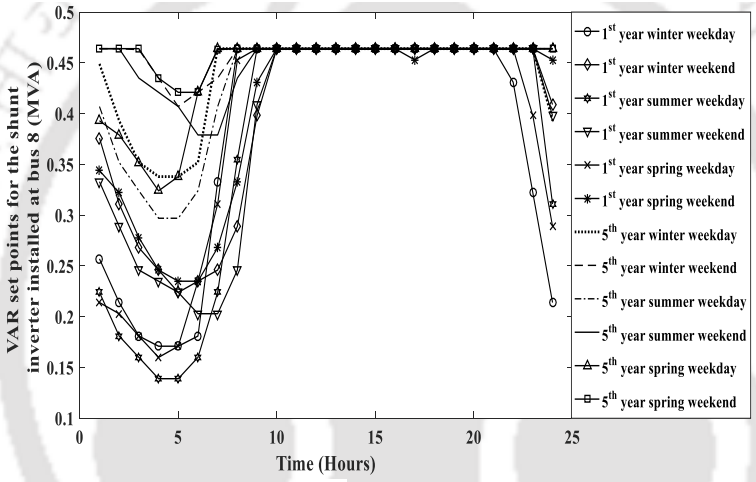

(a)

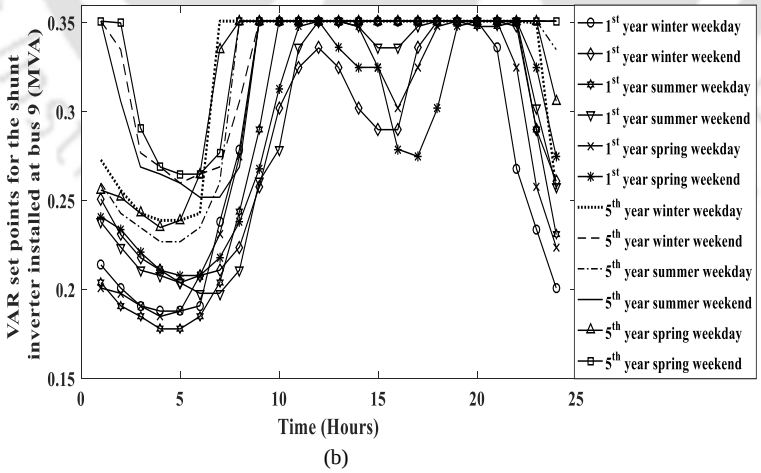

(b)

Fig. 6.12: Optimal VAr set points obtained for the shunt inverters located at: (a) bus 8 and (b) bus 9 in different seasons in the 1st and 5th years

capacity during higher loading conditions. The VAr compensation set points also need to be tuned with the future growth of load. The VAr compensation set points obtained for the

series inverter of UPQC-O during hourly load variation are found to be same in both the planning Cases A(2) and A(3). These are found to be set at the rated VAr capacity of the series inverter.

6.6.1.2 Minimum bus voltage magnitude

The minimum bus voltage magnitudes obtained with Cases A(1)-A(3) are shown in Figs. 6.13(a)-(f) for the weekday and weekend of different seasons considering 6% of annual load growth. The results of the 1st year and 5th year after the UPQC-O installation are shown. The results show that the minimum bus voltage magnitude of network is varying with the variation in load demand. For the obvious reason, the minimum bus voltage magnitude of network is found to be less in the 5th year as compared to the 1st year. In the 5th year, the minimum bus voltage magnitudes obtained without UPQC-O {in Case A(1)} are violating the limit set. However, with the UPQC-O {in Case A(2) and Case A(3)} the bus voltage magnitude is found to be well above the limit. It implies to the fact that the VAr supports provided by the UPQC-O in both the cases improve the bus voltage magnitude of the network. The results also show that the minimum bus voltage magnitude obtained with Case A(3) is slightly better than that of the Case A(2). The reason is that the UPQC-O provides three-point compensation in Case A(3). However, in Case A(2), UPQC-O provides single point compensation with a shunt inverter.

6.6.1.3 Cost benefit analysis

The cost benefit analysis is provided considering two cost components: (i) cost of placement of UPQC-O, and (ii) saving due to the energy loss reduction. The unit cost for placement of UPQC-O is computed as [92]:

$$C_U = 0.0003{S_U}^2 - 0.2691S_U + 188.2 \qquad (\$/kVA) \tag{6.31}$$

where, S_U is the total VA-rating of UPQC-O in MVA.

This does not include the cost of smart grid technologies, such as, costs of communication network, smart meters, high speed computers, control systems. The annual energy loss (in kWh) of distribution network is computed as:

$$AEL = 1000S_{base} \sum_{y\in\Delta} t_y \sum_{w\in\beta} t_w \sum_{d_{yw}\in\Gamma_{yw}} t_{ywh} \sum_{ef\in\mu} I^2_{efd_{yw}} R_{ef} \tag{6.32}$$

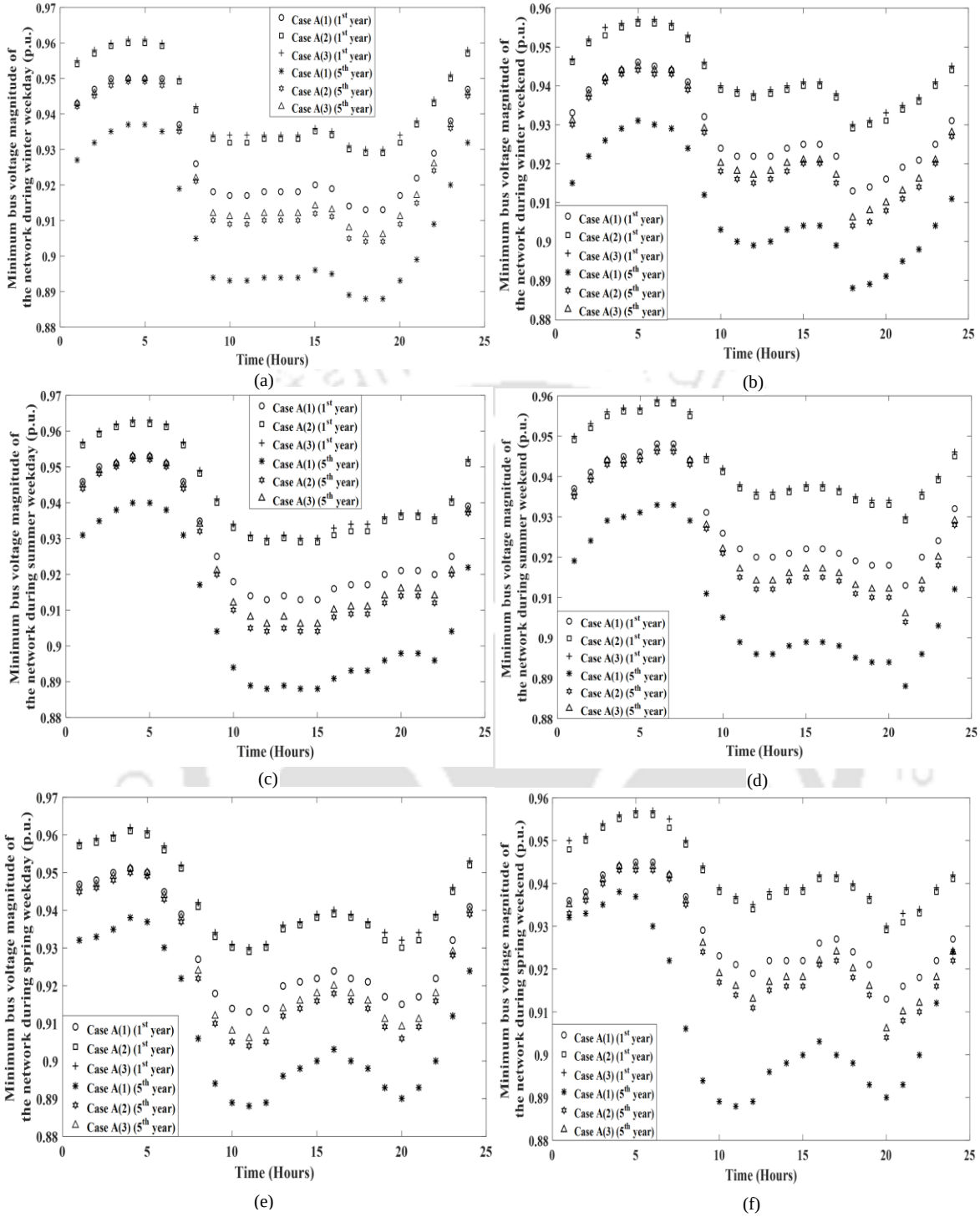

Fig. 6.13: Minimum bus voltage magnitude of the network obtained for: (a) winter weekday, (b) winter weekend, (c) summer weekday, (d) summer weekend, (e) spring weekday, and (f) spring weekend in the 1st and 5th years for Cases A(1)-A(3)

The saving from energy loss reduction in the 1st and 5th years are computed as:

$$C_{AEL1} = C^E(AEL_{base1} - AEL_{U1}) \tag{6.33}$$

$$C_{AEL5} = C^E(1 + r_e)^4(AEL_{base5} - AEL_{U5}) \tag{6.34}$$

where, AEL_{base1} and AEL_{base5} are the annual energy loss of base-case network (without UPQC-O) in 1st and 5th years, respectively; AEL_{U1} and AEL_{U5} are the annual energy loss of network with UPQC-O in 1st and 5th years, respectively. The average annual saving due to the energy loss reduction is computed as:

$$C_{AEL}^{Avg} = \frac{C_{AEL1}+C_{AEL5}}{2} \tag{6.35}$$

The return of investment (%) after completion of planning horizon (T^h) is computed as:

$$IR = 100\frac{T^h C_{AEL}^{Avg}}{1000 C_U S_U} \tag{6.36}$$

Table 6.1 shows the different parameters related to the cost-benefit analysis. The results show that the return of investment in planning Case A(3) is more as compared to Case A(2) because of the less VA-rating requirement of UPQC-O in Case A(3). It is noteworthy that the numerical value provided in Table 6.1 for return of investment is only in view of saving due to the energy loss reduction. There is another important benefit of planning Cases A(2) and A(3). The deployment of UPQC-O in distribution networks defers the network upgrade cost to the future years. The inclusion of this would further increase the percentage of return of investment.

Table 6.1: Cost benefit analysis without and with UPQC-O

Costs and operational parameters	Case A(1)	Case A(2)	Case A(3)
Annual energy loss in the 1st year (MWh)	1233.2115	943.4183	950.4731
Reduction in annual energy loss with UPQC-O in 1st year (%)	-	23.4991	22.9270
Saving from energy loss reduction in 1st year ($)	-	23092.544	22619.072
VA-rating of UPQC-O (MVA)	-	1.7991	1.5811
Installation cost of UPQC-O (×10^5$)	-	3.3793	2.9740
Annual energy loss in the 5th year (MWh)	2038.5334	1570.4532	1583.6506
Reduction in annual energy loss with UPQC-O in 5th year (%)	-	22.9616	22.3142
Saving from energy loss reduction in 5th year ($)	-	43807.0103	42571.8830
Average of 1st and 5th years saving ($)	-	33449.7772	32595.4775
Return of investment after completion of 5 years (%)	-	49.4922	54.8007

6.6.1.4 Comparison of annual energy losses obtained with variable and constant/rated VAr set points of UPQC-O

This section provides the comparison between two approaches of energy loss minimization with UPQC-O. These are: (i) UPQC-O with variable set points and (ii) UPQC-O with constant/rated set point of UPQC-O. The annual energy losses obtained in the 1st year of planning horizon with variable and constant VAr set points of UPQC-O are

shown in Table 6.2 for the planning Cases A(2) and A(3). The simulation results show that the UPQC-O with variable VAr injection set points yields lower energy loss as compared to the UPQC-O with constant/rated VAr injection. The integration of UPQC-O with variable VAr injection set points results in 10611.7 kWhr and 8365.8 kWhr of energy saving for the planning Cases A(2) and A(3), respectively.

Table 6.2: Annual energy loss of distribution network with variable and constant VAr injection set points of UPQC-O

Annual energy loss of the network	Case A(2)	Case A(3)
Without UPQC-O (MWh)	1233.2115	1233.2115
With variable set points of UPQC-O (MWh)	943.4183	950.4731
% reduction *w.r.t.* without UPQC-O	23.4991	22.9270
With constant set point of UPQC-O (MWh)	954.0300	958.8389
% reduction *w.r.t.* without UPQC-O	22.6386	22.2486
Saving of energy with variable set points of UPQC-O *w.r.t.* constant set point of UPQC-O (kWh)	10611.7000	8365.8000

Another case study is provided by varying the load demand of the same network according to the load demand duration curves of different regions of India [163], as shown in Fig. 6.14. The single point compensation using a shunt inverter {i.e., Case A(2)} is chosen for this study. The total energy losses obtained in 1st year of planning horizon with variable and constant/rated VAr set points of UPQC-O are shown in Table 6.3. The load factor (LF) corresponding to each load demand duration curve is also shown in Table 6.3. The results clearly show that the variable VAr injection set points of UPQC-O result in higher energy loss reduction and greater saving in energy as compared to the constant/rated VAr injection. It is also observed that the energy saving with the variable VAr injection set

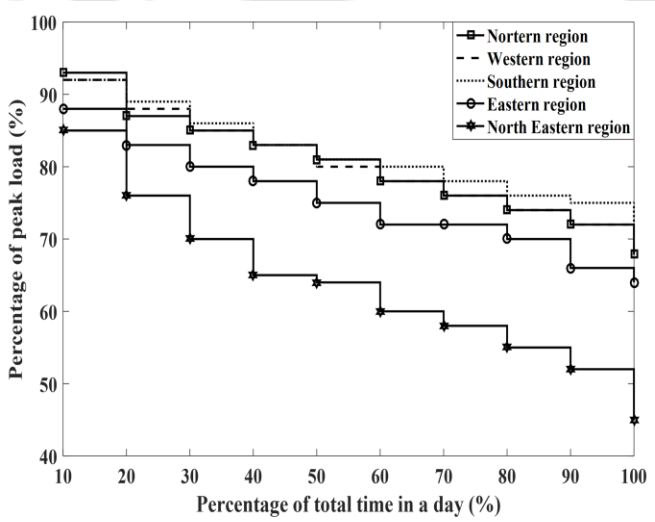

Fig. 6.14: Load demand duration curves for different regions of India [163]

points of UPQC-O is more if the LF of demand duration curve is less. Hence, the proposed approach of energy loss minimization is more effective in those areas where LF is low as the north eastern region of India.

Table 6.3: Annual energy loss obtained by varying the load demand according to the demand duration curves of different regions of India with variable and constant VAr set points of UPQC-O

Annual Energy loss of the network	Load demand variation according to the load demand duration curve of different regions in India				
	Northern region (LF=0.8570)	Western region (LF=0.8641)	Southern region (LF=0.8826)	Eastern region (LF=0.85)	North Eastern region (LF=0.7412)
Without UPQC-O (MWh)	1104.4853	1098.9245	1145.3691	966.8841	691.8902
With variable set points of UPQC-O (MWh)	846.4569	842.2293	877.4489	742.2120	532.7079
% reduction *w.r.t.* without UPQC-O	23.3619	23.3588	23.3916	23.2367	23.0069
With constant set point of UPQC-O (MWh)	853.9861	850.0108	883.0378	755.3617	569.8538
% reduction *w.r.t.* without UPQC-O	22.6802	22.6507	22.9036	21.8767	17.6381
Saving of energy with variable set points of UPQC-O *w.r.t.* constant set point of UPQC-O (kWh)	7529.2	7781.5	5588.9	13149.7	37145.9

6.6.1.5 Comparison among different compensation approaches for the energy loss reduction of distribution network

In the literature, several approaches are reported for energy loss reduction in distribution networks. In this section, a case study is presented for the comparison of the solutions obtained with the proposed approach with two similar approaches. The following approaches of energy loss minimization are considered:

- *Case 1*: In this case, the sizes of series and shunt inverters of UPQC-O in a location are determined using the modelling provided in subsection 2.2.3.
- *Case 2*: In this case, the sizes of series and shunt inverters of UPQC-O are determined through optimization by setting minimum and maximum set values for the VA-ratings.

The Case 1 and Case 2 have two subcases:

  - In Cases 1(a) and 2(a), the energy loss is minimized with variable VAr injection set points of UPQC-O.
  - In Cases 1(b) and 2(b), the energy loss is minimized with constant/rated VAr injection of UPQC-O.

- *Case 3*: In this case, the energy loss is minimized with the allocation of DSTATCOM. The size of DSTATCOM is determined through optimization by setting minimum and maximum set values for the VA-rating of DSTATCOM for energy loss minimization in peak load condition.

- *Case 4*: In this case, the energy loss is minimized with the allocation of fixed capacitor bank. The size of capacitor bank is also determined through the optimization for energy loss minimization in peak load condition.

The single point compensation is chosen for this case study. The results obtained with these four cases are shown in Table 6.4. The results show that the variable VAr set points of UPQC-O in Case 1(a) and 2(a) provide better compensation to obtain higher energy loss reduction as compared to Cases 1(b) and 2(b), respectively. The solutions obtained with Case 1(a) and Case 2(a) show similar annual energy loss reduction. However, the VA-rating requirement for UPQC-O for solution obtained with Case 2(a) is higher as compared to Case 1(a). The allocation of DSTATCOM in Case 3 provides similar annual energy loss reduction as obtained with the solutions of Cases 1(a) and 2(a). The size of DSTATCOM is also found to be similar as obtained with Case 1. Among all the above mentioned approaches, the allocation of fixed capacitor bank results in comparatively lesser energy loss reduction in network because of the constant VAr injection in Case 4. Although the installation of capacitor bank for VAr compensation is an economical option, it is not skilled to mitigate any of the PQ issues. UPQC-O with its series inverter can protect the downstream load from voltage sag occurring in upstream section. The voltage sag mitigation can be done with a DSTATCOM installed in a similar strategic location. However, this needs additional DSTATCOM and it will increase the total VA rating.

Table 6.4: Comparison among different compensation approaches of energy loss reduction

Solution obtained with different types compensation approaches	Case A(1)	UPQC-O Allocation				DSTATCOM allocation (Case 3)	Capacitor allocation (Case 4)
		Case 1		Case 2			
		Case 1(a)	Case 1(b)	Case 2(a)	Case 2(b)		
Annual energy loss (MWh)	1233.2115	943.4183	954.0300	942.5683	963.9156	943.7999	965.0003
VA-rating of shunt compensator (MVA)	-	1.6078	1.6078	1.778	1.778	1.792	1.792
VA-rating of series compensator (MVA)	-	0.1913	0.1913	0.359	0.359	-	-
Total VA-rating	-	1.7991	1.7991	2.137	2.137	1.792	1.792

6.6.2 Simulation results with planning Case B

For planning Case B, single point compensation using one shunt inverter located at bus 6 is considered. The load growth is not considered in this study. The simulation results obtained with planning Case B are discussed in subsequent subsections.

6.6.2.1 PV capacity of each bus

The PV capacity of each bus as obtained with the Stage 1 optimization problem is shown in Fig. 6.15. From the bar chart, it is observed that the buses near to the substation can allow more integration of PV than the buses distant away from the substation. It also provides the information of maximum PV generation that a network can accommodate in each bus during peak generation hour. The allowable maximum PV generation in each bus would be equal to the PV capacities of the respective buses.

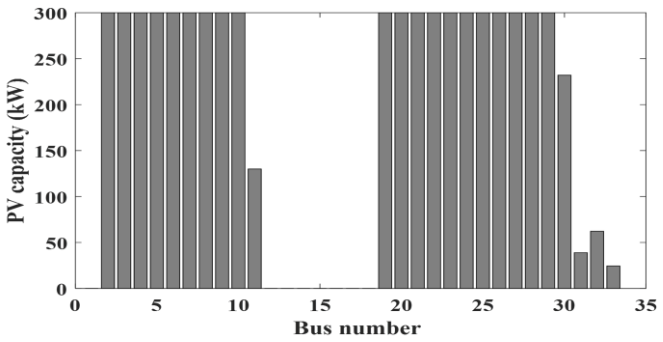

Fig. 6.15: Bar chart for the PV capacities in each bus of 33-bus radial distribution network

6.6.2.2 Hourly energy loss and minimum bus voltage magnitude

The hourly energy loss obtained with Cases B(1)-B(3) are shown in Figs. 6.16 (a)-(c) for the different seasons in a year. The results show that the energy loss of the network is varying with the variations in load demand and PV generation in Cases B(2) and B(3). The energy loss reduction in Case B(2) is observed only during PV generation hours as compared to Case B(1). However, the energy loss reduction in Case B(3) is observed throughout the day as compared to Cases B(1) and B(2). It is due to the VAr compensation provided by the inverters of UPQC-O in addition to the active power compensation provided by the PV. The numerical values for annual energy loss are provided in Table 6.5 for Cases B(1)-(3).

The minimum bus voltage magnitude obtained with Cases B(1)-(3) are shown in Figs. 6.17 (a)-(c) for different seasons in a year. The results show that the minimum bus voltage magnitude is also varying with the variations in load demand and PV generation in Cases B(2) and B(3). In Case B(2), significant improvement in minimum bus voltage

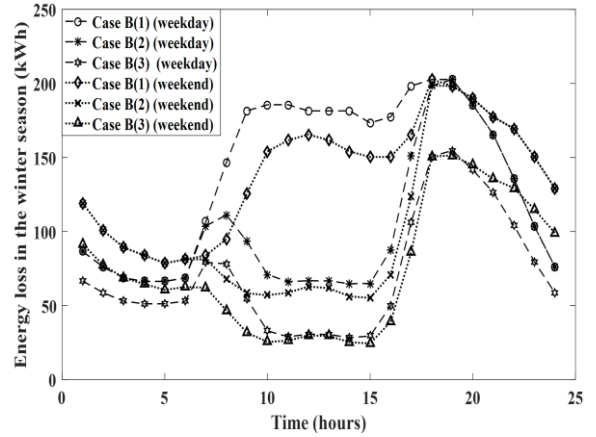

(a)

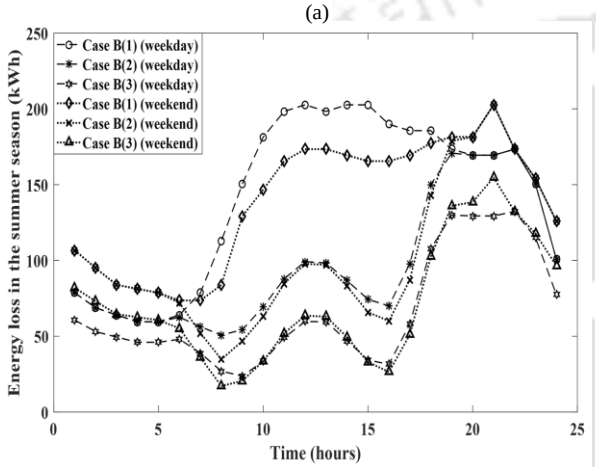

(b)

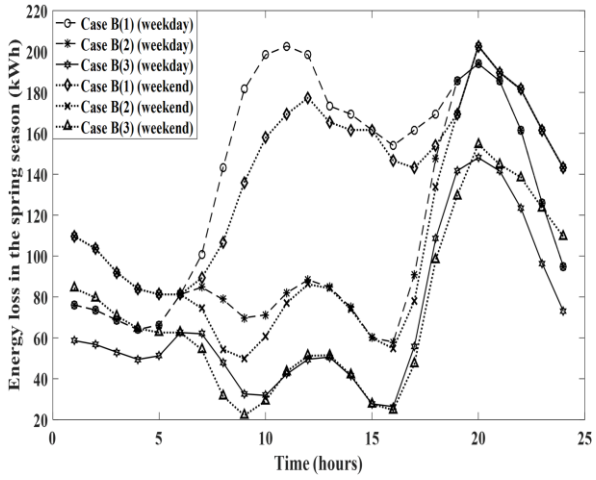

(c)

Fig. 6.16: Hourly energy loss of the network obtained with Cases B(1), B(2), and B(3) for the weekday and weekend of: (a) winter, (b) summer, and (c) spring seasons

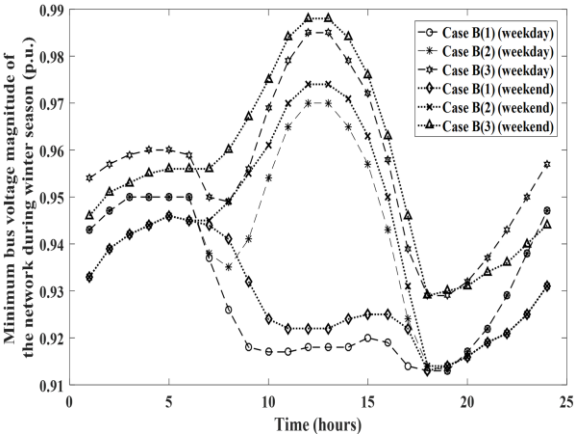

(a)

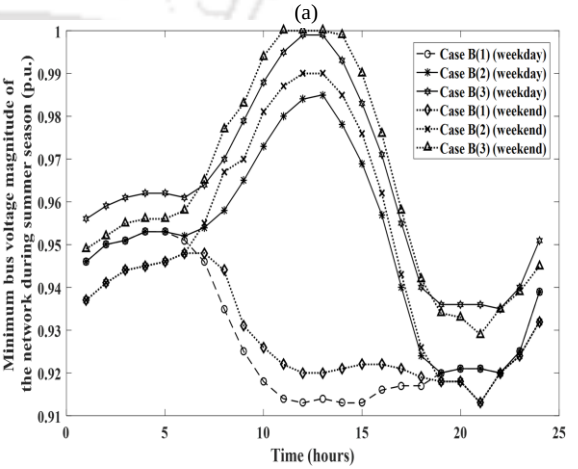

(b)

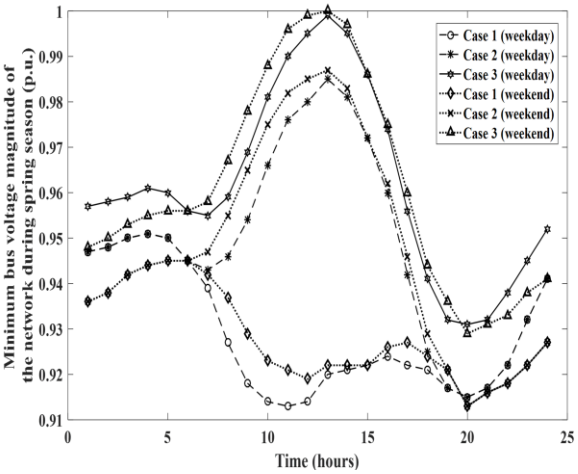

(c)

Fig. 6.17: Minimum bus voltage magnitude of the network obtained with Cases B(1), B(2), and B(3) for the weekday and weekend of: (a) winter, (b) summer, and (c) spring seasons

magnitude is observed during PV generation hours as compared to Case B(1). In Case B(3), the improvement in minimum bus voltage magnitude is observed throughout the day as

compared to Cases B(1) and B(2) due to the VAr compensation provided by the inverters of UPQC-O.

Table 6.5: Annual energy loss obtained for different planning cases of Case B

Parameters	Case B(1)	Case B(2)	Case B(3)
Annual energy loss (MWh)	1233.2115	878.5402	609.3889
% reduction w.r.t. Case B(1)	-	28.7600	50.5852

6.6.2.3 VAr injection set points for the inverters of UPQC-O

The VAr injection set points obtained for the shunt inverter of UPQC-O during hourly load demand and PV generation variations are shown Fig.6.18 for Case B(3). It is observed that the VAr injection set points for the shunt inverter are varying with the variations in load demand and PV generation. It means that different amount of VAr injection is required in different load and PV generation scenario to minimize the energy loss of a distribution network. The results show that the higher amount of VAr injection is required during higher load demand or/and PV generation hours to minimize the energy loss for a distribution network. Thus, the shunt inverter needs to be set at the rated VAr capacity in some of the higher load or/and PV generation hours. The VAr compensation set points obtained for the series inverter of UPQC-O during hourly load demand and PV generation variations are found to be same in the planning Case B(3). These are found to be set at the rated VAr capacity of the series inverter.

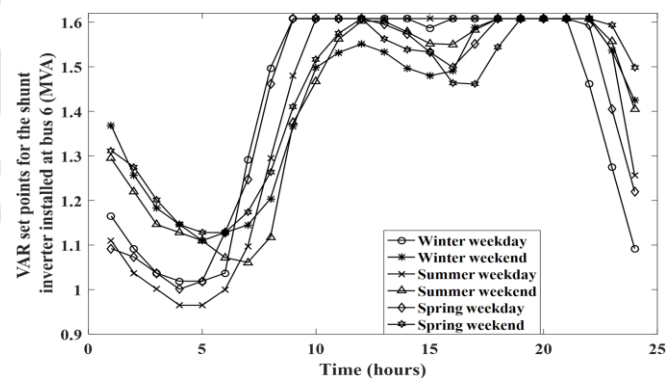

Fig. 6.18: VAR set points obtained for the shunt inverter installed at bus 6 in Case B(3) for different seasons in a year

6.7 Conclusion

In this chapter, an online operational optimization approach for energy loss minimization with load and PV generation variations has been proposed for distribution

networks. The UPQC-O is modeled to provide time varying VAr compensation for the energy loss reduction. The infrastructure required for the real-time implementation of the proposed methodology are also provided. The simulation results obtained with proposed approach provide the following:

- The annual load growth and variations in load demand and PV generation need the tuning of set points of the inverters of UPQC-O to have optimal operation. Hence, the optimal VAr compensation set points for shunt inverter(s) are found to be varying with the load growth and time varying load demand and PV generation.
- The deployment of any of the planning cases (with UPQC-O and/or PV generation) can reduce significant amount of the annual energy loss. It also significantly improves the bus voltage magnitude of distribution networks.
- The deployment of the planning cases with UPQC-O defers the network upgrade cost to future years, as well.
- The planning Case A(3), being a three-point compensation, is the economical option than the Case A(2) (i.e., single point compensation) in view of higher return of investment and less VA-rating of UPQC-O. But, it requires more investment to establish the communication network and control infrastructure.
- The UPQC-O with variable VAr set points can provide better compensation in terms of higher loss reduction as compared to the constant VAr set point approach. The deployment of proposed approach in the areas where load factor is low can save more energy as compared to the constant/rated VAr compensation.
- The deployment of UPQC-O in distribution network along with the PV generation, i.e., Case B(3) shows its effectiveness over the Cases B(1) and B(2) in energy loss reduction and bus voltage improvement. It is due to the time-varying VAr support provided by the UPQC-O.
- The injection of surplus PV generation {i.e., Cases B(2)-B(3)} into a network is advantageous for the utility, because, it reduces the energy loss and improves the bus voltage magnitude during PV generation hours. But, a utility needs to put some limit on the maximum injection of PV generation in each bus, beyond which it may deteriorate the operational performance of the network. The first stage optimization provides the frame work for this.

7

Conclusions

The distribution networks are slowly changing from PDNs to ADNs due to the integration of renewable based DG units. The proper planning of ADN is required to flexibly work with the intermittent renewable generation and continuously varying load demand. The power systems researchers have significantly contributed on ADN planning in last few years. In Chapter-1, different ADN planning approaches reported in the literature have been systematically presented. These approaches are classified according to the three level classification tree developed based on the different attributes of planning. In the literature review, the special focus is given to identify the inclusion of two important features: (i) mitigation of the PQ issues, and (ii) integration of the energy storage unit in ADN planning. The qualitative assessment of presented work on ADN planning provides that there is need of an approach to improve PQ of distribution networks. It is also known that distribution networks suffer from poor energy efficiency and lower bus voltage magnitude due to the high resistance to reactance ratio of distribution line. Thus, there is need of an approach which can simultaneously improve both these aspects. The custom power devices are kind of compensator which can simultaneously provide reactive power compensation and PQ issues mitigation. The UPQC is a type of custom power devices which injects a series voltage and a shunt compensating current by using its series and shunt inverters, respectively to mitigate voltage sag/swell in supply voltage, to provide reactive power compensation, and to eliminate current harmonics. In open UPQC (UPQC-O) model,

the series and shunt inverters can be placed in different locations in a network unlike UPQC. This needs the modelling of UPQC-O and the formulation of planning approach for its optimal allocation in distribution networks. Thus, this thesis is focused on the modelling and allocation planning of UPQC-O to improve operational performance of distribution networks. The contributions of this thesis are summarized as follows:

- In Chapter-2, the modelling of UPQC-O without and with active power injection has been proposed for the distribution networks. A new technical constraint, percentage of voltage sag mitigated load (PVSML) has been formulated to ensure the protection of a minimum amount of load from the supply voltage sag by the series inverter. A planning optimization model has been formulated to optimally place the UPQC-O in distribution network for the energy/power loss reduction. Its placement can also ensure desired PQ level. PSO based solution approach has been used to solve the optimization problem. Two charging schemes for the battery connected to the UPQC/UPQC-O: (i) by consuming/purchasing energy from the grid and (ii) with the installation of a PV array with each battery unit have been proposed. Cost-based analysis has been presented for these two schemes. A comparative study has been carried out among the UPQC and UPQC-O models without and with active power injection to assess the potential of UPQC-O in enhancing the energy efficiency and PQ of distribution networks. The comparative study provides that the placement of UPQC-O results in significant reduction in energy loss and improvement in bus voltage magnitude. It is also found to be an economical option due to the less battery rating requirement as compared to UPQC, if it is designed for active power injection. Otherwise, UPQC placement is more economical option. In the connected UPQC models, the series and shunt inverters locations are found to be near to the substation to protect the given number of loads from voltage sag. But, the same can be done with UPQC-O by placing only the series inverter near to the substation. Hence, UPQC-O has the flexibility to place its shunt inverter at the location which results in higher power loss reduction. The charging of the battery can be done with the installation of PV array. This needs additional investment cost. It is found to be an economical option as compared to the cost of the energy purchase from the grid for the battery charging over a planning horizon.

- In Chapter-3, the modelling of UPQC-O has been proposed with the PV array for distribution networks. The planning optimization model has been formulated to optimally place the multiple UPQC-O in distribution networks for the energy efficiency and PQ improvement. PSO based solution approach has been used to solve the proposed optimization problem. Two case studies have been presented for energy efficiency improvement using two UPQC-O models: (i) UPQC-O with battery and PV array and (ii) UPQC-O without battery and with PV array. The relative merits and demerits of deploying these models in distribution networks have also been provided. The performance of proposed approach has been compared with the other similar approaches of power/energy loss reduction. The simulation studies carried out using two test networks, i.e., 33- and 69-bus networks, provide that the placement of any of the UPQC-O models with PV array can significantly improve energy efficiency, bus voltage profile, and PQ for the distribution networks. Also, the multiple placement of the shunt inverters significantly reduces the overall rating requirement for UPQC-O for certain type of the networks, such as the 33-bus network. It is found that the sizes of the PV array and battery basically depend on the minimum DG penetration limit to be set by the DNO.
- In Chapter-4, mono- and multi-objective planning approaches have been proposed to improve the PVHC and energy efficiency of distribution networks. In this chapter, firstly, mono-objective planning has been carried out to maximize the PVHC of a distribution network. For this, the PVHC is defined considering the network power loss as an operational performance index. The modelling of series and shunt inverters has been formulated to provide reactive power compensation to the distribution networks. The planning optimization model has been formulated to determine the locations of inverters of UPQC-O and PV generation capacity in each bus, except substation bus, by maximizing the PVHC of distribution network constrained by the network power loss. PSO is used as the solution approach. The simulation results obtained with this planning approach provide that the appropriate placement of series and shunt inverters increases the hosting capacity of a network constrained by a permissible power loss. The PVHC of a distribution network can be of higher values if the permissible limit of the network power loss is set to increase. A case study has been carried out to assess the potential of

inverters of UPQC-O in enhancing the energy efficiency of distribution networks during peak load and no PV generation scenario. It is found that the placement of UPQC-O in other loading conditions can improve the energy efficiency and bus voltage magnitude. The impact of placement of single series/shunt inverter on the PVHC has also been provided. It shows that the placement of both series and shunt inverters provides better PVHC as compared to the placement of single series/shunt inverter. The performance of the proposed mono-objective planning approach has been qualitatively compared with the other similar approaches of PVHC maximization. The multi-objective planning has been carried out to simultaneously optimize the PVHC and energy loss of distribution networks with the optimal allocation of inverters of UPQC-O. For this, multi-objective optimization problem is formulated. In this case, Pareto-based MOPSO is used as the solution approach. The results show that the placement of UPQC-O simultaneously improves the PVHC and energy loss of the distribution networks. It also ensures a desired PQ level. The Pareto-approximation front obtained with MOPSO shows the maximization of the PVHC and the energy loss minimization do conflict with each other. This also provides variety of choices to an electric utility, from which it can decide the amount of PV generation that can be accommodated in each bus corresponding to the desired levels of PVHC and energy loss. The impact of set value of maximum PV generation capacity and UPQC-O placement on the Pareto-approximation front is also studied. The PV generation capacities obtained in each load bus from both the approaches show that the buses located near to the substation is capable of accommodating higher capacity of PV generation as compared to the buses located distant away from the substation.

- In Chapter-5, a multi-objective planning approach has been proposed for simultaneous improvement of peak load shaving and PQ of distribution networks. For this, the PV-BESS integrated UPQC-O is optimally allocated in distribution networks by simultaneously optimizing the three objectives: (i) ratio of power supplied by PV-BESS-UPQC-O to the base-case network peak active power demand, (ii) cost of placement of PV-BESS-UPQC-O, and (iii) ratio of total power loss during peak load demand with the placement of PV-BESS-UPQC-O to the base-case network peak power loss. The Pareto-based MOPSO is used to solve the multi-objective planning

problem. This provides a set of solutions, from which a DNO can decide the amount of peak load shaving to be obtained with the placement of PV-BESS-UPQC-O according to its capital expenditure budget and energy economy. The deployment of solution corresponding to the higher peak load shaving requires higher investment and incurs higher power loss. In addition to the peak shaving, the placement of PV-BESS-UPQC-O in distribution networks provides multiple benefits, such as, PQ improvement, power loss reduction in other loading conditions, investment deferral for network reinforcement etc. The performance of proposed approach has also been qualitatively compared with the other similar approaches of peak load shaving.

- In Chapter-6, an operational optimization approach has been proposed to determine the time varying reactive power injection set points of UPQC-O during time varying load demand and PV generation for energy loss minimization in distribution networks. A two–stage optimization problem has been formulated to determine the maximum PV generation capacity in each load bus and to minimize the energy loss in each time step. A suitable solution strategy has been devised to solve the proposed optimization problem. It is found that the CONOPT solver of GAMS takes less than 2 seconds to solve the proposed energy loss minimization problem for single load or/and PV generation scenario. Thus, the proposed methodology can be implemented in real-time with smart grid technologies. For this, the infrastructure required for real-time implementation of proposed methodology has also been provided. Two planning cases are formulated for energy loss minimization in distribution networks with UPQC-O. In case of operational optimization of UPQC-O with time varying load demand, the case study is presented with single and three-point compensations using single and three shunt inverter(s), respectively for energy loss minimization in distribution networks. It also considers the annual load growth. The cost benefit analysis for these two compensation approaches is carried out for a planning horizon. This study provides that the three-point compensation is the economical option than the single point compensation in view of higher return of investment. But, it requires more investment to establish the communication network and control infrastructure. A case study has been presented with the constant and variable VAr set points of UPQC-O for energy loss minimization in distribution networks. The results show that the UPQC-O with

variable VAr set points can provide higher loss reduction as compared to the constant VAr set point approach. The deployment of proposed approach in the areas where load factor is low can save more energy as compared to the constant/rated VAr compensation. The proposed approach of energy loss minimization is compared with the other approaches of energy loss minimization. In case of operational optimization of UPQC-O with time varying load demand and PV generation, the energy loss minimization study is carried out. The simulation results obtained with this planning case provide that the injection of surplus PV generation into a network is advantageous for the utility, because, it reduces the energy loss and improves the bus voltage magnitude during PV generation hours. But, an electric utility needs to put some limit on the maximum injection of PV generation in each bus, beyond which it may deteriorate the operational performance of the network. The first stage optimization provides the frame work for this. In both the planning cases, optimal VAr set points obtained for the shunt inverters show that the annual load growth and variations in load demand and PV generation need the tuning of set points of the inverters to have optimal operation. Hence, the optimal VAr compensation set points for the shunt inverter(s) are found to be varying with the load growth and time varying load demand and PV generation. The deployment of any of the planning cases with UPQC-O or/and PV generation significantly reduces the energy loss and improves the bus voltage profile of distribution networks. It also defers the network upgrade cost to future years.

In this thesis, the modelling and allocation of different UPQC-O models have been presented to improve the energy efficiency, bus voltage profile, PVHC, PQ, and peak load shaving of distribution networks. Also, an operational planning approach has been developed for the operation of UPQC-O during time varying load demand and PV generation. The proposed approaches are compared with the other existing approaches. The major contributions of this thesis are summarized as follows:

- Modelling and allocation planning of UPQC-O without and with active power injection have been proposed to improve energy efficiency of distribution networks by keeping a desired PQ level intact.

- Modelling and allocation planning of UPQC-O integrated PV generation system have been proposed for the improvement of energy efficiency and PQ of distribution networks.
- Mono- and multi-objective planning approaches have been proposed to improve PVHC and energy efficiency of distribution networks with optimal allocation of UPQC-O.
- Multi-objective planning approach has been proposed to simultaneously improve the peak load shaving and PQ of distribution networks with optimal allocation of PV-BESS integrated UPQC-O.
- An operational optimization approach for UPQC-O has been proposed to minimize the energy loss in distribution networks with time varying load demand and PV generation.

There are many practical aspects which can be incorporated in the planning models. The following aspects need to be investigated in future.

- *Consideration of unbalanced and mesh/ring distribution networks in planning models*: The proposed approaches are developed for the balanced radial distribution networks. The study can be extend with the consideration of unbalanced distribution networks. Also, the distribution networks can be of ring/mesh type. Hence, there is need of planning model for ring/mesh type networks.
- *Development of control scheme for UPQC-O*: In UPQC-O, the series and shunt inverters are placed in different locations of a network. Thus, they need coordinated control strategy to change their internal set points and to share the information of VAr sharing to each other during different load and generation scenarios. Although the research work carried out in Chapter-6 provides a frame work for the determination of variable VAr set points during time varying load and generation, this work does not propose any control scheme for the inverters of UPQC-O. Hence, there is need of coordinated control scheme for the optimal operation of inverters of UPQC-O for attaining particular objectives, such as, energy loss reduction, voltage deviation minimization, etc. in distribution networks during time varying load and generation. In case of PV-BESS integrated UPQC-O, the control scheme is required for the coordination among inverters of UPQC-O, PVs, and BESSs.

- *SOC management for battery connected to the UPQC-O*: In UPQC-O models with battery, the batteries connected to the series and shunt inverters need to be charged or discharged based on their SOC level. Since the load and generation are varying throughout the day, these need SOC management for the batteries connected to the inverters of UPQC-O.
- *Consideration of load and generation uncertainties in planning models:* The electric utilities use different forecasting techniques and historical data to predict the future load demand and PV generation. In reality, these might have errors. Thus, the incorporation of load and PV generation uncertainties in the proposed planning models can be possible extension of this work. This needs future investigation.
- *Sensitivity analysis of proposed UPQC-O models to the different simulation parameters:* The variation in the values of different simulation parameters may affect the performance the proposed UPQC-O models. Thus, the sensitivity analysis is required to analyze their sensitivity to the various simulation parameters used in this research.

Bibliography

[1] T. Gönen, and I.J. Ramirez-Rosado, "Review of distribution system planning models: A model for optimal multi-stage planning," *IEE Proceedings C- Generation, Transmission and Distribution*, vol. 133, no. 7, pp. 397–408, 1986.

[2] H.K. Temraz, and V.H. Quintana, "Distribution system expansion models: An overview," *Electric Power Systems Research*, vol. 26, pp. 61–70, 1993.

[3] S.K. Khator, and L.C. Leung, "Power distribution planning: A review of models and issues," *IEEE Trans. on Power Systems*, vol. 12, no. 3, pp. 1151–1159, 1997.

[4] S. ganguly, N.C. Sahoo, and D. Das, "Recent advances on power distribution system planning: A state-of-the-art survey," *Energy Systems*, vol. 4, no. 2, pp. 165–193, 2013.

[5] P.S. Georgilakis, and N.D. Hatziargyriou, "A review of power distribution planning in the modern power system era: Models, methods and future research," *Electric Power Systems Research*, vol. 121, pp. 89–100, 2015.

[6] Y. Xiang, J. Liu, F. Li, et al., "Optimal active distribution network planning: A review," *Electric Power Components and Systems*, vol. 44, no. 10, pp. 1075–1094, 2016.

[7] M. Sedghi, A. Ahmadian, and M. Aliakbar-Golkar, "Assessment of optimization algorithms capability in distribution network planning: Review comparison and modification techniques," *Renewable and Sustainable Energy Reviews*, vol. 66, pp. 415–434, 2016.

[8] S. Ganguly, and D. Samajpati, "Distributed generation allocation on radial distribution networks under uncertainties of load and generation using genetic algorithm," *IEEE Trans. on Sustainable Energy*, vol. 6, no. 3, pp. 688–697, 2015.

[9] Y.M. Atwa, and E.F. El-Saadany, "Probabilistic approach for optimal allocation of wind-based distributed generation in distribution systems," *IET Renewable Power Generation*, vol. 5, no.1, pp. 79–88, 2011.

[10] M-R Haghifam, H. Falaghi, and O.P. Malik, "Risk-based distributed generation placement," *IET Generation, Transmission & Distribution*, vol. 2, no. 2, pp. 252–260, 2008.

[11] A. Zidan, M.F. Shaaban, and E.F. El-Saadany, "Long-term multi-objective distribution network planning by DG allocation and feeders' reconfiguration," *Electric Power Systems Research*, vol. 105, pp. 95–104, 2013.

[12] M.E. Jahromi, M. Ehsan, and A.F. Meyabadi, "A dynamic fuzzy interactive approach for DG expansion planning," *Electrical Power & Energy Systems*, vol. 43, no. 1, pp. 1094–1105, 2012.

[13] A. Soroudi, and M. Afrasiab, "Binary PSO-based dynamic multi-objective model for distributed generation planning under uncertainty," *IET Renewable Power Generation*, vol. 6, no. 2, pp. 67–78, 2012.

[14] A.S.B. Humayd, and K. Bhattacharya, "Comprehensive multi-year distribution system planning using back-propagation approach," *IET Generation, Transmission & Distribution*, vol. 7, no.12, pp. 1415–1425, 2013.

[15] I. Ziari, G. Ledwich, A. Ghosh, et al., "Optimal distribution network reinforcement considering load growth, line loss, and reliability," *IEEE Trans. on Power Systems*, vol. 28, no. 2, pp. 587–597, 2013.

[16] R. Hemmati, R-A. Hooshmand, and N. Taheri, "Distribution network expansion planning and DG placement in the presence of uncertainties," *Electrical Power & Energy Systems*, vol. 73, pp. 665–673, 2015.

[17] V.F. Martins, and C.L.T. Borges, "Active distribution network integrated planning incorporating distributed generation and load response uncertainties," *IEEE Trans. on Power Systems*, vol. 26, no. 4, pp. 2164–2172, 2011.

[18] V.A. Evangelopoulos, and P.S. Georgilakis, "Optimal distributed generation placement under uncertainties based on point estimate method embedded genetic algorithm," *IET Generation, Transmission & Distribution*, vol. 8, no. 3, pp. 389–400, 2014.

[19] Ž.N. Popović, V.Dj. Kerleta, and D.S. Popović, "Hybrid simulated annealing and mixed integer linear programming algorithm for optimal planning of radial distribution networks with distributed generation," *Electric Power Systems Research*, vol. 108, pp. 211–222, 2014.

[20] S-Y. Kim, W-W. Kim, and J-O. Kim, "Determining the optimal capacity of renewable distributed generation using restoration methods," *IEEE Trans. on Power Systems*, vol. 29, no. 5, pp. 2001–2013, 2014.

[21] S. Gill, I. Kockar, and G.W. Ault, "Dynamic optimal power flow for active distribution networks," *IEEE Trans. on Power Systems*, vol. 29, no. 1, pp. 121–131, 2014.

[22] G. Carpinelli, G. Celli, F. Pilo, et al., "Embedded generation planning under uncertainty including power quality issues," *Int. Trans. on Electrical Energy Systems*, vol. 13, no. 6, pp. 381–389, 2003.

[23] C.L.T. Borges, and V.F. Martins, "Multistage expansion planning for active distribution networks under demand and distributed generation uncertainties," *Electrical Power & Energy Systems*, vol. 36, no. 1, pp. 107–116, 2012.

[24] J.A. Martinez, and G. Guerra, "A parallel Monte Carlo method for optimum allocation of distributed generation," *IEEE Trans. Power Systems*, vol. 29, no. 6, pp. 2926–2933, 2014.

[25] W. Yuan, J. Wang, F. Qiu, et al., "Robust optimization-based resilient distribution network planning against natural disasters," *IEEE Trans. on Smart Grid*, vol. 7, no. 6, pp. 2817–2826, 2016.

[26] S.S. Al Kabbi, H.H. Zeineldin, and V. Khadkikar, "Planning active distribution networks considering multi-DG configurations," *IEEE Trans. on Power Systems*, vol. 29, no. 2, pp. 785–793, 2014.

[27] A. Gabash, and P. Li, "Active-reactive optimal power flow in distribution networks with embedded generation and battery storage," *IEEE Trans. on Power Systems*, vol. 27, no. 4, pp. 2026–2035, 2012.

[28] M. Nick, R. Cherkaoui, and M. Paolone, "Optimal allocation of dispersed energy storage systems in active distribution networks for energy balance and grid support," *IEEE Trans. on Power Systems*, vol. 29, no. 5, pp. 2300–2310, 2014.

[29] S. Ganguly, and D. Samajpati, "Distributed generation allocation with on-load tap changer on radial distribution networks using adaptive genetic algorithm," *Applied Soft Computing*, vol. 59, pp. 45–67, 2017.

[30] B.R. Pereira Jr., G.R. Martins da Costa, J. Contreras, et al., "Optimal distributed generation and reactive power allocation in electrical distribution systems," *IEEE Trans. on Sustainable Energy*, vol. 7, no. 3, pp. 975–984, 2016.

[31] C.G. Tarôco, R.H.C. Takahashi, and E.G. Carrano, "Multiobjective planning of power distribution networks with facility location for distributed generation," *Electric Power Systems Research*, vol. 141, pp. 562–571, 2016.

[32] N. Jayasekara, M.A.S. Masoum, and P.J. Wolfs, "Optimal operation of distributed energy storage systems to improve distribution network load and generation hosting capability," *IEEE Trans. on Sustainable Energy*, vol. 7, no. 1, pp. 250–261, 2016.

[33] G. Mokryani, "Active distribution networks planning with integration of demand response," *Solar Energy*, vol. 122, pp. 1362–1370, 2015.

[34] S. Wang, S. Chen, L. Ge, et al., "Distributed generation hosting capacity evaluation for distribution systems considering the robust optimal operation of OLTC and SVC," *IEEE Trans. on Sustainable Energy*, vol. 7, no. 3, pp. 1111–1123, 2016.

[35] A. Bagheri, H. Monsef, and H. Lesani, "Renewable power generation employed in an integrated dynamic distribution network expansion planning," *Electric Power Systems Research*, vol. 127, pp. 280–296, 2015.

[36] H.B. Tolabi, M.H. Ali, and M. Rizwan, "Simultaneous reconfiguration, optimal placement of DSTATCOM, and Photovoltaic array in a distribution system based on Fuzzy-ACO approach," *IEEE Trans. on Sustainable Energy*, vol. 6, no. 1, pp. 210–218, 2015.

[37] H. Saboori, and R. Hemmati, "Maximizing DISCO profit in active distribution networks by optimal planning of energy storage systems and distributed generators," *Renewable and Sustainable Energy Reviews*, vol. 71, pp. 365–372, 2017.

[38] X. Shen, M. Shahidehpour, Y. Han, et al., "Expansion planning of active distribution networks with centralized and distributed energy storage systems," *IEEE Trans. Sustainable Energy*, vol. 8, no. 1, pp. 126–134, 2017.

[39] A. Bagheri, H. Monsef, and H. Lesani, "Integrated distribution network expansion planning incorporating distributed generation considering uncertainties, reliability, and operational conditions," *Electrical Power and Energy Systems*, vol. 73, pp. 56–70, 2015.

[40] G. Mokryani, Y.F. Hu, P. Pillai, et al., "Active distribution network planning with high penetration of wind power," *Renewable Energy*, vol. 104, pp. 40–49, 2017.

[41] S.F. Santos, D.Z. Fitiwi, A.W. Bizuayehu, et al., "Novel multi-stage stochastic DG investment planning with recourse," *IEEE Trans. on Sustainable Energy*, vol. 8, no. 1, pp.164–178, 2017.

[42] G. Munoj-Delgado, J. Contreras, and J.M. Arroyo, "Multistage generation and expansion planning in distribution systems considering uncertainty and reliability," *IEEE Trans. on Power Systems*, vol. 31, no. 5, pp. 3715–3728, 2016.

[43] P.P. Biswas, R. Mallipeddi, P.N. Suganthan, et al., "A multiobjective approach for optimal placement and sizing of distributed generators and capacitors in distribution network," *Applied Soft Computing*, vol. 60, pp. 268–280, 2017.

[44] S. Nejadfard-Jahromi, M. Rashidinejad, and A. Abdollahi, "Multistage distribution network expansion planning under smart grids environment," *Electrical Power & Energy Systems*, vol. 71, pp. 222–230, 2015.

[45] S. Heidari, M. Fotuhi-Firuzabad, and S. Kazemi, "Power distribution network expansion planning considering distribution automation," *IEEE Trans. on Power Systems*, vol. 30, no.3, pp. 1261–1269, 2015.

[46] H.K. Nguyen, H. Mohsenian-Rad, A. Khodaei, et al., "Decentralized reactive power compensation using Nash Bargaining solution," *IEEE Trans. on Smart Grid*, vol. 8, no. 4, pp. 1679–1688, 2017.

[47] Y. Xiang, J. Liu, and Y. Liu, "Optimal active distribution system management considering aggregated plug-in electric vehicles," *Electric Power Systems Research*, vol. 131, pp. 105–115, 2016.

[48] L. Zhou, F. Li, C. Gu, et al., "Cost/benefit assessment of a smart distribution system with intelligent electric vehicle charging," *IEEE Trans. on Smart Grid*, vol. 5, no. 2, pp. 839–847, 2014.

[49] A.A. Eajal, M.F. Shaaban, K. Ponnambalam, et al., "Stochastic centralized dispatch scheme for AC/DC hybrid smart distribution systems," *IEEE Trans. on Sustainable Energy*, vol. 7, no. 3, pp. 1046–1059, 2016.

[50] X. Shen, M. Shahidehpour, S. Zhu, et al., "Multi-stage planning of active distribution networks considering the co-optimization of operation strategies," *IEEE Trans. on Smart Grid*, vol. 9, no. 2, pp. 1425–1433, 2018.

[51] L. Guo, W. Liu, B. Jiao, et al., "Multi-objective stochastic optimal planning method for stand-alone microgrid system," *IET Generation, Transmission & Distribution*, vol. 8, no. 7, pp. 1263–1273, 2014.

[52] S. Bahramirad, W. Reder, and A. Khodaei, "Reliability-constrained optimal sizing of energy storage system in microgrid," *IEEE Trans. on Smart Grid*, vol. 3, no. 4, pp. 2056–2062, 2012.

[53] H. Lofti, and A. Khodaei, "AC versus DC microgrid planning," *IEEE Trans. on Smart Grid*, vol. 8, no. 1, pp. 296–304, 2017.

[54] S.M. Hakimi, and S.M. Moghaddas-Tafreshi, "Optimal planning of a smart microgrid including demand response and intermittent renewable energy resources," *IEEE Trans. on Smart Grid*, vol. 5, no. 6, pp. 2889–2900, 2014.

[55] Z. Wang, B. Chen, J. Wang, et al., "Robust optimization based optimal DG placement in microgrids," *IEEE Trans. on Smart Grid*, vol. 5, no. 5, pp. 2173–2182, 2014.

[56] E. Hajipour, M. Bozorg, and M. Fotuhi-Firuzabad, "Stochastic capacity expansion planning of remote microgrids with wind farms and energy storage," *IEEE Trans. on Sustainable Energy*, vol. 6, no. 2, pp. 491–498, 2015.

[57] M.H. Moradi, M. Eskandari, and S.M. Hosseinian, "Operational strategy optimization in an optimal sized smart microgrid," *IEEE Trans. on Smart Grid*, vol. 6, no. 3, pp. 1087–1095, 2015.

[58] S.A. Arefifar, Y.A-R.I. Mohamed, and T.H.M. EL-Fouly, "Comprehensive operational planning framework for self-healing control actions in smart distribution grids," *IEEE Trans. on Power Systems*, vol. 28, no. 4, pp. 4192–4200, 2013.

[59] Y. Xiang, J. Liu, and Y. Liu, "Robust energy management of microgrid with uncertain renewable generation and load," *IEEE Trans. on Smart Grid*, vol. 7, no. 2, pp. 1034–1043, 2016.

[60] Y. Levron, J.M. Guerrero, and Y. Beck, "Optimal power flow in microgrids with energy storage," *IEEE Trans. on Power Systems*, vol. 28, no. 3, pp. 3226–3234, 2013.

[61] M. Ross, C. Abbey, F. Bouffard, et al., "Multi-objective optimization dispatch for microgrids with a high penetration of renewable generation," *IEEE Trans. on Sustainable Energy*, vol. 6, no. 4, pp. 1306–1314, 2015.

[62] W. Shi, X. Xie, C-C. Chu, et al., "Distributed optimal energy management in microgrids," *IEEE Trans. on Smart Grid*, vol. 6, no. 3, pp. 1137–1146, 2015.

[63] L. Che, X. Zhang, M. Shahidehpour, et al., "Optimal planning of loop-based microgrid topology," *IEEE Trans. on Smart Grid*, vol. 8, no. 4, pp. 1771–1781, 2017.

[64] A. Parisio, E. Rikos, and L. Glielmo, "A model predictive control approach to microgrid operation optimization," *IEEE Trans. on Control Systems Technology*, vol. 22, no. 5, pp. 1813–1827, 2014.

[65] E. Dall'Anese, H. Zhu, and G.B. Gian, "Distributed optimal power flow for smart microgrids," *IEEE Trans. on Smart Grid*, vol. 4, no. 3, pp. 1464–1475, 2013.

[66] T. Som, and N. Chakraborty, "Studies on economic feasibility of an autonomous power delivery system utilizing alternative hybrid distributed energy resources," *IEEE Trans. on Power Systems*, vol. 29, no. 1, pp. 172–181, 2014.

[67] H. Yang, H. Pan, F. Luo, et al., "Operational planning of electric vehicles for balancing wind power and load fluctuations in a microgrid," *IEEE Trans. on Sustainable Energy*, vol. 8, no. 2, pp. 592–604, 2017.

[68] H. Wang, and J. Huang, "Cooperative planning of renewable generations for interconnected microgrids," *IEEE Trans. on Smart Grid*, vol. 7, no. 5, pp. 2486–2496, 2016.

[69] A. Khodaei, S. Bahramirad, and M. Shahidehpour, "Microgrid planning under uncertainty," *IEEE Trans. on Power Systems*, vol. 30, no. 5, pp. 2417–2425, 2015.

[70] A. Ghosh, and G. Ledwitch, "*Power quality enhancement using custom power devices*," Springer, New York, 2009.

[71] M. Brenna, R. Faranda, and E. Tironi, "A new proposal for power quality and custom power improvement: OPEN UPQC," *IEEE Trans. Power Delivery*, vol. 24, no. 4, pp. 2107–2116, 2009.

[72] S. Ganguly, "Impact of unified power-quality conditioner allocation on line loading, losses, and voltage stability of radial distribution systems," *IEEE Trans. Power Delivery*, vol. 29, no. 4, pp. 1859–1867, 2014.

[73] S. Ganguly, "Multi-objective planning for reactive power compensation of radial distribution networks with unified power quality conditioner allocation using particle swarm optimization," *IEEE Trans. Power Systems*, vol. 29, no. 4, pp. 1801–1810, 2014.

[74] S. Ganguly, "Unified power quality conditioner allocation for reactive power compensation of radial distribution networks," *IET Generation, Transmission & Distribution*, vol. 8, no. 8, pp. 1418–1429, 2014.

[75] J. Sarker, and S. K. Goswami, "Optimal location of unified power quality conditioner in distribution system for power quality improvement," *Int. Journal of Electrical Power and Energy Systems*, vol.83, pp. 309–324, 2016.

[76] V. Khadkikar, "Enhancing electric power quality using UPQC: A comprehensive overview," *IEEE Trans. Power Electronics*, vol. 27, no. 5, pp. 2284–2297, 2012.

[77] H. Fujita, and H. Akagi, "The unified power quality conditioner: the integration of series- and shunt-active filters," *IEEE Trans. Power electronics*, vol. 13, no. 2, pp. 315–322, 1998.

[78] M. Basu, S.P. Das, and G.K. Dubey, "Comparative evaluation of two models of UPQC for suitable interface to enhance power quality," *Electric Power Systems Research*, vol. 77, pp. 821–830, 2007.

[79] V. Khadkikar, and A. Chandra, "UPQC-S: A novel concept of simultaneous voltage sag/swell and load reactive power compensations utilizing series inverter of UPQC," *IEEE Trans. Power Electronics*, vol. 26, no. 9, pp. 2414–2425, 2011.

[80] D.O. Kisck, V. Navrapescu, and M. Kisck, "Single-phase unified power quality conditioner with optimum voltage angle injection for minimum VA requirement," *IEEE Proc. Power Electronics Specialists Conference*, Bucharest, pp. 574–579, 2007.

[81] V. Khadkikar, and A. Chandra, "A novel structure for three-phase four-wire distribution system utilizing unified power quality conditioner (UPQC)," *IEEE Trans. Industry Applications*, vol. 45, no. 5, pp. 1897–1902, 2009.

[82] A.K. Jindal, A. Ghosh, and A. Joshi, "Interline unified power quality conditioner," *IEEE Trans. on Power Delivery*, vol. 22, no. 1, pp. 364-372, 2007.

[83] K. Senthilnathan, and I. Annapoorani, "Implementation of unified power quality conditioner (UPQC) based on current source converters for distribution grid and performance monitoring through LabVIEW Simulation Interface Toolkit server: a cyber physical model," *IET Generation, Transmission & Distribution*, vol. 10, no. 11, pp. 2622–2630, 2016.

[84] V. Khadkikar, and A. Chandra, "A new control philosophy for a unified power quality conditioner (UPQC) to coordinate load-reactive power demand between shunt and series inverters," *IEEE Trans. Power Delivery*, vol. 23, no. 4, pp. 2522–2534, 2008.

[85] A. Ghosh, and G. Ledwich, "A unified power quality conditioner (UPQC) for simultaneous voltage and current compensation," *Electric Power Systems Research*, vol. 59, pp. 55–63, 2001.

[86] S.B. Karanki, M.K. Mishra, and B.K. Kumar, "Particle swarm optimization-based feedback controller for unified power-quality conditioner," *IEEE Trans. Power Delivery*, vol. 25, no. 4, pp. 2814–2824, 2010.

[87] V. Khadkikar, "Fixed and variable power angle control methods for unified power quality conditioner: operation, control and impact assessment on shunt and series inverter kVA loadings," *IET Power Electronics*, vol. 6, no. 7, pp. 1299–1307, 2013.

[88] J. Ye, H.B. Gooi, and F. Wu, "Optimization of the size of UPQC system based on data-driven control design," *IEEE Trans. Smart Grid*, vol. 9, no. 4, pp. 2999–3008, 2018.

[89] J. Ye, H.B. Gooi, and F. Wu, "Optimal design and control implementation of UPQC based on variable phase angle control method," *IEEE Trans. Industrial Informatics*, vol. 14, no. 7, pp. 3109–3123, 2018.

[90] Q. Trinh, and H. Lee, "Improvement of unified power quality conditioner performance with enhanced resonant control strategy," *IET Generation, Transmission & Distribution*, vol. 8, no. 12, pp. 2114–2123, 2014.

[91] A. Patel, H.D. Mathur, and S. Bhanot, "An improved control method for unified power quality conditioner with unbalanced load," *Electric Power and Energy Systems*, vol. 100, pp.129–138, 2018.

[92] H. Heydari, and A.H. Moghadasi, "Optimization scheme in combinatorial UPQC and SFCL using normalized simulated annealing," *IEEE Trans. Power Delivery*, vol. 26, no. 3, pp. 1489–1498, 2011.

[93] B. Han, B. Bae, H. Kim, et al., "Combined operation of unified power-quality conditioner with distributed generation," *IEEE Trans. Power Delivery*, vol. 21, no. 1, pp. 330–338, 2006.

[94] N.G. Jayanti, M. Basu, M.F. Conlon, et al., "Rating requirements of the unified power quality conditioner to integrate the fixed speed induction generator-type wind generation to the grid," *IET Renewable Power Generation*, vol. 3, no. 2, pp. 133–143, 2009.

[95] S. Devassy, and B. Singh, "Design and performance analysis of three-phase solar PV integrated UPQC," *IEEE Trans. on Industry Applications*, vol. 54, no. 1, pp. 73–81, 2018.

[96] G. D'Antona, R. Faranda, H. Hafezi, et al., "Open UPQC: A possible solution for power quality. Series unit analysis," *Proc. of Int. Symposium on Power Electronics, Electrical Drives, Automation and Motion (SPEEDAM)*," pp. 1104–1109, 2014.

[97] G. D'Antona, R. Faranda, H. Hafezi, et al., "Open UPQC: A possible solution for customer power quality improvement. Shunt unit analysis," *Proc. of Int. Conference on Harmonics and Quality of Power (ICHQP)*, pp. 596–600, 2014.

[98] G. Accetta, G. D'Antona, D.D. Giustina, et al., "Power Quality improvement in LV smart grid by using the open UPQC device," *Int. Conference on Renewable Energies and Power Quality*, Bilbao, Spain, vol. 1, no. 11, pp. 540–545, 2013.

[99] G. D'Antona, D.D. Giustina, R. Faranda, et al., "Open UPQC power quality manager within distributed generation systems," *Proc. of IEEE 10th Int. Symposium on Diagnostics for Electrical Machines, Power Electronics and Drives (SDEMPED)*, pp. 501–507, 2015.

[100] A. Teke, M.E. Meral, M.U. Cuma, et al., "Open Unified power quality conditioner with control based on enhanced phase locked loop," *IET Generation, Transmission & Distribution*, vol. 7, no. 3, pp. 254–264, 2013.

[101] H. Hafezi, G. D'Antona, A. Dedè, et al., "Power quality conditioning in LV distribution networks: Results by field demonstration," *IEEE Trans. Smart Grid*, vol. 8, no. 1, pp. 418–427, 2017.

[102] J. Kotturu, and P. Agarwal, "Comparative performance analysis of UPQC and open UPQC," *Annual IEEE India Conference (INDICON)*, New Delhi, India, December, 2015.

[103] M. Basu, S.P. Das, and G.K. Dubey, "Comparative evaluation of two models of UPQC for suitable interface to enhance power quality," *Electric Power Systems Research*, vol. 77, no. 7, pp. 821–830, 2007.

[104] Y.Y. Kolhatkar, and S.P. Das, "Experimental investigation of a single-phase UPQC with minimum VA loading," *IEEE Trans. Power Delivery*, vol. 22, no. 1, pp. 373–380, 2007.

[105] J.A.M. Rupa, and S. Ganesh, "Power flow analysis for radial distribution system using backward/forward sweep method," *Int. Journal of Electrical and Computer Engineering*, vol. 8, no. 10, pp. 1628–1632, 2014.

[106] S. Ghosh, and D. Das, "Method for load-flow solution of radial distribution networks," *IEE Proc. Generation, Transmission, and Distribution*, vol. 146, no. 6, pp. 641–648, 1999.

[107] J. Kennedy, and R. Eberhart, "Particle swarm optimization," *Proc. of IEEE Int. Conference on Neural Networks*, Pearth, Australia, pp. 1942–1948, 1995.

[108] Y. Shi, and R. Eberhart, "A modified particle swarm optimizer," *In Proc. IEEE Int. Conference on Evolutionary Computation*, pp. 69–73, 1998.

[109] J.S. Savier, and D. Das, "Impact of network reconfiguration on loss allocation of radial distribution systems," *IEEE Trans. Power Delivery*, vol. 22, no. 4, pp. 2473–2480, 2007.

[110] M.E. Baran, and F.F. Wu, "Network reconfiguration in distribution systems for loss reduction and load balancing," *IEEE Trans. Power Delivery*, vol. 4, no. 2, pp. 1401–1407, 1989.

[111] N. DiOrio, A. Dobos, and S. Janzou, "Economic analysis case studies of battery energy storage with SAM," *National Renewable Energy Laboratory Technical Report*, NREL/TP-6A20-64987, November 2015.

[112] W.G. Manuel, "TURLOCK Irrigation District Energy Storage Study 2014," *California Energy Commission Report*, September 2014.

[113] "Distributed generation renewable energy estimate of costs," *Technical report*, NREL, USA, February 2016, https://www.nrel.gov/analysis/tech-lcoe-re-cost-est.html (accessed on 28th September, 2018).

[114] A. Keane, L.F. Ochoa, C.L.T. Borges, et al., "State-of-the-Art techniques and challenges ahead for distributed generation planning and optimization," *IEEE Trans. Power Systems*, vol. 28, no. 2, pp. 1493–1502, 2013.

[115] F. Abbasi, and S.M. Hosseini, "Optimal DG allocation and sizing in presence of storage systems considering network configuration effects in distribution systems," *IET Generation Transmission & Distribution*, vol. 10, no. 3, pp. 617–624, 2016.

[116] S. Ganguly, N.C. Sahoo, and D. Das, "Multi-objective particle swarm optimization based on fuzzy-Pareto-dominance for fuzzy-based planning of electrical distribution systems incorporating distributed generation," *Fuzzy Sets and Systems*, vol. 213, pp. 47–73, 2013.

[117] S. Jazebi, S.H. Hosseinian, and B. Vahidi, "DSTATCOM allocation in distribution networks considering reconfiguration using differential evolution algorithm," *Energy Conversion and Management*, vol. 52, pp. 2777–2783, 2011.

[118] "Year End Review 2017," Published in *Press Information Bureau, Government of India, Ministry of New and Renewable Energy*, web-link (Last access on May, 2018): http://pib.nic.in/newsite/PrintRelease.aspx?relid=174832.

[119] P.K.C. Wong, A. Kalam, and R. Barr, "Modelling and analysis of practical options to improve the hosting capacity of low voltage networks for embedded photo-voltaic generation," *IET Renewable Power Generation*, vol. 11, no. 5, pp. 625–632, 2017.

[120] M.M. Haque, and P. Wolfs, "A review of high PV penetrations in LV distribution networks: Present status, impacts and mitigation measures," *Renewable and Sustainable Energy Reviews*, vol. 62, pp. 1195–1208, 2016.

[121] P. Chaudhary, and M. Rizwan, "Voltage regulation mitigation techniques in distribution system with high PV penetration: A review," *Renewable and Sustainable Energy Reviews*, vol. 82, pp. 3279–3287, 2018.

[122] M. Karimi, H. Mokhlis, K. Naidu, et al., "Photovoltaic issues and impacts in distribution network- A review," *Renewable and Sustainable Energy Reviews*, vol. 53, pp. 594–605, 2016.

[123] S. Hashemi, and J. Østergaard, "Methods and strategies for overvoltage prevention in low voltage distribution systems with PV," *IET Renewable Power Generation*, vol. 11, no. 2, pp. 205–214, 2017.

[124] T. Jamal, T. Urmee, M. Calais, et al., "Technical challenges of PV deployment into remote Australian electricity networks: A review," *Renewable and Sustainable Energy Reviews*, vol. 77, pp. 1309–1325, 2017.

[125] F. Ding, B. Mather, and P. Gotseff, "Technologies to increase PV hosting capacity in distribution feeders," *Proc. IEEE Power and Energy Society General Meeting*, Boston, MA, USA, pp. 1–5, July 2016.

[126] S.N. Salih, P. Chen, O. Carlson, et al., "Optimizing wind power hosting capacity of distribution systems using cost benefit analysis," *IEEE Trans. on Power Delivery*, vol. 29, no. 3, pp. 1436–1445, 2014.

[127] F. Ding, and B. Mather, "On distributed PV hosting capacity estimation, sensitivity study, and improvement," *IEEE Trans. on Sustainable Energy*, vol. 8, no. 3, pp. 1010–1020, 2017.

[128] S.F. Santos, D.Z. Fitiwi, M. Shafie-Khah, et al., "New multistage and stochastic mathematical model for maximizing RES hosting capacity–Part I: Problem formulation," *IEEE Trans. on Sustainable Energy*, vol. 8, no. 1, pp. 304–319, 2017.

[129] S.F. Santos, D.Z. Fitiwi, M. Shafie-Khah, et al., "New multistage and stochastic mathematical model for maximizing RES hosting capacity–Part II: Numerical results," *IEEE Trans. on Sustainable Energy*, vol. 8, no. 1, pp. 320–330, 2017.

[130] A. Dubey, and S. Santoso, "On estimation and sensitivity analysis of distribution circuit's photovoltaic hosting capacity," *IEEE Trans. on Power Systems*, vol. 32, no. 4, pp. 2779–2789, 2017.

[131] R.G. Wandhare, and V. Agarwal, "Reactive power capacity enhancement of a PV-grid system to increase PV penetration level in smart grid scenario," *IEEE Trans. on Smart Grid*, vol. 5, no. 4, pp. 1845–1854, 2014.

[132] F. Capitanescu, L.F. Ochoa, H. Margossian, et al., "Assessing the potential of network reconfiguration to improve distributed generation hosting capacity in active distribution systems," *IEEE Trans. on Power Systems*, vol. 30, no. 1, pp. 346–356, 2015.

[133] C. Li, V.R. Disfani, Z.K. Pecenak, et al., "Optimal OLTC voltage control scheme to enable high solar penetrations," *Electric Power Systems Research*, vol. 160, pp. 318–326, 2018.

[134] D.A. Quijano, J. Wang, M.R. Sarker, et al., "Stochastic assessment of distributed generation hosting capacity and energy efficiency in active distribution networks," *IET Generation, Transmission & Distribution*, vol. 11, no. 18, pp. 4617–4625, 2017.

[135] P.H. Divshali, and L. Söder, "Improving hosting capacity of rooftop PVs by quadratic control of an LV-central BSS," *IEEE Trans. on Smart Grid*, vol.10, no.1, pp. 919–927, 2019.

[136] H. Pezeshki, A. Arefi, G. Ledwich, et al., "Probabilistic voltage management using OLTC and dSTATCOM in distribution networks," *IEEE Trans. on Power Delivery*, vol. 33, no. 2, pp. 570–580, 2018.

[137] K. Deb, "*Multi-Objective Optimization using Evolutionary Algorithms*," New York, NY, USA, Wiley, 2004.

[138] E. Zitzler, M. Laumanns, and L. Thiele, "SPEA2: Improving the Strength Pareto Evolutionary Algorithm," *TIK-Report* 103, 2001.

[139] M.H.J. Bollen, and F. Hassan, "*Integration of distributed generation in power system*," Wiley IEEE Press, Hoboken, NJ, USA, 2011.

[140] M.R. Sierra, and C.A.C. Coello, "Multi-objective particle swarm optimizers: A survey of the-state-of-the-art," *Int. Journal of Computational Intelligence Research*, vol. 2, no. 3, pp. 287–308, 2006.

[141] S. Ganguly, N.C. Sahoo, and D. Das, "Mono- and Multi-objective planning of electrical distribution networks using particle swarm optimization," *Applied Soft Computing*, vol. 11, no. 2, pp. 2391–2405, 2011.

[142] M. Mahmoodi, P. Shamsi, and B. Fahimi, "Optimal scheduling of microgrid operation considering the time-of-use price of electricity," *39th Annual Conference of the IEEE Industrial Electronics Society* 2013, Vienna, Austria, November 2013.

[143] M. Uddin, M.F. Romlie, M.F. Abdullah, et al., "A review on peak load shaving strategies," *Renewable and Sustainable Energy Reviews*, vol. 82, pp. 3323–3332, 2018.

[144] M. Zheng, C.J. Meinrenken, and K.S. Lackner, "Smart households: Dispatch strategies and economic analysis of distributed energy storage for residential peak shaving," *Applied Energy*, vol. 147, pp. 246–257, 2015.

[145] A.J. Pimm, T.T. Cockerill, and P.G. Taylor, "The potential for peak shaving on low voltage distribution networks using electricity storage," *Journal of Energy Storage*, vol. 16, pp. 231–242, 2018.

[146] Y. Yang, H. Li, A. Aichhorn, et al., "Sizing strategy of distributed energy storage system with high penetration of photovoltaic for voltage regulation and peak load shaving," *IEEE Trans. on Smart Grid*, vol. 5, no. 2, pp. 982–991, 2014.

[147] Y. Shi, B. Xu, D. Wang, et al., "Using battery storage for peak shaving and frequency regulation: Joint optimization for superlinear gains," *IEEE Trans. on Power Systems*, vol. 33, no. 3, pp. 2882–2894, 2018.

[148] E. Reihani, M. Motalleb, R. Ghorbani, et al., "Load peak shaving and power smoothing of a distribution grid with high renewable energy penetration," *Renewable Energy*, vol. 86, pp. 1372–1379, 2016.

[149] T. Jiang, Y. Cao, L. Yu, et al., "Load shaping strategy based on energy storage and dynamic pricing in smart grid," *IEEE Trans. on Smart Grid*, vol. 5, no. 6, pp. 2868–2876, 2014.

[150] A-H Mohsenian-Rad, and A. Leon-Garcia, "Optimal residential load control with price prediction in real-time electricity pricing environments," *IEEE Trans. on Smart Grid*, vol. 1, no. 2, pp. 120–133, 2010.

[151] A.S.A. Awad, T.H.M. EL-Fouly, and M.M.A. Salama, "Optimal ESS allocation for benefit maximization in distribution networks," *IEEE Trans. on Smart Grid*, vol. 8, no. 4, pp. 1668–1678, 2017.

[152] A.S.A. Awad, T.H.M. EL-Fouly, and M.M.A. Salama, "Optimal ESS allocation for load management application," *IEEE Trans. on Power Systems*, vol. 30, no. 1, pp. 327–336, 2015.

[153] M.G. Damavandi, J.R. Marti, and V. Krishnamurthy, "A methodology for optimal distributed storage planning in smart distribution grids," *IEEE Trans. on Sustainable Energy*, vol. 9, no. 2, pp. 729–740, 2018.

[154] H.R. Baghee, M. Mirsalim, G.B. Gharehpetian, et al., "Reliability/cost-based multi-objective Pareto optimal design of stand-alone wind/PV/FC generation microgrid system," *Int. Journal of Energy*, vol. 115, pp. 1022–1041, 2016.

[155] H.R. Baghee, M. Mirsalkim, G.B. Gharehpetian, "Multi-objective optimal power management and sizing of a reliable wind/PV microgrid with hydrogen storage using MOPSO," *Journal of Intelligent and Fuzzy Systems*, vol. 32, pp. 1753–1773, 2017.

[156] H.R. Baghaee, M. Mirsalim, G.B. Gharehpetian, et al., "A decentralized robust mixed H_2/ H_∞ voltage control scheme to improve small/large-signal stability and FRT capability of islanded multi-DER microgrid considering load disturbances," *IEEE Systems Journal*, vol. 12, no. 3, pp. 2610–2621, 2018.

[157] "*A guide to understanding battery specifications*," MIT Electrical Vehicle Team, 2008.

[158] J.F. Franco, M.J. Rider, M. Lavorato, et al., "A mixed-integer LP model for the optimal allocation of voltage regulators and capacitors in radial distribution systems," *Int. Journal of Electrical Power and Energy Systems*, vol. 48, pp. 123–130, 2013.

[159] https://www2.ee.washington.edu/research/pstca/rts/pg_tcarts.htm (Last access on January, 2019).

[160] "*Solar radiant energy over India*," India Meteorological Department, Ministry of Earth Sciences, New Delhi, 2009.

[161] G. G. Karady, S. Saksena, B. Shi, et al., "Effects of voltage sag on loads in a distribution system," *Project report from the Power Systems Engineering Research Center*, Cornell University, USA, October 2005.

[162] "*Energy Statistics 2017*," Central Statistics Office, Ministry of Statistics and Programme Implementation, Government of India, 2017.

[163] "*Electricity load factor in Indian power system*," Power System Operation Corporation Ltd., India, January 2016, web-link: https://posoco.in/download/electricity-load-factor-in-india-power-system/?wpdmdl=709 (Last access on February, 2019).

Indian Institute of Technology Guwahati

Appendix

This Appendix provides the simulation data for all the test networks used in the simulation which includes the bus data, line data, base MVA, base kV etc. Bus data provides the information of active and reactive power load demand of each bus of a network. However, line data of the network provides the information of connectivity of each bus to other buses and the values of resistance and reactance of each line of the network. The simulation data for the time varying load demand and PV generation are also provided in this Appendix.

A.1 Simulation data for 33-bus radial distribution network

The 33-bus radial distribution network is a single feeder network with single substation. The bus 1 of this network is the substation bus and rest all are load buses. Simulation data for the 33-bus radial distribution network are taken from [110]. The bus data and line data for the 33-bus radial distribution network are shown in Tables A.1 and A.2, respectively. The base VA and base kV of the network are 100 MVA and 12.66 kV, respectively. The single line diagram of 33-bus network is shown in Fig. A.1.

Table A.1: Bus data of 33-bus radial distribution network

Bus number	Load demand		Bus number	Load demand		Bus number	Load demand	
	Active power (kW)	Reactive power (kVAr)		Active power (kW)	Reactive power (kVAr)		Active power (kW)	Reactive power (kVAr)
1	0	0	12	60	35	23	90	50
2	100	60	13	60	35	24	420	200
3	90	40	14	120	80	25	420	200
4	120	80	15	60	10	26	60	25
5	60	30	16	60	20	27	60	25
6	60	20	17	60	20	28	60	20
7	200	100	18	90	40	29	120	70
8	200	100	19	90	40	30	200	600
9	60	20	20	90	40	31	150	70
10	60	20	21	90	40	32	210	100
11	45	30	22	90	40	33	60	40

Table A.2: Line data of 33-bus radial distribution network

Sending end	Receiving end	Resistance (Ω)	Reactance (Ω)		Sending end	Receiving end	Resistance (Ω)	Reactance (Ω)
1	2	0.0922	0.047		17	18	0.732	0.574
2	3	0.493	0.2511		2	19	0.164	0.1565
3	4	0.366	0.1864		19	20	1.5042	1.3554
4	5	0.3811	0.1941		20	21	0.4095	0.4784
5	6	0.819	0.707		21	22	0.7089	0.9373
6	7	0.1872	0.6188		3	23	0.4512	0.3083
7	8	0.7114	0.2351		23	24	0.898	0.7091
8	9	1.03	0.74		24	25	0.896	0.7011
9	10	1.044	0.74		6	26	0.203	0.1034
10	11	0.1966	0.065		26	27	0.2842	0.1447
11	12	0.3744	0.1238		27	28	1.059	0.9337
12	13	1.468	1.155		28	29	0.8042	0.7006
13	14	0.5416	0.7129		29	30	0.5075	0.2585
14	15	0.591	0.526		30	31	0.9744	0.963
15	16	0.7463	0.545		31	32	0.3105	0.3619
16	17	1.289	1.721		32	33	0.341	0.5302

A.2 Simulation data for 69-bus radial distribution network

The 69-bus radial distribution network is also a single feeder network with single substation. The bus 1 of this network is the substation bus and rest all are load buses. Simulation data for the 69-bus radial distribution network are taken from [109]. The bus data and line data for the 69-bus radial distribution network are shown in Tables A.3 and A.4, respectively. The base VA and base kV of the network are 10 MVA and 12.66 kV, respectively. The single line diagram of 69-bus network is shown in Fig. A.2.

Table A.3: Bus data of 69-bus radial distribution network

Bus number	Load demand			Bus number	Load demand			Bus number	Load demand	
	Active power (kW)	Reactive power (kVAr)			Active power (kW)	Reactive power (kVAr)			Active power (kW)	Reactive power (kVAr)
1	0	0		24	28	20		47	0	0
2	0	0		25	0	0		48	79	56.4
3	0	0		26	14	10		49	384.7	274.5
4	0	0		27	14	10		50	384.7	274.5
5	0	0		28	26	18.6		51	40.5	28.3
6	2.6	2.2		29	26	18.6		52	3.6	2.7
7	40.4	30		30	0	0		53	4.35	3.5
8	75	54		31	0	0		54	26.4	19
9	30	22		32	0	0		55	24	17.2
10	28	19		33	14	10		56	0	0
11	145	104		34	19.5	14		57	0	0
12	145	104		35	6	4		58	0	0
13	8	5.5		36	26	18.55		59	100	72
14	8	5.5		37	26	18.55		60	0	0
15	0	0		38	0	0		61	1244	888
16	45.5	30		39	24	17		62	32	23
17	60	35		40	24	17		63	0	0
18	60	35		41	1.2	1		64	227	162
19	0	0		42	0	0		65	59	42
20	1	0.6		43	6	4.3		66	18	13
21	114	81		44	0	0		67	18	13
22	5.3	3.5		45	39.22	26.3		68	28	20
23	0	0		46	39.22	26.3		69	28	20

Table A.4: Line data of 69-bus radial distribution network

Sending end	Receiving end	Resistance (Ω)	Reactance (Ω)		Sending end	Receiving end	Resistance (Ω)	Reactance (Ω)
1	2	0.0005	0.0012		3	36	0.0044	0.0108
2	3	0.0005	0.0012		36	37	0.064	0.1565
3	4	0.0015	0.0036		37	38	0.1053	0.123
4	5	0.0251	0.0294		38	39	0.0304	0.0355
5	6	0.366	0.1864		39	40	0.0018	0.0021
6	7	0.3811	0.1941		40	41	0.7283	0.8509
7	8	0.0922	0.047		41	42	0.31	0.3623
8	9	0.0493	0.0251		42	43	0.041	0.0478
9	10	0.819	0.2707		43	44	0.0092	0.0116
10	11	0.1872	0.0691		44	45	0.1089	0.1373
11	12	0.7114	0.2351		45	46	0.0009	0.0012
12	13	1.03	0.34		4	47	0.0034	0.0084
13	14	1.044	0.345		47	48	0.0851	0.2083
14	15	1.058	0.3496		48	49	0.2898	0.7091
15	16	0.1966	0.065		49	50	0.0822	0.2011
16	17	0.3744	0.1238		8	51	0.0928	0.0473
17	18	0.0047	0.0016		51	52	0.3319	0.1114
18	19	0.3276	0.1083		9	53	0.174	0.0886
19	20	0.2106	0.0696		53	54	0.203	0.1034
20	21	0.3416	0.1129		54	55	0.2842	0.1447
21	22	0.014	0.0046		55	56	0.2813	0.1433
22	23	0.1591	0.0526		56	57	1.59	0.5337
23	24	0.3463	0.1145		57	58	0.7837	0.263
24	25	0.7488	0.2745		58	59	0.3042	0.1006
25	26	0.3089	0.1021		59	60	0.3861	0.1172
26	27	0.1732	0.0572		60	61	0.5075	0.2585
3	28	0.0044	0.0108		61	62	0.0974	0.0496
28	29	0.064	0.1565		62	63	0.145	0.0738
29	30	0.3978	0.1315		63	64	0.7105	0.3619
30	31	0.0702	0.0232		64	65	1.041	0.5302
31	32	0.351	0.116		11	66	0.2012	0.0611
32	33	0.839	0.2816		66	67	0.0047	0.0014
33	34	1.708	0.5646		12	68	0.7394	0.2444
34	35	1.474	0.4873		68	69	0.0047	0.0016

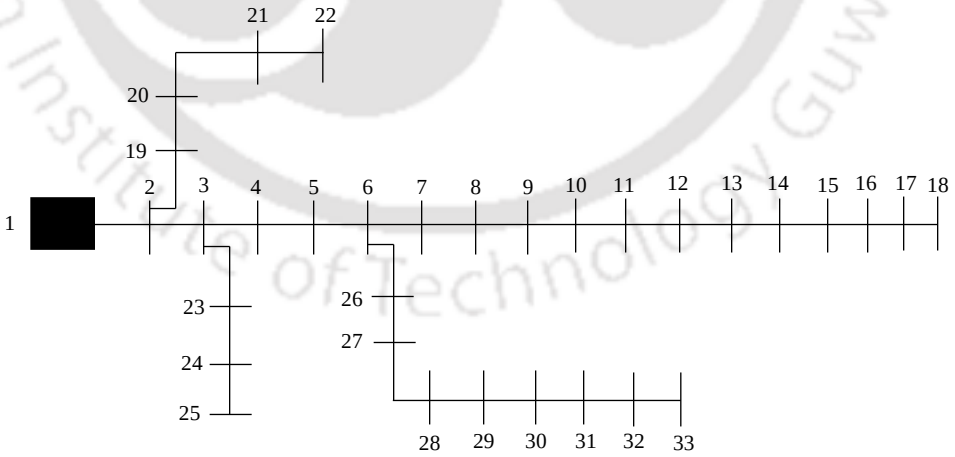

Fig. A.1: Single line diagram of 33-bus radial distribution network

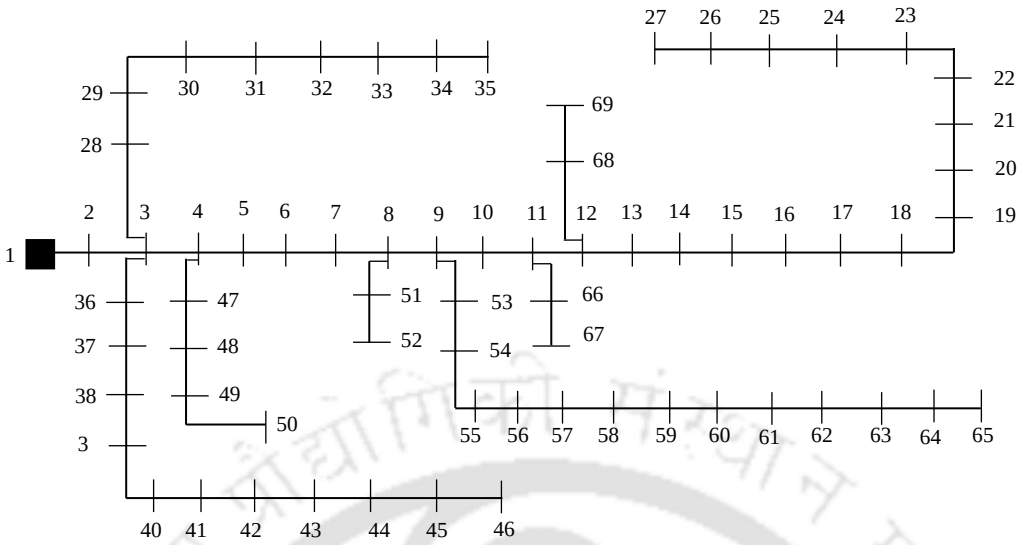

Fig. A.2: Single line diagram of 69-bus radial distribution network

A.3 Simulation data for time varying load demand

The hourly average load data of three different seasons of IEEE reliability test system [159] are considered in this thesis to have daily variation in load demand. The hourly average load demand data in terms of percentage of peak load demand for three different seasons of a year are shown in Table A.5.

Table A.5: Hourly average load demand in percentage of peak load

Hour	Hourly average load demand in percentage of peak load (%)					
	Winter weeks (1 -8 & 44 – 52)		Summer weeks (18 -30)		Spring weeks (9-17 & 31 – 43)	
	Weekday	Weekend	Weekday	Weekend	Weekday	Weekend
12-1 am	67	78	64	74	63	75
1-2	63	72	60	70	62	73
2-3	60	68	58	66	60	69
3-4	59	66	56	65	58	66
4-5	59	64	56	64	59	65
5-6	60	65	58	62	65	65
6-7	74	66	64	62	72	68
7-8	86	70	76	66	85	74
8-9	95	80	87	81	95	83
9-10	96	88	95	86	99	89
10-11	96	90	99	91	100	92
11-noon	95	91	100	93	99	94
Noon-1pm	95	90	99	93	93	91
1-2	95	88	100	92	92	90
2-3	93	87	100	91	90	90
3-4	94	87	97	91	88	86
4-5	99	91	96	92	90	85
5-6	100	100	96	94	92	88
6-7	100	99	93	95	96	92
7-8	96	97	92	95	98	100
8-9	91	94	92	100	96	97
9-10	83	92	93	93	90	95
10-11	73	87	87	88	80	90
11-12	63	81	72	80	70	85

A.4 Simulation data for time varying PV generation

The simulation data for time varying PV generation are taken from [160]. The PV generation data of three different months of a year are considered to have the seasonal variation in PV generation. The hourly average PV generation data in terms of peak PV generation are shown in Table A.6.

Table A.6: Hourly average PV generation in percentage of peak PV generation

Hour	Hourly average PV generation in percentage of peak PV generation (%)		
	Winter season	Summer season	Spring season
12-1 am	0	0	0
1-2	0	0	0
2-3	0	0	0
3-4	0	0	0
4-5	0	0	0
5-6	0	0.696864	0
6-7	1.0453	10.80139	6.2718
7-8	11.8467	31.70732	25.4355
8-9	31.7073	55.74913	50.1742
9-10	51.2195	77.35192	72.1254
10-11	65.8537	92.68293	87.108
11-noon	72.8223	100	93.0314
Noon-1pm	72.4739	99.65157	92.3345
1-2	64.8084	91.2892	85.3659
2-3	51.9164	77.00348	69.338
3-4	33.4495	55.74913	49.1289
4-5	13.2404	30.66202	25.784
5-6	1.0453	10.10453	6.2718
6-7	0	0.696864	0
7-8	0	0	0
8-9	0	0	0
9-10	0	0	0
10-11	0	0	0
11-12	0	0	0

भारतीय प्रौद्योगिकी संस्थान गुवाहाटी
Indian Institute of Technology Guwahati

Publications from This Thesis

Journal

[1] S. Lakshmi, and S. Ganguly, "An on-line operation optimization approach for open unified power quality conditioner for energy loss minimization of distribution networks," *IEEE Transactions on Power Systems* (Accepted), May 2019, DOI:10.1109/TPWRS.2019.2919786.

[2] S. Lakshmi, and S. Ganguly, "Modelling and allocation of open-UPQC-integrated PV generation system to improve the energy efficiency and power quality of radial distribution networks," *IET Renewable Power Generation*, vol. 12, no. 5, pp. 605–613, 2018.

[3] S. Lakshmi, and S. Ganguly, "Modelling and allocation planning of voltage-sourced converters to improve the rooftop PV hosting capacity and energy efficiency of distribution networks," *IET Generation, Transmission & Distribution*, vol. 12, no. 20, pp. 4462–4471, 2018.

[4] S. Lakshmi, and S. Ganguly, "Simultaneous optimization of photovoltaic hosting capacity and energy loss of radial distribution networks with open unified power quality conditioner allocation," *IET Renewable Power Generation*, vol. 12, no. 12, pp. 1382–1389, 2018.

[5] S. Lakshmi, and S. Ganguly, "A comparative study among UPQC models with and without real power injection to improve energy efficiency of radial distribution networks," *Journal of Energy Systems*, Springer, pp. 1–26, 2018.

[6] S. Lakshmi, and S. Ganguly, "Multi-objective planning for the allocation of PV-BESS integrated open unified power quality conditioner for peak load shaving of radial distribution networks," *Journal of Energy storage*, Elsevier, vol. 22, pp. 208–218, 2019.

Book Chapter

[1] S. Lakshmi, and S. Ganguly, "Transition of power distribution system planning from passive to active networks: a state-of-the-art review and a new proposal," *Sustainable Energy Technology and Policies*, Springer, Singapore, pp. 87–117, 2018.

Conference

[1] S. Lakshmi, and S. Ganguly, "Energy loss minimization with open unified power quality conditioner placement in radial distribution networks using particle swarm optimization," *7th International Conference on Power Systems (ICPS)*, Pune, India, pp. 55–60, 2017.

[2] S. Lakshmi, S. Ganguly, and U. Sarma, "Open unified power quality conditioner model with and without storage units to improve power quality and losses of radial distribution networks," *14th IEEE India Council International Conference (INDICON)*, Roorkee, India, pp. 1–6, 2017.

[3] S. Lakshmi, and S. Ganguly, "Steady-state model for open unified power quality conditioner for power quality and energy efficiency improvement of radial distribution networks," *2nd International Conference on Energy, Power, and Environment (ICEPE)*, Shillong, India, 2018.

[4] S. Lakshmi, and S. Ganguly, "Centralized and distributed battery energy storage system for peak load demand support of radial distribution networks," *13th IEEE PowerTech 2019 Conference*, Milano, Italy, 2019.

Author's Biography

Shubh Lakshmi was born on 26 February 1992 at Muzaffarpur in Bihar, India. She obtained Bachelor of Technology degree in Electrical Engineering from Muzaffarpur Institute of Technology, Muzaffarpur in 2013. She received Master of Technology degree in Power System Engineering from Indian School of Mines, Dhanbad {Now, Indian Institute of Technology (Indian School of Mines), Dhanbad} in 2015. She joined the Ph.D. programme in the Department of Electronics and Electrical Engineering, Indian Institute of Technology Guwahati in 2015. Her research interest includes active distribution system planning and optimization, multi-objective optimization, custom power devices, and distributed generation.